Stony Brook University

Anti-Backbiting in Alternating Ring-Opening Metathesis Polymerization and Applications of Alternating Copolymers

A Dissertation Presented

by

Li Tan

to

The Graduate School

in Partial Fulfillment of the

Requirements

for the Degree of

Doctor of Philosophy

in

Chemistry

Stony Brook University

December 2014

Stony Brook University

The Graduate School

Li Tan

We, the dissertation committee for the above candidate for the

Doctor of Philosophy degree, hereby recommend

acceptance of this dissertation.

Nicole S. Sampson– Dissertation Advisor

Professor and Chair of Chemistry

Robert B. Grubbs - Chairperson of Defense

Associate Professor of Chemistry

Iwao Ojima – Third member of Defense

Distinguished Professor of Chemistry

Jin Kim Montclare - Outside member of Defense

Associate Professor of Chemical and Biomolecular Engineering

NYU Polytechnic School of Engineering

This dissertation is accepted by the Graduate School

Charles Taber

Dean of the Graduate School

Abstract of the Dissertation

Anti-Backbiting in Alternating Ring-Opening Metathesis Polymerization and Applications of Alternating Copolymers

by

Li Tan

Doctor of Philosophy

in

Chemistry

Stony Brook University

2014

Linear alternating copolymers have potential use as tools in the biochemical and material sciences. Cyclobutene-1-carboxylate esters and cyclohexene participate in an alternating ring-opening metathesis polymerization (AROMP) [Song, A.; Parker, K. A.; Sampson, N. S. *J. Am. Chem. Soc.* **2009**, *131*, 3444]. However, the molecular weight homogeneity of the copolymers resulting from the 1-cyclobutene ester/cyclohexene pair is limited by "cross metathesis" reactions that lead to undesired polymer dispersities and cyclic polymers. Therefore, strategies to inhibit intramolecular cross metathesis and to obtain linear alternating copolymers were undertaken.

We set out to improve the AROMP process by screening reaction conditions to inhibit intramolecular cross metathesis. These conditions included co-solvents, additives, different catalysts and variation of monomers. Altering monomer steric contraints proved the most effective. Incorporation of bulky side chains provided linear alternating copolymers of limited lengths. These alternating copolymers support efficient energy transfer between side chains

[Romulus, J.*; Tan, L.*; Weck, M.; Sampson, N. S. *ACS Macro. Lett.* **2013**, *2*, 749]. Linear alternating copolymers are synthetically accessible via AROMP with bicylic carbomethoxy olefin monomers and cyclohexene. Importantly, monomer methyl bicyclo[4.2.0]oct-7-ene-7-carboxylate in which the cyclobutene ring is fused to a cyclohexane provides rigorously linear (as opposed to cyclic), alternating copolymers free of cross metathesis. This pair was used to prepare alternating copolymers substituted with bromide and aldehyde moieties. These orthogonal functionalities provide an efficient route for post-polymerization modification with functional groups that are not compatible with AROMP. To demonstrate the utility of this approach, a tryptophan and dansyl fluorophore pair was conjugated onto the bromide/aldehyde derivatized polymers. FRET was observed between fluorophores confirming the substitutions, and illustrating the use of the polymer backbone for functional group presentation.

Further investigation of the [4.2.0] monomers yielded bicyclo[4.2.0]oct-7-ene-7-carboxamides of primary amines. Theses amides were found to be susceptible to isomerization in the presence of $(H_2IMes)(PCy_3)(Cl)_2Ru{=}CHPh$ and yielded tetra-substituted bicyclo[4.2.0]oct-1(8)-ene-8-carboxamides. The isomerized amides underwent ring-opening metathesis in situ, and upon addition of cyclohexene, alternating copolymers were obtained. The tetrasubstituted amide monomers polymerize more rapidly than methyl bicyclo[4.2.0]oct-7-ene-7-carboxylate, enabling the construction of linear and extremely long alternating polymers. These synthetic methods provide an entry to applications requiring controlled polymer architectures.

Table of Contents

List of Figures

List of Tables

List of Schemes

List of Abbreviations

m-CPBA	*meta*-Chloroperoxybenzoic acid
APT	Attached proton test
AROM	Alternating ring-opening metathesis
AROMP	Alternating ring-opening metathesis polymerization
ATRP	Atom transfer radical polymerization
AMPs	Antimicrobial peptides
CBE	Cyclobutene
CH	Cyclohexene
COE	Cyclooctene
CPE	Cyclopentene
CRPs	Controlled radical polymerizations
DAN	Dialkoxynaphthalene
DH	Dansyl
DMF	Dimethylformamide
DP	Degree of polymerization
$Đ_M$	Molar-mass dispersity
EDC•HCl	*N*'-ethylcarbodiimide hydrochloride
FRET	Förster/fluorescence resonance energy transfer
GPC	Gel permeation chromatography
HRMS	High resolution mass spectroscopy
HSQC	Heteronuclear single quantum coherence spectroscopy

NALDI	Nanostructure-assisted laser desorption/ionization
NBE	Norbornene
NHS	N-Hydroxysuccinimide
NMR	Nuclear magnetic resonance
OLEDs	Organic Light Emitting Diodes
PEDTA	*N,N,N',N'',N''*-Pentamethyldiethylenetriamine
PDI	Pyromellitic dianhydride
RAFT	Reversible addition−fragmentation chain-transfer polymerization
ROM	Ring-opening metathesis
ROMP	Ring-opening metathesis polymerization
[Ru]	Ruthenium catalyst
TLC	Thin layer chromatography
Trp	Tryptophan
TFE	Trifluoroethanol
THF	Tetrahydrofuran
UV-vis	Ultraviolet visible spectroscopy

Acknowledgments

We thank the National Institutes of Health (NIH) for grants R01GM097971/R01HD38519 (N.S.S.), R01GM74776 (K.A.P) and RR021008-01-001, and National Science Foundation for grant CHE1058349.We also thank Dr. Francis Picart and Dr. James Marecek for their assistance with NMR spectroscopy and Dr. Bela Ruzsicska for his assistance with HRMS and NALDI.

Chapter 1. Introduction of Sequence-Controlled Polymer and Alternating Ring-Opening Metathesis Polymerization

1.1. Specific Aims

Song, et al[1] previously reported alternating ROMP (AROMP) of cyclobutene-1-carboxylic esters (**A**) and cyclohexene (**B**) with $(H_2IMes)(3\text{-Br-Pyr})_2Cl_2Ru{=}CHPh$. They obtained highly alternating copolymers, owing to the combination of two monomers. Neither of the monomers forms a homopolymer via ROMP. Moreover, the monomers have alternate affinities to the ruthenium catalyst. However, AA dyads were observed, suggesting that intramolecular cross metathesis (backbiting) occurs during AROMP. In this study, we set out to improve AROMP and to eliminate intramolecular cross metathesis which is also called 'backbiting'. Our goal was to synthesize rigorously pure, linear and alternating copolymers and to advance the applications for alternating copolymers.

1.1.1. Exploration of AROMP conditions to prevent backbiting.

In an optimal polymerization process, $k_{polymerization}$ (k_p) must be greater than $k_{backbiting}$ (k_b). Various temperatures, solvents, monomer feed ratios and additives were tested to alter the partitioning between k_p and k_b.

1.1.2. Redesign of polymer backbone to introduce steric hindrance and prevent backbiting.

Bicyclic monomers were designed and applied in AROMP in order to introduce rings into the polymer backbone to prevent the occurrence of backbiting. We hypothesized that the rings would reduce k_b, preferentially to minimize intramolecular backbiting reactions.

1.1.3. Application of alternating copolymers.

We investigated the utility of the "alternating" characteristic of our copolymers. Functional groups which communicate with each other were coupled to the copolymers in order to enhance their interactions. These functional groups include electron donors and acceptors used in solar cells and OLEDs.

1.2. Overview of Polymers

Polymers are macromolecules consisting of repeating subunits known as "monomers" which are typically connected by covalent bonds. They are natural and synthetic materials with various properties and functions. Natural biopolymers such as DNA and proteins are vital to biological structures and functions. Synthetic polymers mimicking biopolymers or possessing other chemical, physical, physiological properties have received wide attentions. Applications of synthetic polymers build up the modern world and play essential roles in everyday life.[2]

1.2.1. Application of Synthetic Polymers

Polymers have found their wide applications in material science. With further advances in the understanding of polymers, and also with new applications being studied, there is no reason to believe that the revolution will stop any time soon. Plastics (including polystyrene (PS), polyvinyl chloride (PVC), polyamide (PA, trade name Nylon), etc.), elastomers (for example, rubber), and fibers (such as nylon, polyester, rayon, and acrylic, etc.) have had a major impact on the way we live. They have also been utilized in the cosmetics industry, military protection clothing, nano sensors and filtration media to name but a few applications. Recently, their applications have been extended into the biomedical sciences.

In biological contexts, essentially all biological macromolecules, such as polypeptides, polynucleotides and polysaccharides, are polymeric, or are composed in large part of polymeric components, e.g., isoprenylated/lipid-modified glycoproteins.[3] Synthetic polymers have been designed to mimic biological macromolecules for their biochemical activities. Peptidomimetic, for example, is defined as "a compound that is able to emulate the properties or biologically

activity of a peptide".[4] Polymer-based peptidomimetics, or proteinomimetics mimicking the biochemical activity of antimicrobial peptides (AMPs) have been realized in the development of antibiotics and in the mechanism studies of AMPs.[5-9]

The use of polymers for the administration of pharmaceutical agents has increased dramatically over the past decades. Polymers applied in controlled release technology have gained a significant impact.[10-13] The advances in the development of biodegradable polymers has enabled site-specific or systemic administration of pharmaceutical agents without the need for subsequent retrieval of the delivery system.[14]

Polymer-based stents or polymer-coated stents have been applied to clinical studies.[15-17] Polymer-based, paclitaxel-eluting stents remarkably reduced the risk of clinical and angiographic restenosis as compared with the implantation of a bare-metal stent in patients with a wide range of previously untreated coronary lesions.[16] Polymer-based (polyglycolic acid, PGA) absorbable sutures have been available as early as 1971. PGA outperforms other materials with respect to handling, tensile strength, knot security, lack of toxicity, and minimal tissue reaction, and it does not interfere with wound healing.[18, 19] Medical polymer adhesives[20, 21] and other implantable polymer-based medical devices[22, 23] have also been applied to clinical use.

1.2.2. Classification of Synthetic Polymers

Typically, polymers can be classified in regards to their architectures, including star polymers, comb polymers, brush polymers, dendronized polymers, ladders, and dendrimers.

Based on repeating units, they can be also categorized into homopolymers and copolymers. Homopolymers contain a single type of repeating unit, for example, poly(styrene), which is used

where a rigid, economical plastic is desired, e.g. disposable plastic cutlery and dinnerware. Copolymers contain a mixture of repeating units, for example, ethylene vinyl acetate (EVA), which is used in hot melt adhesives, hot glue sticks, top of the line soccer cleats and more.

Copolymers can be further divided into the following four groups based on the arrangement along the chain:[24, 25] a) Alternating copolymers consist of alternating A and B units (e. g. (A-B-A-B-A-B-A-B)$_n$); b) periodic copolymers consisting of A and B units arranged in a repeating sequence (e.g.(A-B-A-B-B-A-A-A-A-B-B-B)$_n$); c) statistical copolymers such as random copolymers consisting two or more monomeric units polymerized simultaneously; d) block copolymers consisting of two or more homopolymer subunits connected by covalent bonds (e.g. -A-A-A(B-B-B)$_m$-A-A-A-, (A-A-A)$_n$-(B-B-B)$_m$); e) graft or grafted copolymers consisting of polymeric side chains that have a different composition or configuration than the main chain.

1.3. Development of Synthetic Polymers and Current Advances

In recent years, the most popular methods of making polymers include living/controlled radical polymerizations (CRPs) and ring-opening metathesis polymerization, as well as ring opening polymerization of cyclic esters. They are the focus of polymer sciences as a result of improved molar-mass dispersities provided by these methodologies.

1.3.1. Living/Controlled Radical Polymerizations (CRPs)

In radical polymerization methods, polymers are formed from the successive addition of free radical monomers. CRP continuously polymerizes until the monomeric unit nears a complete conversion (usually not to complete conversion) and the reaction will not be terminated by most of the impurities. The polymerization continues upon the addition of more monomer.

There are three main types of CRPs, atom-transfer radical polymerization (ATRP), reversible addition-fragmentation chain-transfer polymerization (RAFT) and nitroxide-mediated radical polymerization.

ATRP, discovered in 1995, is based on the formation of a carbon-carbon bond through a transition metal catalyst (Scheme 1-1). This method requires reversible activation of a dormant species (such as an alkyl halide) and a transition metal halide catalyst.[26-28] The transition metal halide is used to activate the dormant species. The atom transfer step is the key step in the reaction responsible for uniform polymer chain growth. Polymers generally synthesized by ATRP includes polystyrene, poly(methyl methacrylate) and poly(*N*-alkylacrylamide)s.

RAFT makes use of a compound that can act as a reversible chain transfer agent, such as thiocarbonyl compounds to afford control over the generated molecular weight and molar-mass dispersities during a free-radical polymerization (Figure 1-1). The thiocarbonylthio compounds can be dithioesters, thiocarbamates, and xanthates, and related compounds. RAFT has been successfully applied to the synthesis of a wide range of polymers with a promising control over the molecular weight and molar-mass dispersities ($\mathit{Đ}_M$ between 1.06 and 1.40). One of its most prominent applications is the production of smart materials such as drug-delivery system with temperature or pH sensitivity.

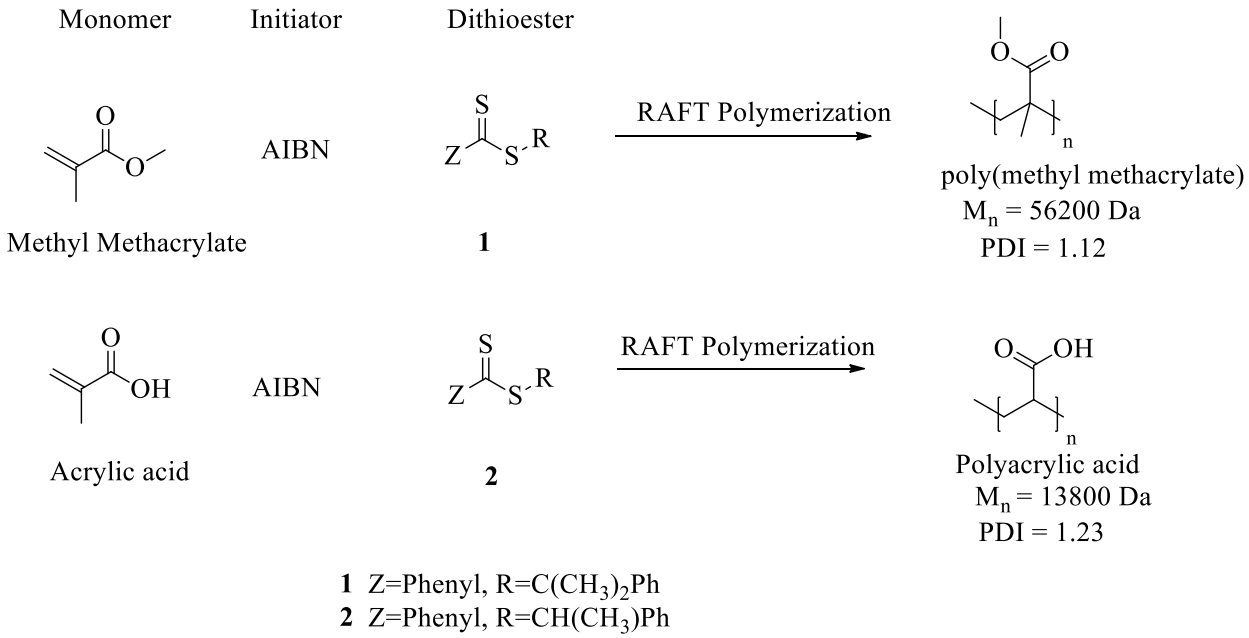

Figure 1-1. Examples of the major reagents and products in two RAFT polymerizations. This figure was adapted from Chiefari, et al.[29]

1.3.2. Ring-Opening Metathesis Polymerization (ROMP).

The story of ROMP began more than five decades ago when the first carbon-carbon double bond rearrangement reaction was reported by Anderson and Merckling.[30] The patent describes the synthesis of polybicyclo[2,2,1]-2-heptene catalyzed by titanium compounds. The term "ROMP" was coined by Robert H. Grubbs, which is a variant of olefin metathesis. ROMP is a chain-growth polymerization reaction based on the ring opening of cyclic olefins. Generally, there are three key steps in ROMP which utilizes a transition metal (Mo- or Ru-) catalyst: (i) initiation, (ii) propagation, and (iii) termination (Scheme 1-2).

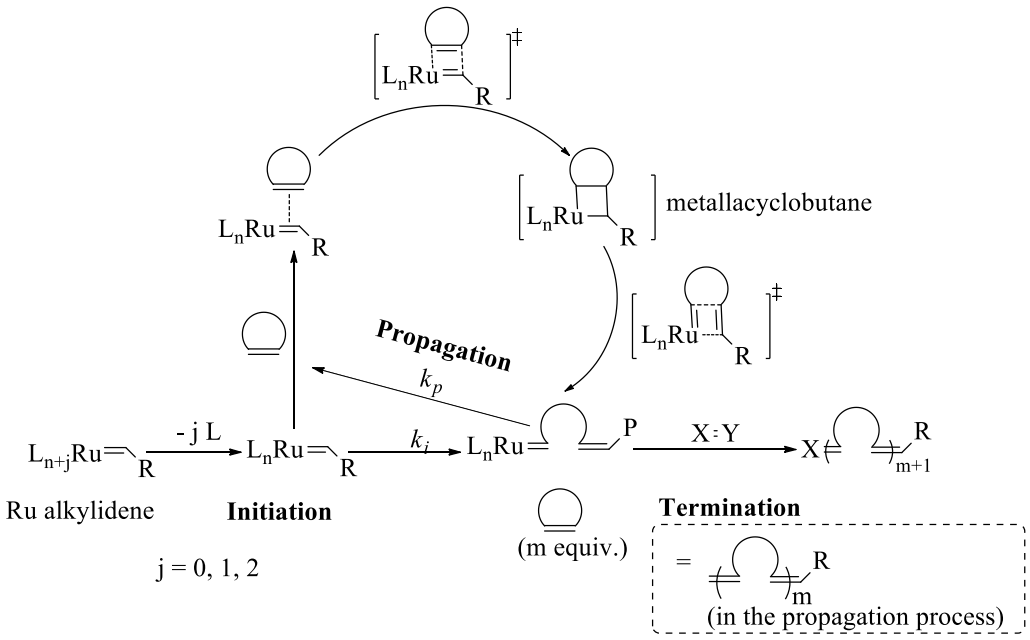

Scheme 1-1. Mechanism of a typical ROMP reaction using transition metal ruthenium catalyst. This scheme was adapted from Song, et al.[31]

A "Living" polymerization proceeds without termination or transfer reactions. It will give a linear relationship between M_n and conversion and is especially desirable because it offers precision and control in polymer synthesis without chain transfer or termination.

A good "living" ROMP exhibits three features: a) initiation be much faster than chain propagation ($k_i >> k_p$) and it must be complete; b) a linear relationship must be established between the number-averaged molecular weight of the polymer (M_n) and monomer conversion; and c) molar-mass dispersities ($Đ_M$) below 1.5.[31, 32]

Polymerization usually is a process of decreasing entropy (ΔH_p), and the driving force for ROMP is the release of ring strain in cyclic olefins upon ring opening. Hence, ring-strain energy, in addition to high initial monomer concentration ($[M]_e$) and low reaction temperature is ideally

required (Equation 1-1). However, available ROMP catalysts are less reactive at low temperatures. Therefore, ROMP reactions are generally carried out at room temperature. In order for ROMP to occur, the strain energy of the monomers should be greater than 5 kcal/mol to compensate the entropy loss in polymerization.[33] Commonly used cyclic olefin monomers include cyclopropene, norbornene, cyclobutene, cyclopentene and cyclooctene (Figure 1-2).[34-36]

$$In[M]_e = \frac{\Delta H_p}{RT} - \frac{\Delta S^\theta}{T} \qquad \textbf{(Equation 1-1)}$$

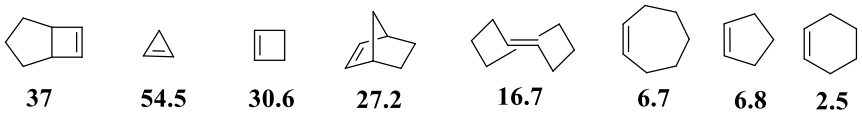

Figure 1-2. Relative ring strain for selected cyclic olefins (kcal/mol).[37, 38]

ROMP Catalysts Development. ROMP reactions are catalyzed by transition metal complexes which have come a long way since they were first reported almost 50 years ago.[39-41] Thereafter, catalyst development has been driven by many preeminent scientists especially Yves Chauvin,[42-44] Robert H. Grubbs,[45-51] Richard R. Schrock,[52-57] Amir H. Hoveyda,[52, 58, 59] Karol Grela[60-62] and Steven. P. Nolan,[63, 64] etc. The first three of them were collectively awarded the 2005 Nobel Prize in Chemistry for their work in the field of olefin metathesis.[65] Modern metathesis catalysts used in ROMP are well-defined organometallic compounds; they include but are not limited to the following two categories based on the transition metal utilized.

Molybdenum(IV)- and Tungsten(IV)-based catalysts. Molybdenum(IV)- and tungsten(IV)-based catalysts are known to be fast initiators for living ROMP, especially with norbornenes and substituted norbornadienes.[53, 54, 66-72] The development of the well-defined, activity-tunable Mo(IV)-based metathesis catalysts (Figure 1-3) stands as a very important milestone in this area. However, they are still more reactive towards acids, alcohols or aldehydes than with olefins.

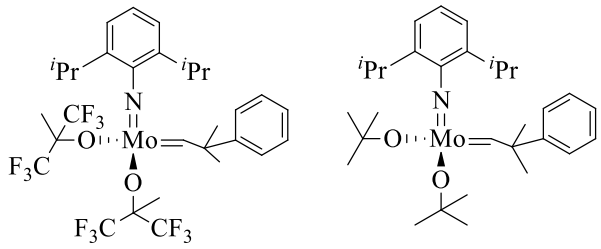

Figure 1-3. Structures of commonly used Schrock's Mo-based imido alkylidene catalysts.[52, 55, 57]

Ruthenium-based Catalysts. Meanwhile, development of ruthenium-based catalysts progressed slower, even though ruthenium (Ru) catalysts were considered excellent candidates for ROMP due to high oxidation state and low oxophilicity.[48] Previously reported, ill-defined Ru complexes, such as $RuCl_3(H_2O)_n$, initiate too slowly in ROMP. However, it was determined that the ROMP reactions were actually catalyzed by the Ru alkylidene species, which shed light on the direction for the future active Ru catalyst design.[45, 73-75]

The first well-defined Ru catalyst for ROMP, $(PPh_3)_2(Cl)_2Ru{=}CHCH{=}CPh_2$ **G1**, was published in 1992 (Figure 1-4), and exhibited efficient activity for ROMP of norbornene (NBE) and cyclobutene (CBE) with high tolerance towards alcohols in protic solvents.[37, 76] This led to the production of the Grubbs I catalyst $(PCy_3)_2(Cl)_2Ru{=}CHPh$ **G2**, in 1995.[50, 51] The broad

functional group tolerance and thermal stability of **G2** relative to previous catalysts (half-life > 1 week at 55 °C) marked its importance in the development of Ru catalysts.[50, 51, 77-79] However, it still requires strictly inert storage and handling conditions for a long shelf life. The poor molecular weight control and the resulting high molar-mass dispersities in ROMP of NBE with **G2** derivatives posed a new challenge for catalyst design.

Mechanistic studies suggested that the chain propagation is catalyzed by the Ru carbene species with only one phosphine ligand bound to Ru.[47, 80-84] Hence, Grubbs II catalyst $(H_2IMes)(PCy_3)(Cl)_2Ru{=}CHPh$ **G3**, was designed by replacing one of the PCy_3 ligand with an *N*-heterocyclic carbene (NHC).[85-87] NHC forms a stronger coordination with Ru and is a better electron donating ligand to the ruthenium alkylidene.[88] As a result, catalyst **G3** displays much better thermostability towards air and moisture, higher ROMP activity and functional group tolerance than catalyst **G2**.

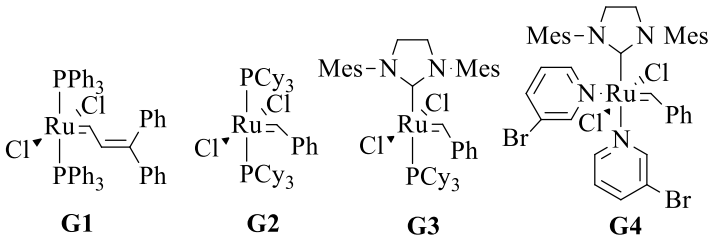

Figure 1-4. Most popular Grubbs' Ru catalysts for ROMP.[58, 89]

Later, a benzylidene ligand which has a chelating *ortho*-isopropoxy group attached to the benzene rings was introduced into **G2** and **G3** and formed new catalysts known as Hoveyda-Grubbs catalysts, **H1** and **H2** (Figure 1-5).[52, 58, 59] The Hoveyda-Grubbs catalysts, while more expensive and even slower to initiate than **G2** and **G3**, are popular because of their improved

stability.[90] Applications of these catalysts are mainly limited to ring-closing metathesis (RCM) due to a decreased initiation rate, comprising a major disadvantage for this series of catalysts. A variety of steric and electronic modifications of the chelating benzylidene ether ligand have been undertaken aiming at resolving this problem.[90]

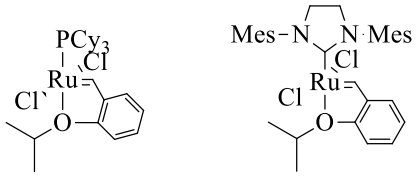

H1 **H2**

Figure 1-5. Early Hoveyda-Grubbs' catalysts.[58, 89]

To improve the poor initiation rates of Grubbs' catalysts, the phosphine ligand was replaced with a more labile ligand. Fast-initiating catalysts were obtained as a result of using pyridine ligands.[91] **G4**, for example, initiates cross metathesis (CM) reactions at least six orders of magnitude faster than **G3**.[91] Though initial studies of **G4** were done in CM, the principle application of the fast-initiating catalysts is as initiators for ROMP. The high ratio of the rate of initiation to the rate of propagation makes these catalysts useful in living polymerization, yielding polymers with low molar-mass dispersities. Because of their excellent performance in ROMP, these catalysts are sometimes referred to as Grubbs III catalysts.

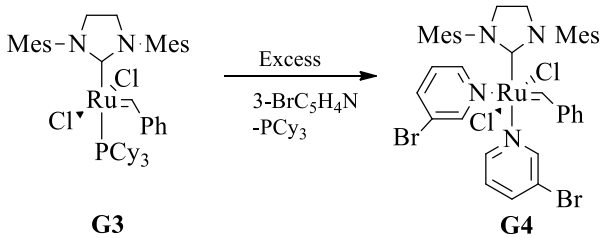

G3 **G4**

Scheme 1-2. Facile synthesis of bispyridine complex **G4** from **G3**.[91]

1.3.3. Secondary Metathesis Reactions of Polymers.

Secondary metathesis reactions include intermolecular chain transfer and intramolecular cross metathesis (backbiting) reactions. In cross metathesis, one or two active Ru alkylidene containing polymers may be involved, generating four possible new polymers at most as shown in Scheme 1-4 (shows the possibility with two active Ru alkylidene containing polymers). New Ru containing polymers can further undergo a new cycle of cross metathesis. Molar-mass dispersities can be calculated using Equation 1-2, where M_w is the weight-average molar mass and M_n is the number-average molar mass. As a result of cross metathesis, M_w of the final polymer is increased while M_n stays the same, hence, $Đ_M$ is increased. In backbiting reactions, the active Ru alkylidene reacts with its own "tail", forming cyclic polymers, and results in a high $Đ_M$s and a lower M_n than the expected value.

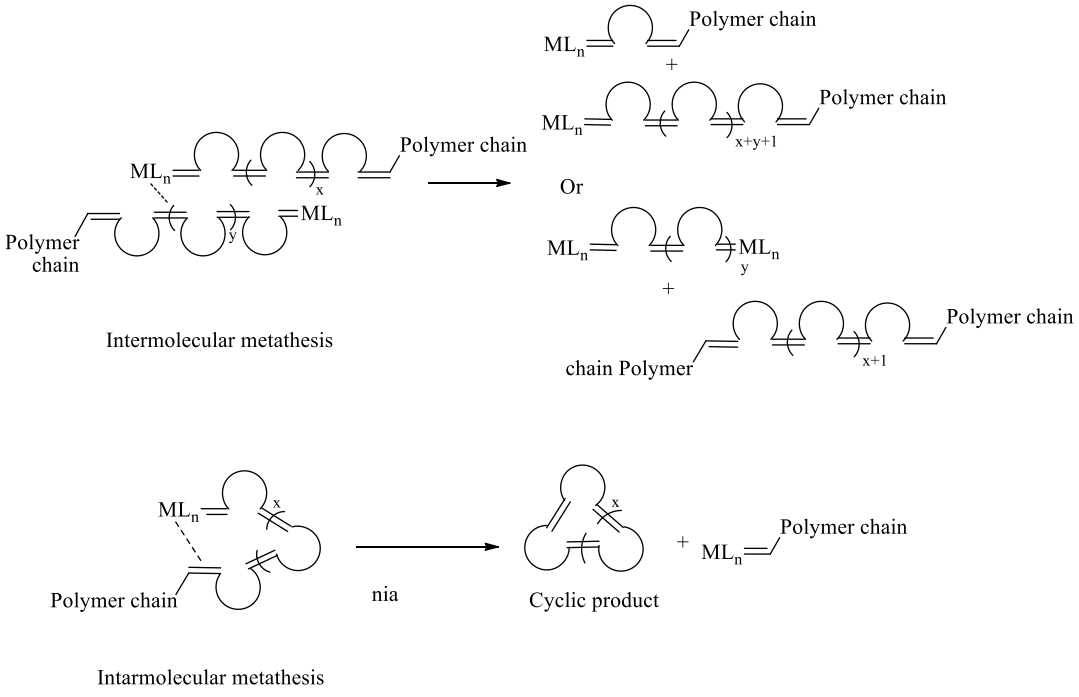

Scheme 1-3. Illustration of typical secondary metathesis reactions in ROMP. This scheme was

adapted from Song, et al.[31]

$$Đ_M = M_w/M_n \qquad \textbf{(Equation 1-2)}$$

$$M_w = \frac{\sum_i N_i M_i^2}{\sum_i N_i M_i} \qquad M_n = \frac{\sum_i N_i M_i}{\sum_i N_i}$$

Where N_i is the number of molecules of molecular mass M_i.

The most commonly believed cause for the secondary metathesis reactions in ROMP is the high activity of the metal alkylidene intermediate. As the consumption of monomer and ROMP reaction progress, the concentration of double bonds on the polymer backbone increase. These double bonds are able to compete with the remaining monomers for the active Ru carbene. The effect of ring-strain energy stored in the monomer becomes less predominant as its concentration decreases especially towards the end of the reaction.

Two strategies have been developed based on the mechanism of secondary metathesis reactions to improve the ratio of k_p/k_s (where *p*: polymerization and *s:* secondary metathesis). The first strategy is to decrease the activity of the Ru alkylidene. The addition of a small amount of THF into ROMP solvent or the use of THF alone as the solvent has been shown to effectively suppress secondary metathesis.[32, 76, 92-95] Other additives such as PPh_3 or PPh_2H have also been shown to be useful in some cases.[32] The two examples are based on the coordination ability of the additives to the Ru alkylidene. The second strategy is to introduce steric hindrance into the polymer backbone to block it from reacting with the active Ru alkylidene. Norbornene derivatives and 1-substituted cyclic olefins have been used for this purpose.[32]

Monomer concentration has also been shown to be important for high quality ROMP reactions.[96, 97] If the initial monomer concentration is less than a critical monomer concentration $[M]_c$, only low molecular weight cyclic and linear oligomers are formed. Also, it has been demonstrated that as the monomer concentration in solution decreases, the k_p decreases, and k_s increases.[92] Furthermore, it has been shown that critical monomer concentration is directly related to monomer ring strain.[49, 76] Therefore, low ring-strain monomers require higher concentration in ROMP than highly strained monomers, and it is difficult for low ring-strain monomers to form high molecular weight polymers.

1.4. Application of ROMP in Our Demonstrations.

The catalysts used for ROMP in the following examples are Grubbs' catalysts. They have very long shelf lives when stored properly and are tolerant of many functional groups and do not require highly rigorous removal of oxygen and other impurities.[49] Removal of Grubbs' catalysts can be easily achieved by precipitation of polymers[49] or by using $P(CH_2OH)_3$[98] and salts[99] or silica supported isocyanide reagents.[100]

1.4.1. Application of 1-Substituted Cyclobutenes in ROMP.

Our research group has accumulated years of experience in ROMP. We chose to focus on cyclobutene derivatives because in norbornene-based systems, stereocontrol of the polymerization reaction is not always possible. For example, Ru catalyzed polymerization of 5-substituted norbornene and oxanorbornene monomers provide stereochemically heterogeneous materials.[101, 102] 1-Substituted cyclobutenes contain no chiral center, and the results show that

cyclobutenecarboxamide is regio- and stereoselective and affords functionalized polymers with $\not{D}_M$s ranging from 1.2 to1.6 (Scheme 1-5).[103]

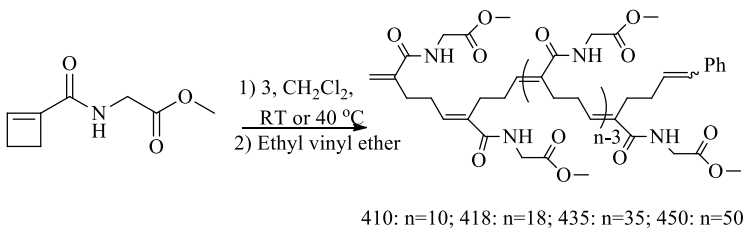

Scheme 1-4. Ring-opening metathesis polymer formation of secondary amide of 1-cyclobutene. This scheme was adapted from Lee, et al.[103]

By exploiting other 1-substituted cyclobutenes, we discovered that these olefins behave differently depending on charge distribution and steric interactions during the formation of the metallocyclobutane intermediates.[104] Substituents such as amides, esters and ethers were studied and divided into four groups based on the result when subjected to ROMP conditions (Figure 1-6). All secondary amides examined (group I) provide polymers with translationally invariant backbones and excellent $\not{D}_M$s, whereas ROMP of the 1-cyclobutene-1-methanol esters (group IV) is neither regio- nor stereoselective. Both 1-cyclobutenecarboxylic acid tertiary amides (group II) and 1-cylobutenecarboxylic acid esters (group III) undergo only one single ring-opening metathesis cycle (ROM) without polymerization.

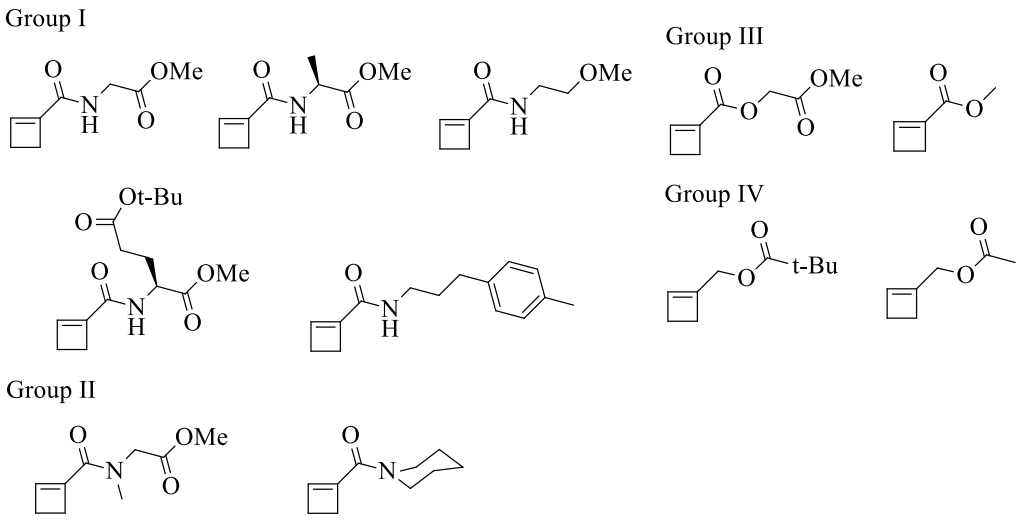

Figure 1-6. 1-Substituted cyclobutene derivatives subjected to ROMP. This figure was adapted from Song, et al.[104]

1.4.2. Sequence-Controlled Polymers Using 1-Substituted Cyclobutenes.

Sequence-controlled polymers consist of repeating units of different chemical composition arranged in a well-defined order. Nucleic acids and proteins are examples of sequence-controlled polymers which are vital to the living world. Hence, synthetic polymers with precisely controlled monomer sequences are predicted to have an enormous effect in the material sciences. Common synthetic polymers are usually homopolymers with simple chain microstructures or copolymers, such as random or block copolymers, which do not have molecular precision. These polymers are widely applied but do not have the same structural and functional complexity as sequence-controlled biopolymers created by nature. In synthetic polymers, the sequential arrangement of monomeric units in a polymer chain is generally poorly controlled. As a result, developing synthetic polymers with sequence-controlled monomers is an important area for research.[105-107]

Applications of ROMP in sequence-controlled polymerizations have been studied extensively owing to well-defined metathesis catalysts. Two approaches are frequently used to produce sequence-controlled polymers: the catalyst-controlled approaches and monomer-controlled approaches.[108] Various catalysts have been developed in this regard and their efficacies are summarized in Table 1-1. Unfortunately, even with carefully designed catalysts, a high alternating ratio is still hard to obtain unless a large excess of the less reactive monomer, such as cyclooctene or cyclopentene, is used.

Table 1-1. Catalyst-controlled approaches for alternating copolymers. This table was adapted from Chang et al.[108]

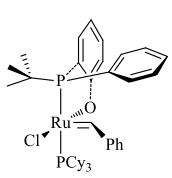

9

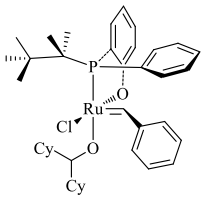

10

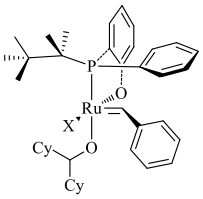

11

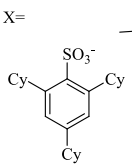

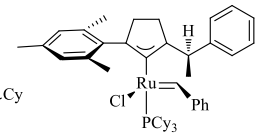

12

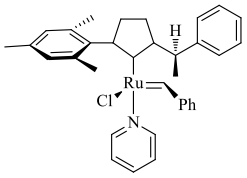

13

Entry	Catalyst	Monomer A	Monomer B	[A]:[B]	A,B Dyads(%)
1	WCl_6/Et_3Al	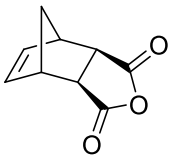		1:1	-[109]
2	$RuCl_3/PhOH$			1:8	-[35, 110]
3	**G1**	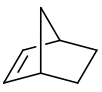	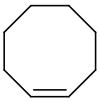	1:200	67[36, 111]
4	**G2**	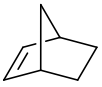	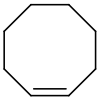	1:20	97[112]
5	**G3**		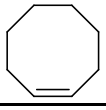	1:20	97[112, 113]

6	**G4**		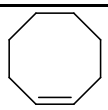	1:50	97[114, 115]
7	**G5**	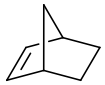	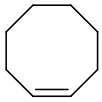	1:50	97[114, 115]
8	**G5**	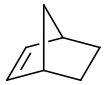		1:8	90[114, 115]
9	**G4**	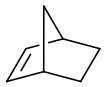	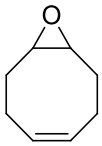	1:1	72[114]
10	**G4**		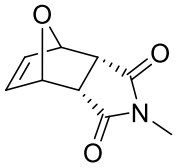	1:1	48[114]

[a]Determined by ^{1}H NMR

Monomer approaches, which have been reported to be capable of yielding precise sequence-controlled polymers, are considered an extension of the catalyst approaches. The use of polar and nonpolar monomers to obtain alternating copolymer was first reported by Ilker and Coughlin in 2002 using **G2**, a catalyst displaying no selectivity for alternation in the copolymerization of cyclic olefins with similar double-bond polarity (Table 1-2, entry 1-3).[111, 116] Highly alternating polymers were obtained from the ROMP of an equimolar mixture of polar 2,3-difunctionalized 7-oxanorbornene derivatives with a series of nonpolar cycloalkenes. Acid-base interaction inspired alternating ROMP was exemplified by Sanda and coworkers' report.[117] The ROMP of two norbornene-based monomers, functionalized with carboxyl groups and amino groups, respectively, yields highly alternating copolymers (Table 1-2, Entry 5). The authors proposed that it was the acid-base interaction that enabled the sequence-control instead of electronic and steric characters, since the electronic and steric differences between the monomers were negligible. Grubbs and coworkers reported the first example of sequence-editing alternating

copolymers with up to 99% alternating dyads from the ROMP of an equimolar mixture of a diacrylate and a cycloalkene, initiated by **G3** (Table 1-2, Entries 6 and 7). Rapid homopolymerization of cyclooctene proceeds first as the diacrylate and cyclooctene are mixed, followed by cross metathesis of the diacrylate which is selectively inserted into the unsaturated backbone.[118]

Table 1-2. Monomer-controlled approaches for alternating copolymers. This table was adapted from Chang, et al.[108]

Entry	Catalyst	Monomer A	Monomer B	[A]:[B]	A,B-Dyads (%)
1	**G6**	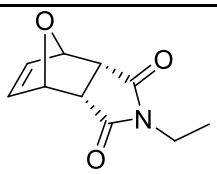	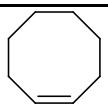	1:1	98[34]
2	**G6**	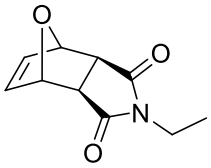	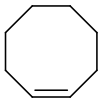	1:1	80[34]
3	**G6**	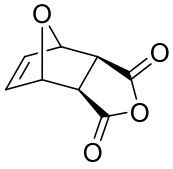	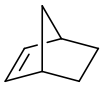	1:1	40[34]
4	**G8**	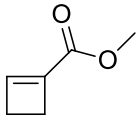		1:2	91[1]
5	**G7**	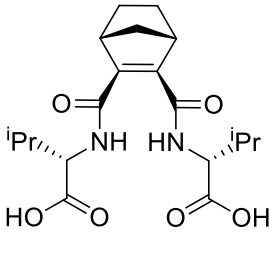	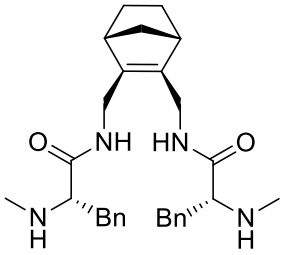	1:1	-[117]

6	**G7**	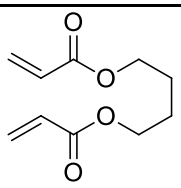	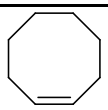	1:1	99[118]
7	**G7**	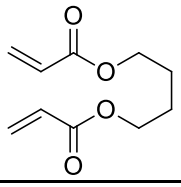	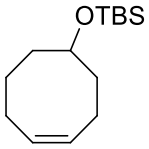	1:1	95[118]

[a]Determined by ^{1}H NMR

Instead of focusing on the development of polymerization techniques, novel catalysts, monomers or templates, Hillmyer (2012) introduced sequence specificity via synthesis of sequence-specific vinyl copolymers through the regioselective ROMP of multiply substituted cyclooctenes (Figure 1-7).[119]

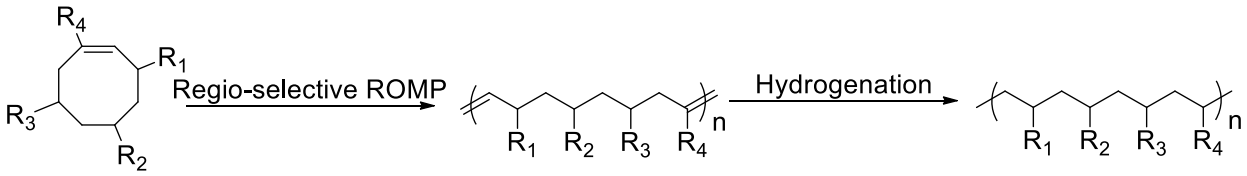

Figure 1-7. Proposed synthesis of sequence-specific polymers by regioselective ROMP of a multisubstituted cyclooctene ($R_1 \neq H$). Note that the substituents (except R1) could also be on other ring carbons and are not limited to the positions shown here. This figure was adapted from Zhang et al.[119]

Previously Song discovered that methyl cyclobut-1-ene carboxylate (Figure 1-6, Group III) undergoes ring-opening metathesis (ROM) when mixed with fast-initiating Grubbs catalyst **G4**, but does not further polymerize after forming the Ru enoic carbene due to electronic and steric effects.[104] He also found that the Ru enoic carbene ring-opens cyclohexene and provides a new

ruthenium alkylidene (Scheme 1-6). The new alkylidene ring-opens methyl cyclobut-1-ene carboxylate and regenerate the Ru enoic carbene while not reacting with cyclohexene. As a result, the alternating ring-opening metathesis activity enables two different monomers to propagate along the polymer chain in an equal ratio.[1] This pioneering discovery using ROMP to generate sequence-controlled polymers provided rigorous alternating dyads.

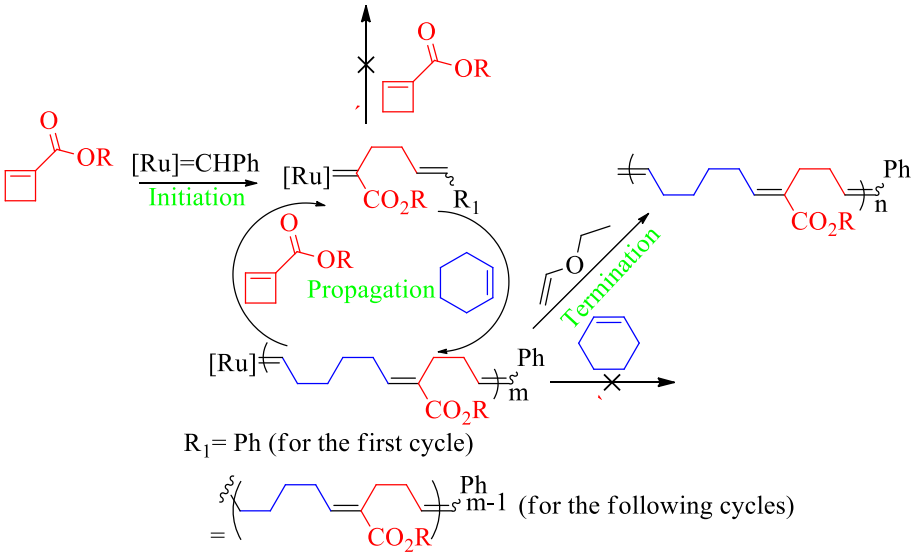

Scheme 1-5. Alternating ring-opening metathesis polymerization of methyl cyclobut-1-ene carboxylate and cyclohexene with Ru catalyst. This scheme was adapted from Song, et al.[1, 120]

1.4.3. Backbiting in AROMP.

In the purification of the alternating polymers, Song isolated a fraction that contained an AA substructure ("A" is defined as the cyclobutene counterpart, as indicated by a triplet at 6.8 ppm in Figure 1-8a). Further investigation suggested that this AA repeat was generated by backbiting to the unstrained olefinic bonds in the growing polymer chain during AROMP of the 1-substituted cyclobutene and cyclohexene. This significantly affects molecular weight (M_n) and

molar-mass dispersities of alternating copolymers, as well as the structure. The proposed mechanism of backbiting in this system is shown in Figure 1-8b. The much smaller experimental M_n values and the broad $Đ_M$s (Table 1-3) indicated that backbiting predominates and competes with the chain propagation of AROMP. GPC traces were also bimodal which supported this conclusion (Figure 1-8c).

a)

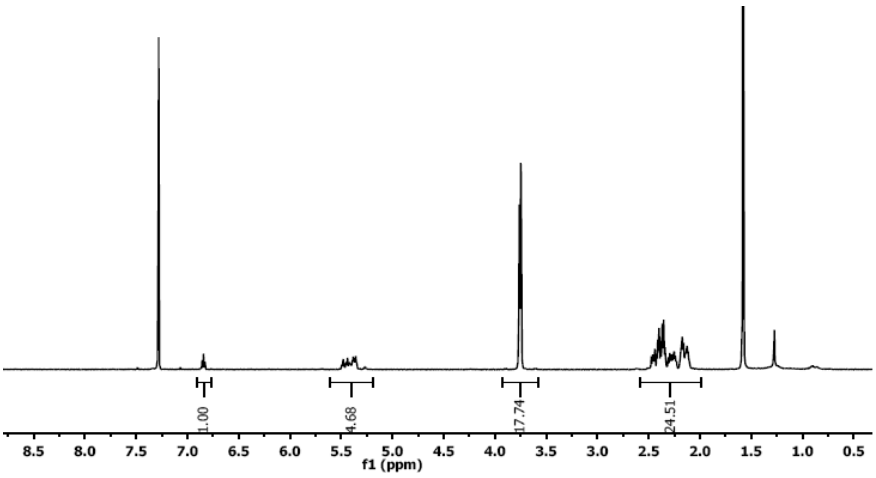

b)

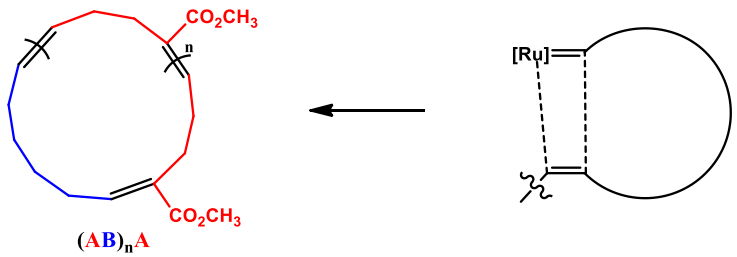

$(AB)_nA$

A: ring-openned cyclobutene
B: ring-openned cyclohexene

Backbiting happens only at the disubstituted olefin bonds

c)

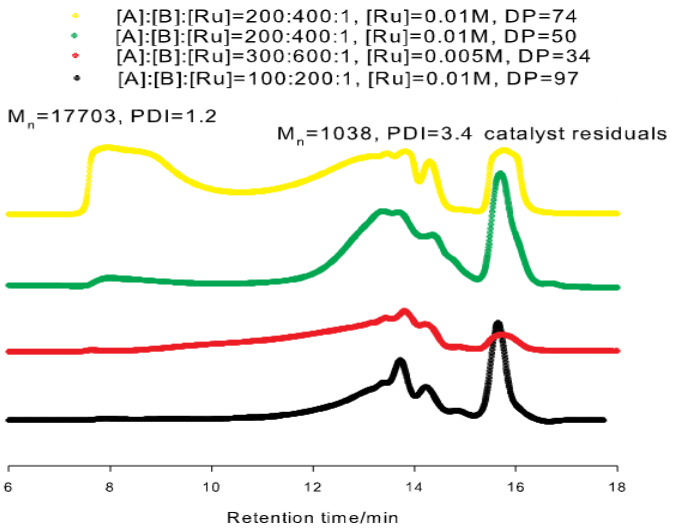

Figure 1-8. Backbiting evidence of poly(cyclobutene-1-methyl ester-*alt*-cyclohexene)$_n$. a) ^{1}H NMR spectrum of backbiting product in alternating copolymers. b) The formation of cyclic polymers by backbiting. c) Bimodal GPC traces of **AB** 100-mer and **AB** 200-mer. This figure was reprinted with permission from Song, et al; copyright 2009, Stony Brook University.[120]

Table 1-3. Alternating ring-opening metathesis polymerization of cyclobutene-1-methyl ester and cyclohexene. This table was adapted from Song, et al.[120]

[G4]	A:B:G4	%Con[a]	M_n^{Calcd}	M_n^{PSS}	M_w^{PSS}	$Đ_M$
0.01	10:20:1	98	2044	376	962	2.6
0.01	20:40:1	98	3984	668	1816	2.7
0.01	50:100:1	98	9804	652	2634	4.0
0.01	100:200:1	97	19504	1869	10872	5.8
0.01	200:400:1	50	29010	3201	18106	5.7
0.01	300:600:1	34	19504	1892	7181	3.8
0.01	200:400:1	74	29010	7749	18501	2.4

[a]Conversion of monomer was determined by ^{1}H NMR. [b]Molecular weights and $Đ_M$s were determined by GPC using polystyrene standards.

Efforts have been applied to minimize backbiting and the results are summarized in Scheme 1-7. Since backbiting can only take place at the disubstituted double bonds, Song employed 1-methylcyclohexene in anticipation that the steric effects of the 1-methyl group may slow down the chain transfer rate with the ruthenium carbene center. However, the styrene bond at the end of the polymer chain could still undergo intramolecular cross metathesis reaction. This was identified by a very low M_w and NMR analysis. The use of substituted cyclohexenes as well as different solvents including THF and benzene was also attempted without success. Catalyst screening including **G2**, **H2**, and Nolan's catalysts with an unsaturated N-heterocyclic carbene (1,3-bis(2,4,6-trimethylphenyl)imidazole) was applied in AROMP to no avail. Therefore, backbiting remains the biggest challenge in AROMP of 1-substituted cyclobutenes and cyclohexenes.

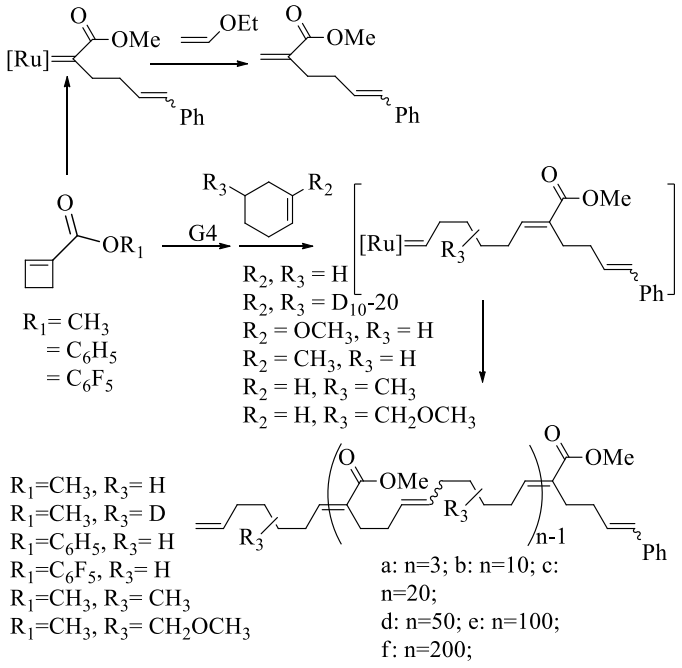

Scheme 1-6. AROMP of different monomers. This scheme was adapted from Song, et al.[120]

Chapter 2. Anti-Backbiting Studies and Linear Alternating Copolymer Syntheses via AROMP

2.1. Introduction

In recent decades, copolymers have been widely studied for their uses in the biomedical and material sciences.[13, 121, 122] Block copolymers, already established as thermoplastic elastomers, detergents, cosmetics and pharmaceutical preparations, promise to contribute to new applications based on nanoscale structures, membranes, and drug and gene delivery.[123] Much less explored are alternating copolymers. For applications in which two different polymer-borne moieties must interact[124-128] (e.g. as in organic light emitting diodes and solar cells), alternating copolymers should impose consistently optimal positioning of the participating substituents.

Alternating copolymers are generally synthesized by radical polymerization in which the alternating order of addition of monomers at the end of the growing chain is kinetically controlled.[129-131] However, the conditions required for radical propagation are not compatible with a number of functional groups that might be desired in the polymer target. Furthermore, with some exceptions,[132-134] such polymerizations are generally not "living." Therefore they do not afford polymer products with narrow molecular weight distributions (low molar-mass dispersities or $Đ_M$s) that are advantageous for certain applications.

Living polymerizations based on the functional group-tolerant ruthenium metathesis catalysts have the potential to provide alternating copolymers that have low $Đ_M$s and bear a

variety of functional groups. In metathesis, alternation of the incorporation of two monomers requires alternation of the affinities of the monomer **A** and monomer **B** to the living metal alkylidene. There are few solutions to this problem and consequently few examples of completely alternating metathesis copolymers. Rooney,[35, 101, 135] Chen,[36, 111-113] Blechert and Buchmeiser[114, 136, 137] have focused on the design of asymmetric catalysts that provide alternating selectivity for different pairs of monomers. Typically variation in steric bulk about the catalyst results in alternating reactivity of very strained and moderately strained, but more sterically demanding monomers. Despite impressive catalyst designs, more than a ten-fold excess of the moderately-strained monomer is required to maintain alternation.[112]

Monomer-design approaches take advantage of the different properties of two monomers such as polarity,[34] electron density and steric hindrance,[1] and acid-base interactions,[117] and in the latter two cases, provide perfectly alternating copolymers without use of excess monomer. Herein, we describe new pairs of monomers that generate, sequentially, two different ruthenium carbenes. One of these pairs efficiently provides completely alternating, linear copolymers.

We discovered that cyclobutene-1-carboxylate esters undergo ring-opening metathesis (ROM), but they do not undergo ROMP.[1] Nonetheless, in solution with cyclohexene (which also does not ROMP on its own), the cyclobutenecarboxylic esters participate in an alternating ring-opening metathesis polymerization (AROMP or *alt*ROMP). The high fidelity of the alternation in the chain extending steps can be attributed to the complementary reactivities of the two intermediate ruthenium carbenes.[138] There is a high kinetic barrier to cyclobutene ester homopolymerization and the low ring strain of the cyclohexene monomer does not overcome the entropic penalty for its homopolymerization.[1] Moreover, the substitution of the cyclobutene alkene provides regiochemical and stereochemical control of the polymerization.

The molecular weight homogeneity of the copolymers resulting from our cyclohexene/1-cyclobutene ester pair was limited by "backbiting" reactions, intramolecular cross metathesis that lead to the formation of cyclic polymers, shortened chains, and compromised molar-mass dispersities ($Đ_M$s). Indeed, we discovered that the use of the Hoveyda-Grubbs II catalysts, which favor cyclizations, resulted in the exclusive formation (within the limits of detection) of cyclic alternating copolymers.[139] Recently, we observed complete inhibition of backbiting upon introduction of bulky side chains into the AROMP monomers. However, the increased steric hindrance near the double bond slows the polymerization propagation rate resulting in shorter polymers, and thus, limits the utility of this approach.[126]

Cognizant of the desirability of high molecular weight linear polymers with narrow molecular weight distributions, we set out to find a pair of monomers that would give longer and linear AROMP polymers with low molar-mass dispersities. Here we report the results of this search to date.

2.2. Results

2.2.1. Design and Synthesis of Novel Monomers.

We noted that using Grubbbs III catalyst for the incorporation of rings into the propagating chain backbone limits backbiting in the case of the well-investigated norbornene ROMP.[140] Therefore we decided to examine norbornene ester **2** as a partner for cyclohexene in AROMP. We prepared monomer **2** (Figure 2-1) by a modification of the method of Elsheimer (see the Experimental Section).[141] However, when we subjected norbornene **2** to AROMP conditions with cyclohexene **6a**, we observed no polymerization. Furthermore, when the catalyst was mixed

with monomer **2**, no ring-opened product was observed at all. We attributed the loss of ROMP activity of monomer **2** to the steric hindrance posed by the bridging methylene group and the ester.

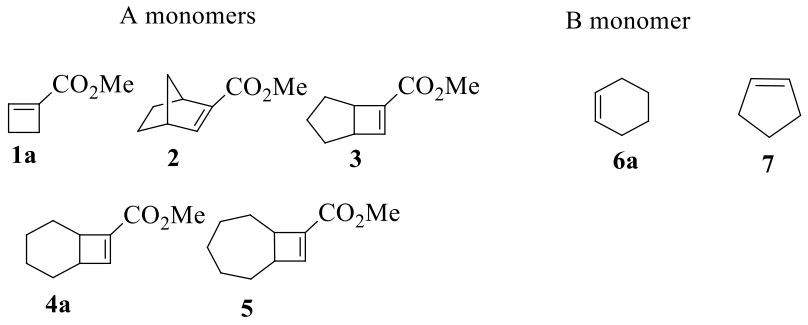

Figure 2-1. Cyclobutene and its cis bicyclic derivatives employed in alternating ring-opening metathesis polymerization for anti-backbiting study.

We next designed bicyclic monomers **3, 4a** and **5** (Figure 2-1) for their ring strain and lower steric hindrance around the alkenes. We first used [1,2-bis-diphenylphosphinoethane]cobalt (II) bromide ($Co(dppe)Br_2$) catalyzed [2+2] cycloaddition of alkenes and alkynes to provide bicyclic monomers. However, instead of getting target compounds, we observed signals indicating the [2+2+2] cycloaddition of the terminal alkynes.[142-144] Since terminal alkynes could undergo trimerization reactions in this condition, we decided to use an alternative route reported by Snider and Dang, et al, a Lewis acid catalyzed approach.[145] For practicality, we developed a simplified purification procedure for monomer **4a** to remove the isomeric by-product **4b** by subjecting the mixture to *m*-CPBA (Scheme 2-1). A white precipitate was observed indicating the formation of a peroxide of the by-product **4b**. The epoxide can be easily removed by suspending the reaction mixture in hexanes and followed by filtration.

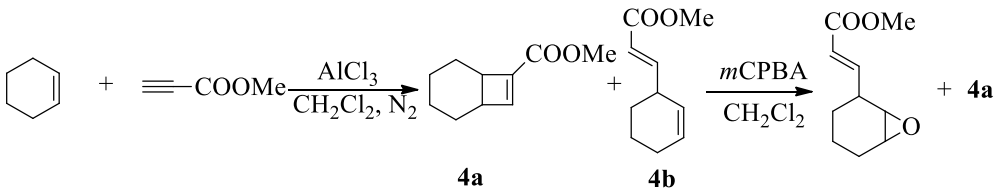

Scheme 2-1. Optimized scheme for the synthesis of bicyclic monomer **4a**.

2.2.2. Metathesis of Bicyclic Monomers.

2.2.2.1. Relative Kinetics of Ring-Opening Metathesis (ROM).

Based on ring strain values available,[38, 146-148] we predicted that the monomers we designed follow the order of **3** > **4a** > **5** > **1a**. First, we undertook kinetic monitoring of the initial ring-opening metathesis (ROM) reactions for each of these monomers by ^{1}H NMR spectroscopy and compared them with that of methyl cyclobutenene-1-carboxylate, **1a**. In each of the experiments, an equimolar amount of each monomer A (the bicycloalkene ester) and catalyst **G4** were mixed in CD_2Cl_2. The disappearance of the alkylidene signal of the catalyst at 19.1 ppm was followed by ^{1}H NMR spectroscopy, and was integrated relative to the methyl ester signals between 3.5-3.8 ppm (Figure 2-2). Under the conditions of the experiment, 50% of monomer **3** was ring opened in 25 minutes; whereas 50% of monomer **1a** was ring opened in 40 minutes. Under the same conditions, monomer **4a** underwent 50% ring opening in 100 minutes and monomer **5** required 300 minutes for 50% ring opening. Thus, upon addition of **G4**, monomer **3** has the fastest ring-opening rate, in accordance with the predicted ring strains. Notably, the fusing ring also poses steric hindrance to ROM, therefore, **4a** and **5** were found to ROM slower than **1a**.

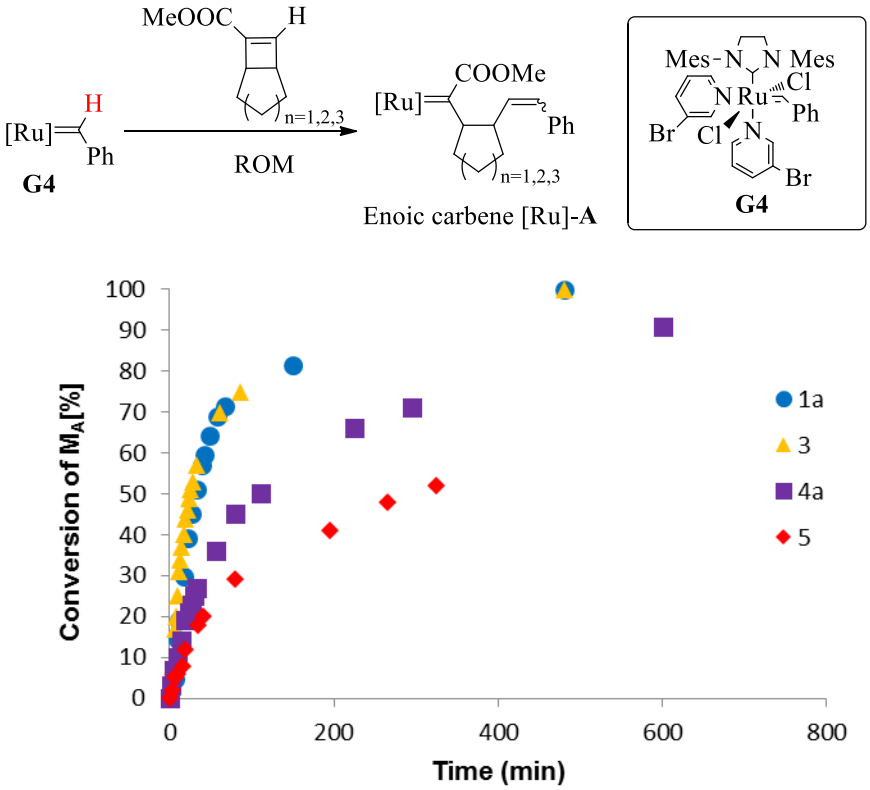

Figure 2-2. Kinetic monitoring of ring-opening metathesis of monomers **1a**, **3, 4a** and **5**. Monomer and **G4** were mixed in a 1:1 ratio, C = 0.03 M. Percent conversion was determined by ^{1}H NMR spectroscopy and integration of the Ru alkylidene α proton resonance at 19.1 ppm (in red) relative to methyl ester resonances between 3.5-3.8 ppm. $t_{1/2}$ were obtained from the plot, monomer **1a**: $t_{1/2}$ = 40 min, monomer **3**: $t_{1/2}$ = 25 min, monomer **4a**: $t_{1/2}$ = 100 min; monomer **5**: $t_{1/2}$ = 300 min.

2.2.2.2. Alternating poly(Cyclobutenes-Cyclohexenes)

When subjected to **G4** in the absence of cyclohexene **6a**, each of the three bicyclic monomers **3**, **4a**, and **5** underwent ring-opening; however, no polymerization could be detected. Thus, we established that these monomers are suitable for the preparation of alternating

copolymers because their rate of homopolymerization is zero. All three monomers produced copolymers with cyclohexene **6a** in the presence of **G4** (Table 2-1).

The lengths of the polymers were determined by integration of alkene proton signals relative to the phenyl end group in the ^{1}H NMR spectra. Copolymerization of monomer **3** or **5** with monomer **6a** yielded much shorter polymers than did monomer **4a** with **6a** under the same conditions (Table 2-1, entries 3 and 4 vs. entry 5). The rates of polymerization varied substantially and all were slower than the AROMP between cyclobutene **1a** and cyclohexene **6a** as determined by ^{1}H NMR spectroscopy. Take monomer **3** for example, though it has the fastest ROM rate, polymerization is very slow and only an **AB** 13-mer was obtained in a 24 hour reaction. Later on, we characterized the purified polymers by GPC and found polymers from AROMP of **4a** and **6a** provide smaller molar-mass dispersities than do cyclobutene **1a** (Table 2-2).

Table 2-1. AROMP applications of sterically hindered monomers with cyclohexene.

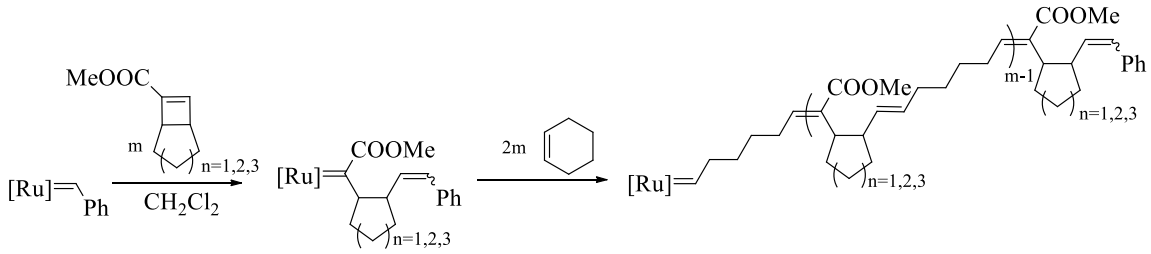

Entry	**A**	**B**	**[A]:[B]:[G4]**	Temp	Time (h)	%Conv[a]	$DP_{[AB]}$[b]
1	**1a**	**6a**	10:20:1	25 ℃	3	98	10
2	**2**	**6a**	10:20:1	25 ℃	3	0	---
3	**3**	**6a**	20:40:1	25 ℃	19	NA[c]	13
4	**3**	**6a**-D_{10}	20:40:1	25 ℃	8	80	6
5	**4a**	**6a**	20:40:1	25 ℃	8	96	17
6	**4a**	**6a**	20:40:1	35 ℃	8	97	16
7	**4a**	**6a**-D_{10}	20:40:1	35 ℃	8	85	15
8	**4a**	**6a**	50:100:1	35 ℃	8	68	34
9	**4a**	**6a**	50:100:1	60 ℃	2	72	36
10	**5**	**6a**	50:100:1	35 ℃	24	85	10

[a]Percent conversion determined by integration of ^{1}H NMR spectra of monomer **A** unless specified otherwise. [b]$DP_{[AB]}$ was determined by ^{1}H NMR with integration relative to the phenyl end group and represents the average numbers of **AB** dyads incorporated in linear copolymers. [c]%Conv could not be determined by ^{1}H NMR due to overlap of alkene and polymer peaks.

Table 2-2. Molecular weights and $Đ_M$s determined by GPC using polystyrene standards.

Entry	Polymer	Temp	M_n^{Calc}	M_n	M_w	$Đ_M$
1	poly(**4a**-*alt*-**6a**)$_{20}$	35 ℃	5064	10005	18855	1.8
2	poly(**4a**-*alt*-**6a**)$_{50}$	50 ℃	12504	14552	26512	1.8
3	poly(**4a**-*alt*-**6a**)$_{50}$	60 ℃	12504	11420	24936	2.1
4	poly(**3**-*alt*-**6a**-**D$_{10}$**)$_6$	25 ℃	1556	2046	7677	3.75
5	poly(**1a**-*alt*-**6a**)$_{50}$	25 ℃	9804	652	634	4.0

The AROMP of monomer **4a** with cyclohexene **6a** is limited by the polymer length with a maximum of 36 **AB** repeating units in attempts to obtain **AB** 50-mers (Table 2-2, entry 7 and 8) as a result of probably long reaction time which allows the decomposition of **G4** to occur. To address, we attempted replacement of cyclohexene with cyclopentene **7** to improve reaction rates (Table 2-3). All reactions proceeded faster than those with cyclohexene: monomer **1a**, **3** and **4a**

reached 100% conversion within 5 hours. Monomer **2** was still not able to react, so only a homopolymer of cyclopentene was observed. However, a cyclopentene homopolymer block was observed in all polymers before complete conversion of monomer **A**.

Table 2-3. AROMP applications of sterically hindered monomers with cyclopentene.

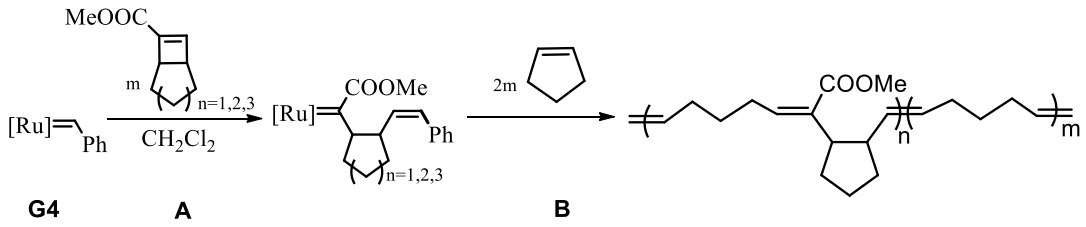

Entry	**A**	**B**	[**A**]:[**B**]:[**G4**]	Temp	Time (h)	%Conv[a]	$DP_{[AB]}$[b]
1	**1a**	**7**	10:20:1	25 ℃	3	100	10
2	**2**	**7**	10:20:1	25 ℃	3	NR	0
3	**3**	**7**	10:20:1	25 ℃	3	100	6
4	**4a**	**7**	10:20:1	25 ℃	5	100	9
5	**5**	**7**	10:20:1	25 ℃	3	60	5

[a]Percent conversion determined by integration of ^{1}H NMR spectra of monomer **A** unless specified otherwise. [b]$DP_{[\mathbf{AB}]}$ was determined by ^{1}H NMR with integration relative to the phenyl end group and represents the average numbers of **AB** dyads incorporated in linear copolymers.

In addition to cyclopentene, other additives were also applied to improve the propagation rate of monomer **4a**. Sanford and coworkers[93] reported that halide ligands around the Ru metal center have an effect on both k_i and k_p. Exchange of the chloride ligands for the less electronegative ligands results in the formation of species in which k_i is enhanced but at the expense of propagation rate. However, the effect is not drastic in case of bromide ligands. Rankin et al.,[149] for example, employed bromide counterions in the copolymerization of cationic *exo*-7-oxanorbornene derivatives and reported a promoted initiation of **G2** and smaller

dispersities. Hence, we included 1 equivalent of LiBr in methanol (relative to **G4**) in the AROMP of monomer **4a** and **6a**. However, in this case the propagation rate was significantly suppressed (Table 2-4, entry 1).

Methanol was used as a co-solvent to dissolve LiBr. Therefore, we tested AROMP without LiBr in pure methanol and observed no polymerization (Table 2-4, entry 2). It was assumed that the sp^3 hybridized oxygen in methanol coordinates to the Ru alkylidene. We then replaced methanol with tetrafluoroethanol (TFE), a less electron-rich alcohol. AROMP propagation was faster in TFE than in methanol, but still slower than without alcohols. The reaction was able to generate a short polymer (Table 2-4, entry 3). The inclusion of LiBr in TFE (Table 2-4, entry 4) suppressed propagation. The reaction only yielded an **AB** 1-2 mer. The AROMP system is extremely sensitive to structural changes in the catalyst; replacing chloride ligands with bromide ligands slows down propagation and was not able provide long polymers.

Table 2-4. AROMP trials with LiBr as a counterion in different solvents.

Entry	[a]Solvents	**A**	**B**	**[G4]**	**[A]:[B]:[G4]:[LiBr]**	Time (h)	$DP_{[AB]}$ [b]
1	MeOH/LiBr/CD_2Cl_2	**4a**	**6a**	0.01	10:20:1:0	3	NR
2	MeOH/CD_2Cl_2	**4a**	**6a**	0.01	10:20:1:0	3	NR
3	TFE/CD_2Cl_2	**4a**	**6a**	0.01	10:20:1:0	7	3
4	LiBr/TFE/CD_2Cl_2	**4a**	**6a**	0.01	10:20:1:1	7	1

[a]Solvent mixture was used to dissolve **G4** and LiBr. [b]$DP_{[AB]}$ was determined by ^1H NMR with integration relative to the phenyl end group and represents the average numbers of AB dyads incorporated in polymers.

Modifications on the Ru catalysts have provided new catalysts specialized for ROMP. There are reports of catalysts with improved propagation and some have very different steric requirements compared to **G4** (Figure 2-3). Curious as to their performance in AROMP, we applied them to both the poly(**1a**-*alt*-**6a**)$_n$ and the poly(**4a**-*alt*-**6a**)$_n$ reactions (Table 2-5). So far, no catalyst outperforms **G4** with regards to polymer length and propagation rate.

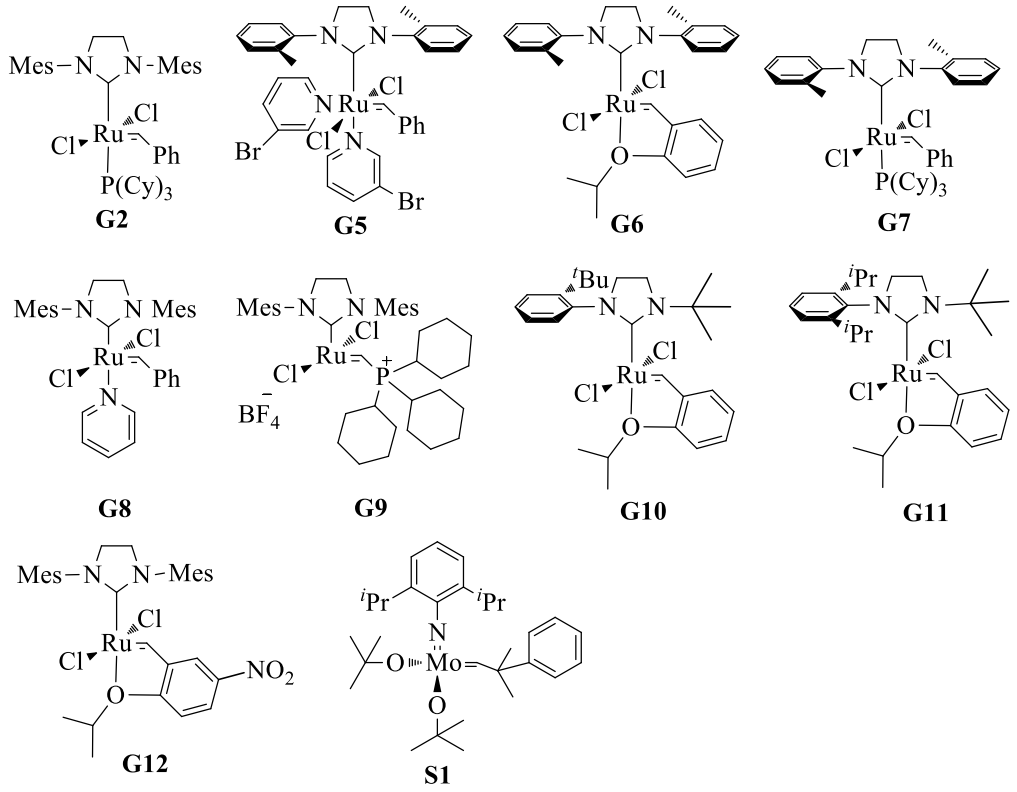

Figure 2-3. Catalysts utilized in our AROMP reactions to improve propagation rate.

Table 2-5. Utilization of other catalysts in AROMP of monomer **1a** or **4a** with cyclohexene **6a**.

Entry	[A]:[B]:[Ru]	Observations
1a	**4a**:**6a**:**G2**=50:100:1	Obtained a 35 mer with alternating sequence
2a	**4a**:**6a**:**G5**=10:20:1	Initiation 100% within 60 min, no polymerization

2b	**1a**:**6a**:**G5**=10:20:1	10mer with backbiting
3a	**4a**:**6a**:**G6**=10:20:1	10% initiation, no polymerization
3b	**1a**:**6a**: **G6**=10:20:1	10mer with backbiting
4a	**4a**:**6a**:**G7**=10:20:1	Initiation 100% within 60 min, no polymerization
5a	**4a**:**6a**:**G8**=10:20:1	10 mer, failed in making longer polymers
5b	**1a**:**6a**:**G8**=10:20:1	10mer with backbiting
6a	**4a**:**6a**:**G9**=10:20:1	1-2 mer was observed
6b	**1a**:**6a**:**G9**=10:20:1	10 mer with backbiting
7	**2**:**6a**:**G10**=10:20:1	No initiation was observed
8a	**4a**:**6a**:**G11**=10:20:1	Initiation but no polymerization
9a	**4a**:**6a**:**S1**=10:20:1	Initiation but no polymerization
10	**4a**:**6a**:**G12**=50:100:1	Obtained a 35 mer with alternating sequence

2.2.3. Other Attempts to Inhibit Backbiting in AROMP

AROMP of different **A** and **B** monomers has also been attempted (Scheme 2-2). We utilized methyl propiolate and methyl but-2-ynoate, respectively, as AROMP monomer **A** and cyclohexene as **B** in order to generate a conjugated double bond which is more rigid than [Ru]-cyclobutene to inhibit backbiting (route a-b). We observed a color change in the reaction which is considered to be evidence of catalyst activation, and also observed disappearance of the Ru alkylidene peak of **G4** in the ^{1}H NMR spectrum. However, no polymer was formed even in the cases for which the catalyst was initiated by ethylene or monomer **1a** before adding methyl propiolate (Scheme 2-2, route c-f). In Tam's work,[150] they proposed that terminal alkynes have a

strong affinity for ruthenium and can inactivate its activity by trapping the alkylidene. Although the structures of the catalysts are not identical, according to our observations, **G4** is very likely to be inactivated by the alkyne.

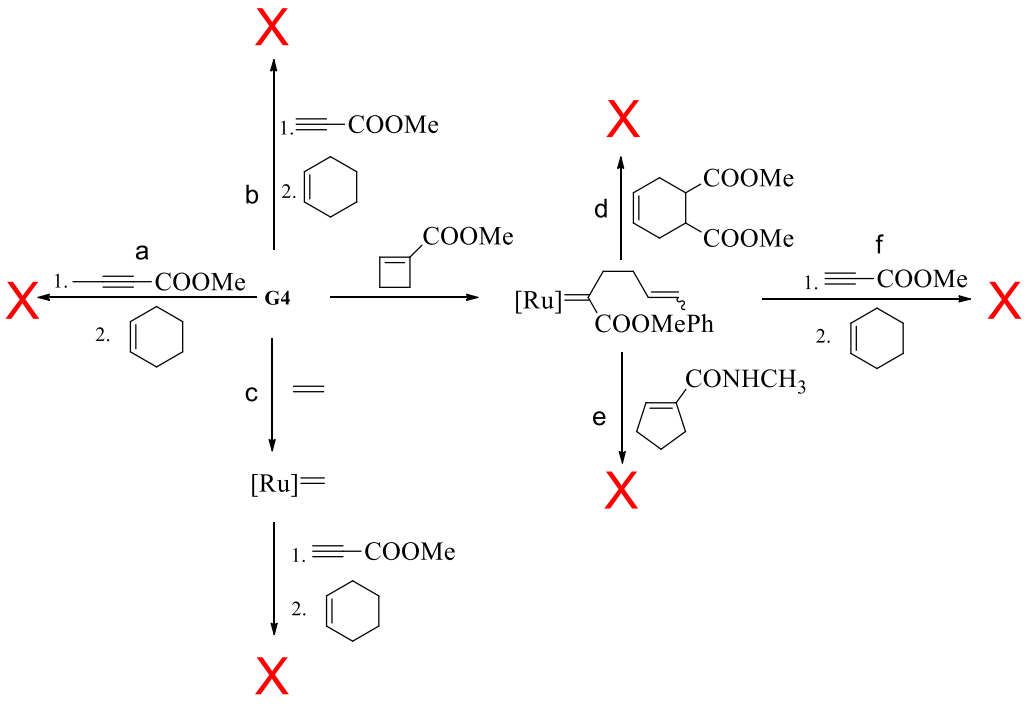

Scheme 2-2. Other monomers utilized in AROMP to prevent backbiting.

The effects of additives on the **1a** and **6a** AROMP were also investigated. There are reports of additives that coordinate with Ru and prevent backbiting, such as THF, pyridine, 2-NO_2-ArOH and triphenylphosphine.[32, 47, 92, 93, 151] These additives were tested at different concentrations ranging from 0.1 to 10 equivalents relative to the catalyst. Based on monitoring the integral of the intensity of the triplet signal from cyclic polymer, at low concentrations (<1 equivalent) no significant prevention of backbiting was observed whereas, at high

concentrations, additives inhibited propagation or even completely blocked the activity of the catalyst in the case of triphenylphosphine (Table 2-6).

Table 2-6. AROMP of **1a** and **6a** with additives.

Entry	Additive/equiv [a]	A	B	[**G4**]	[A]:[B]:[Ru]	Time (h)	$DP_{[AB]}$ [b]
1	Pyridine/0.1	**1a**	**6a**	0.01	20:40:1	6	18
2	Pyridine/1	**1a**	**6a**	0.01	20:40:1	8	18
3	Pyridine/10	**1a**	**6a**	0.01	20:40:1	10	18
4	2-NO_2-ArOH/0.1	**1a**	**6a**	0.01	10:20:1	12	8
5	2-NO_2-ArOH/1	**1a**	**6a**	0.01	20:40:1	12	18.5
6	2-NO_2-ArOH/3	**1a**	**6a**	0.01	10:20:1	12	9
7	Triphenylphosphine/1	**1a**	**6a**	0.01	10:20:1	3	NR
8	Triphenylphosphine/10	**1a**	**6a**	0.01	10:20:1	3	NR

[a]relative to the catalyst. [b]$DP_{[AB]}$ was determined by ^{1}H NMR with integration relative to the phenyl end group and represents the average numbers of AB dyads incorporated in linear copolymers.

2.2.2.3. Intrinsic Rates of Chain Propagation

We set out to explore the kinetics of the AROMP reactions of the bicyclic monomers and cyclohexene to explain why **4a** is a better monomer than **3**. Since AROMP is very fast, it is very hard to monitor the progress. Therefore, we carried out a simplified reaction AROM-1 (formation of **BA** dimer) of **A** and **B** monomers. In this experiment, we first mixed monomer **3**

or **4a** with **G4**; when **G4** reached >90% initiation determined by kinetic monitoring using ^{1}H NMR spectroscopy, 10 equivalents of cyclohexene was added.

We observed the appearance of a new signal at 19.0 ppm from [Ru]-**B**-**A** and obtained it intensity change as a function of time (Figure 2-4). The formation of [Ru]-**6a**-**3** is faster than that of [Ru]-**6a**-**4a**. After the initial phase, however, the concentration of [Ru]-**6a**-**3** reached a plateau before all [Ru]-**3** had turned to [Ru]-**6a**-**3**, then it started to decrease until it completely disappeared in 5 hours after addition of cyclohexene. Meanwhile, [Ru]-**6a**-**4a** was formed slowly but continued to grow even after [Ru]-**6a**-**3** had completely died. The experiment is strong evidence that [Ru]-**6a**-**4a** is much more stable than [Ru]-**6a**-**3**.

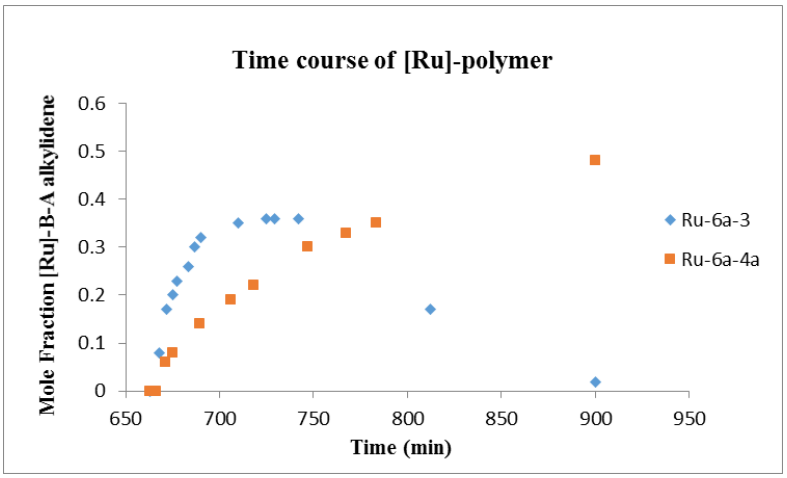

Figure 2-4. Kinetic monitoring of the Ru alkylidene in propagating polymers in AROM-1 of monomer **3** and **4a** with cyclohexene **6a**, respectively, by ^{1}H NMR. The alkylidene signals were integrated relative to signals from ester peaks between 3.5 -3.8 ppm.

Then we undertook kinetic monitoring of AROM with monomers **3** or **4a** and cyclohexene **6a** by ^{13}C NMR spectroscopy (Scheme 2-3). In both reactions, we observed formation of [Ru]-**A**

upon addition of the **A** monomer to **G4** (Figure 2-5, [Ru]+**3** and [Ru]+**4a**). In the case of [Ru]-**3**, two closely related species were produced (311.5 and 311.8 ppm). Addition of cyclohexene cleanly yielded [Ru]-**6a**-**4a** (338.0 ppm, Figure 2-5, [Ru]+**4a**+**6a**) in 1.5 hours, and there was no further change in the NMR spectrum over 30 hours. However, in the (**3**-*alt*-**6a**)$_1$ reaction, we observed regeneration of the **G4** (316.1 ppm) in addition to the [Ru]-**6a**-**3** carbene (337.8 ppm, Figure 2-5, [Ru]+**3**+**6a**) during the first 2 hours of reaction. Within 5 hours of cyclohexene addition, both the [Ru]-**6a**-**3** and Ru catalyst carbene resonances disappeared and no new carbene resonances appeared. We analyzed products of the AROM-1 reaction, and obtained Ph-(**3**-*alt*-**6a**)-Ph, *E*-stilbene and *cyc*-(**3**-*alt*-**6a**)$_1$.

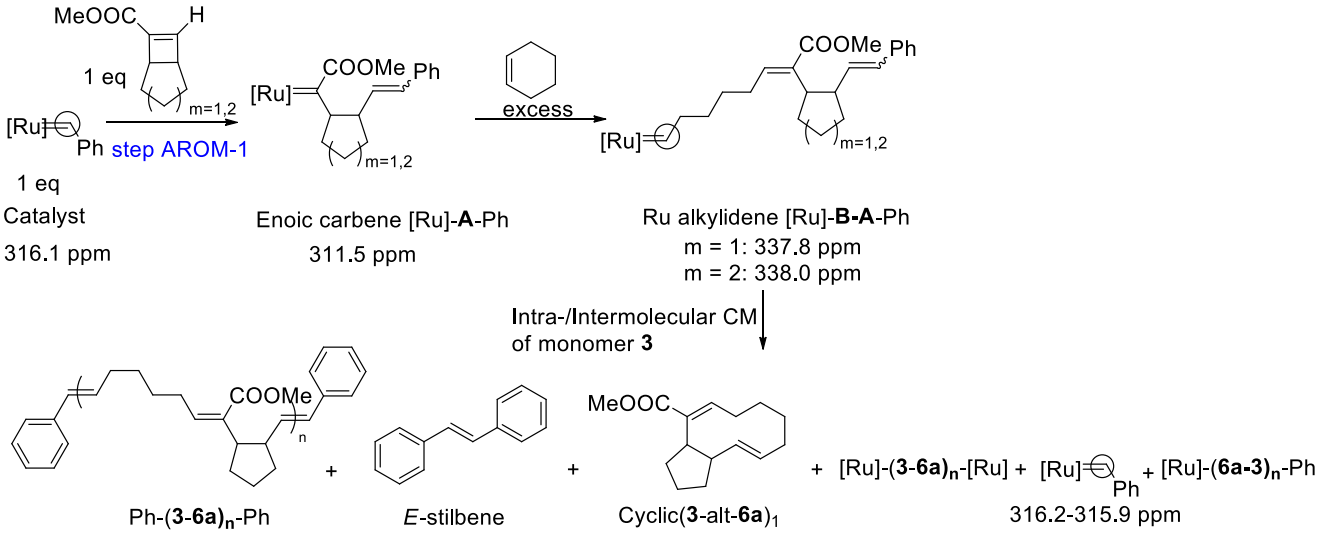

Scheme 2-3. Alternating ring-opening metathesis (AROM-1) of **3** or **4a** with cyclohexene to form BA dimer and proposed intra- and intermolecular cross metathesis for (**3**-*alt*-**6a**)$_1$. Carbenes (circled) were monitored by ^{13}C NMR spectroscopy.

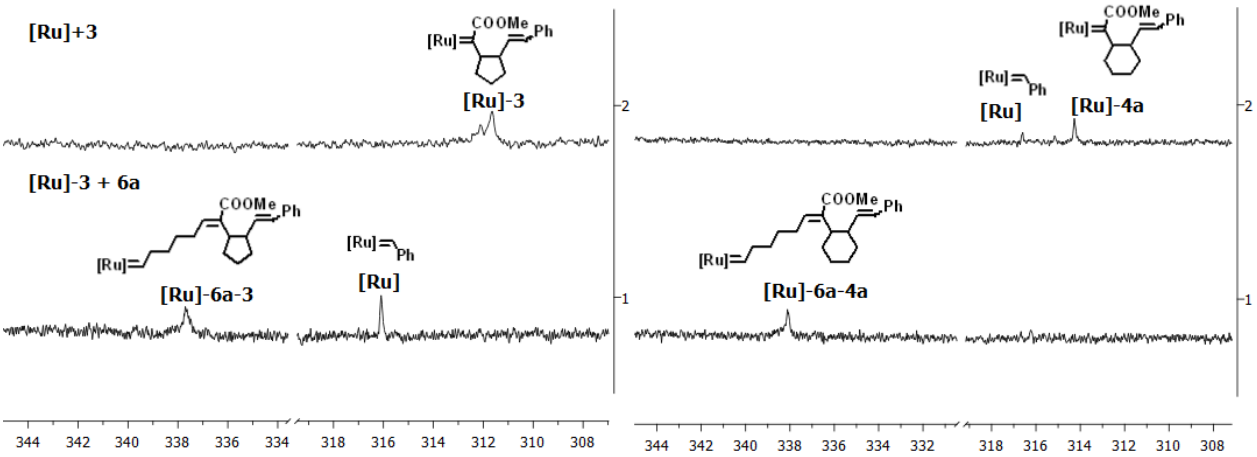

Figure 2-5. Alternating ring-opening metathesis (AROM-1) of monomers **3** and **6a**, and monomers **4a** and **6a**. The carbene regions of ^{13}C NMR spectra of (**3**-*alt*-**6a**)$_1$ (left) and (**4a**-*alt*-**6a**)$_1$ (right) are shown. In the [Ru]+**3** and [Ru]+**4a** spectra, [Ru] catalyst was mixed with **3** or **4a** in CD_2Cl_2 for 10-12 h. Cyclohexene was added after >90% of [Ru] catalyst was consumed as determined by ^1H NMR spectroscopy and the ^{13}C NMR spectra of [Ru]+**6a**+**3** and [Ru]+**6a**+**4a** were acquired after approximately 30-50 min upon addition of cyclohexene.

We also carried out double AROM (AROM-2) experiments with monomers **3** and **4a** to compare their behavior in systems with longer chains (Scheme 2-4a). In these experiments, we mixed monomer **A** and catalyst in a 1:1 ratio in an NMR tube to form [Ru]-**A**, and monitored the reactions by ^1H NMR spectroscopy. These mixtures were allowed to react for 10-12 hours to ensure nearly complete conversion to [Ru]-**A** (the benzylidene proton signal at 19.1 ppm was reduced to less than 10% of its original intensity). At this time, 10 equivalents of cyclohexene (monomer **B**) were added to generate [Ru]-**B**-**A**. The formation of [Ru]-**B**-**A** was monitored by the appearance of a new multiplet resonance at 19.0 ppm corresponding to the alkylidene proton. We found that cyclohexene **6a** reacts with ring-opened monomer **3** enoic carbene 1.5 times faster

($t_{1/2}$ = 28 ± 1 min) than with the corresponding enoic carbene from monomer **4a** ($t_{1/2}$ = 43 ± 5 min) (Scheme 2-4b). When the formation of Ru alkylidene ([Ru]-**B**-**A**) was complete as judged by integration of the resonance at 19.0 ppm, one equivalent of monomer **A'** was added to

a)

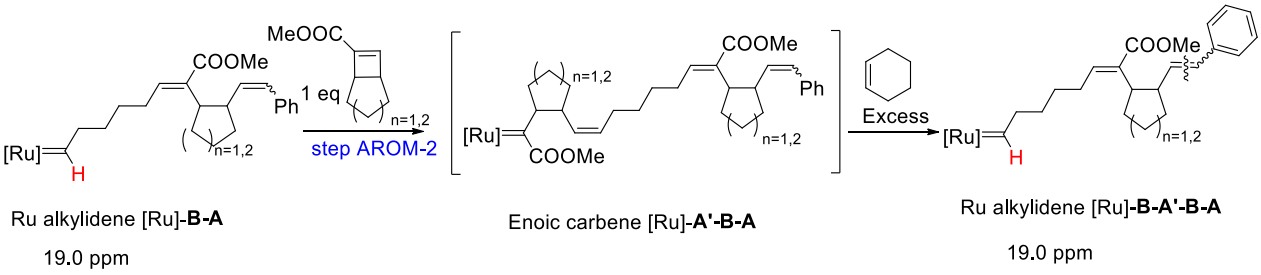

b)

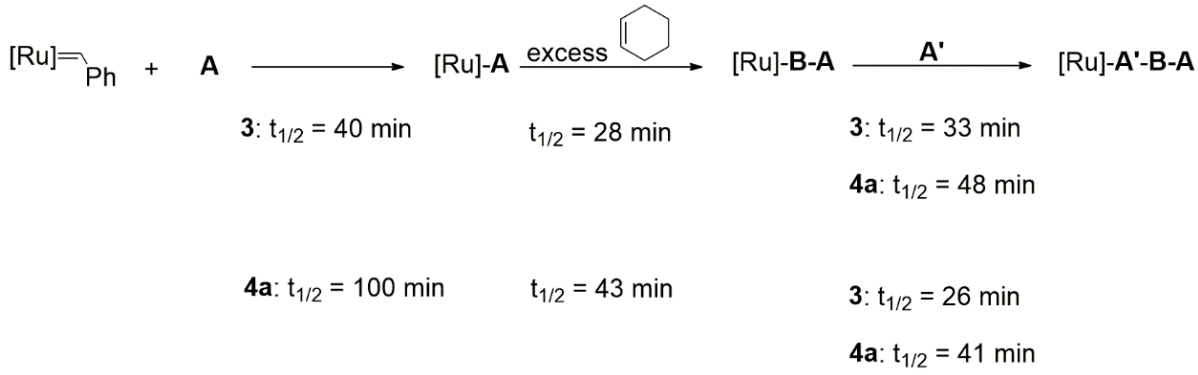

Scheme 2-4. Double alternating ring-opening metathesis (AROM-2). a) Mechanism of AROM-2 to form BA'BA tetramer. The proton resonances monitored are colored red (Figure 2-6). b) $t_{1/2}$ for each AROM-2 reaction step.

investigate the rate of ring-opening catalyzed by [Ru]-**B**-**A**. We examined all four cases of double ROM: ROM of **3** with [Ru]-**6a**-**3** and with [Ru]-**6a**-**4a**, and ROM of **4a** with [Ru]-**6a**-**4a** and with [Ru]-**6a**-**3**. The disappearance of the monomer **A'** alkene signal at 6.7 ppm and the [Ru]-**B**-**A** alkylidene signal at 19.0 ppm were monitored as a function of time. Both signals

disappeared at the same rate as measured by comparison of the integrals with that of the signal for ester peaks. We found that reaction of monomer **3** with [Ru]-**6a**-**4a** ($t_{1/2}$ = 26 ± 1 min) was 27% faster than its reaction with [Ru]-**6a**-**3** ($t_{1/2}$ = 33 ± 1 min). In the case of monomer **4a** reacting with [Ru]-**6a**-**A**, the rate of the reaction with [Ru]-**6a**-**4a** ($t_{1/2}$ = 41 ± 4 min) is 17% faster than the reaction with [Ru]-**6a**-**3** ($t_{1/2}$ = 48 ± 2 min). Moreover, oligomers containing ring-opened **3** as either **A** or **A'** failed to completely convert to [Ru]-**6a**-**A'**-**6a**-**A**, consistent with competing cross-metathesis reactions dominating the reaction.

Although the rates of the second ROM did not vary widely, the ROM reaction appears to be very sensitive to long range polymer structure, i.e., the presence of a five membered ring in the backbone one position removed from the living [Ru] species reduces the reaction rate of either bicyclic monomer with the unhindered [Ru]-alkylidene. The rates of reaction indicate that the backbone containing a six-membered ring (derived from [4.2.0] monomer) is superior to the backbone containing a five-membered ring (derived from [3.2.0] monomer) for propagating polymerization.

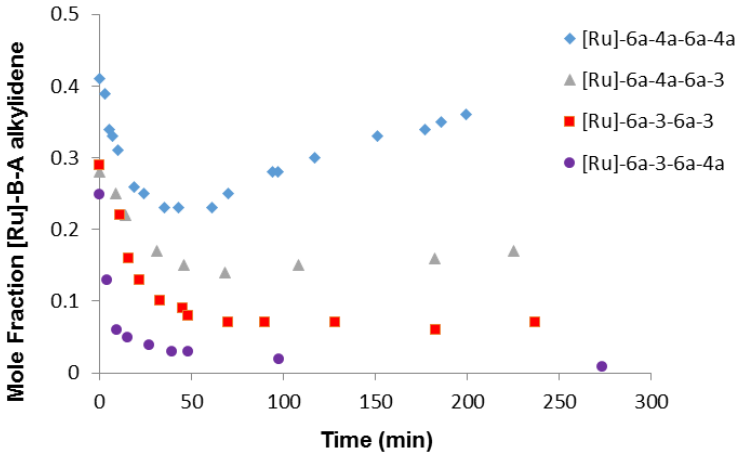

Figure 2-6. Kinetic monitoring of double ring-opening metathesis (AROM-2) reactions of

monomer **A** (**3** or **4a**) with [Ru]-**6a**-**A**. Time zero corresponds to the addition of one equivalent of monomer **A'** (**3** or **4a**) to one equivalent of [Ru]-**6a**-**A** in the presence of excess cyclohexene **6a**. Mole fraction of Ru alkylidene at 19.0 ppm was determined by integration of the Ru alkylidene resonance relative to the methyl ester resonances between 3.5-3.8 ppm. After 15-18 hours, only 30-42% of [Ru]-**6a**-**A** was generated due its instability and the extended reaction time in the first step.

2.3. Discussion

2.3.1. Relative Kinetics of Ring-Opening Metathesis (ROM).

The ring strains of our bicyclic monomers have not all been specially calculated but the relative strain energies can be inferred based on what has been published (Figure 2-7).[37, 38, 146] Thus, upon addition of **G4**, monomer **3** was predicted to have the fastest ring-opening rate and monomer **5** the slowest. The result is in accordance with our prediction (Figure 2-2). Monomer **3** has the shortest $t_{1/2}$ (25 min): it undergoes ROM even faster than monomer **1a** ($t_{1/2}$ = 40 min), despite the steric hindrance caused by the fused ring.[38, 146-148] Monomer **4a** was predicted to have a similar ROM activity to monomer **1a** based on the ring strains of the corresponding cycloalkanes. However, the steric hindrance posed by the cyclohexyl ring hampers the coordination and formation of the metallocyclobutane ring during metathesis and results in a slower ROM rate ($t_{1/2}$ = 100 min). Herein, we proposed that monomer **3** should AROMP the fastest and the fusing ring should inhibit backbiting of the disubstituted double bond along the polymer backbone during polymerization.

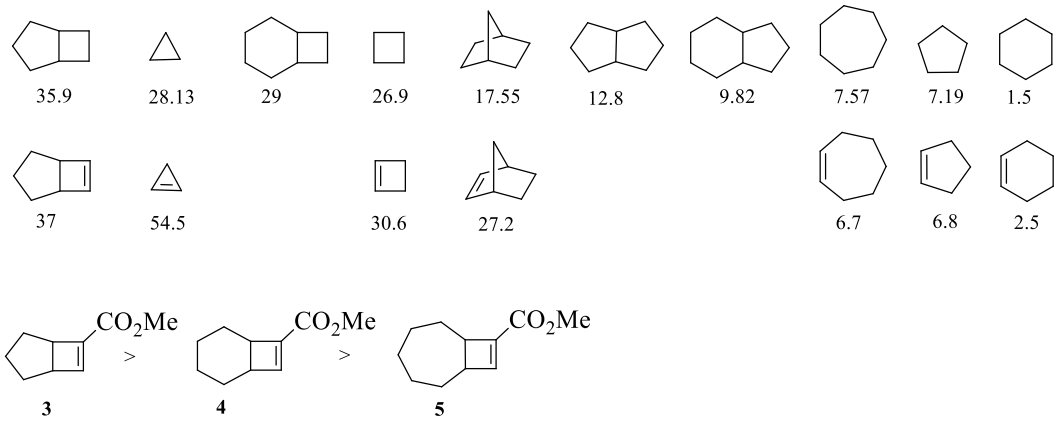

Figure 2-7. Ring strains of different cyclic alkanes and alkenes (kcal/mol).[37, 38, 146]

2.3.2. Alternating ROMP for poly(Cyclobutenes-Cyclohexenes).

The three bicyclic monomers **3**, **4a** and **5** produced copolymers with cyclohexene **6a** in the presence of **G4** (Table 2-1). However, the propagation did not proceed as fast as we had expected. The overall slower polymerizations of the bicyclic monomer in AROMP were rationalized by the steric hindrance introduced by the fused ring and the ROM products of bicyclic monomers are more rigid and steric than that of monomers **1a**, as a result, coordination and ROM of cyclohexene is slower in the former (Figure 2-8).

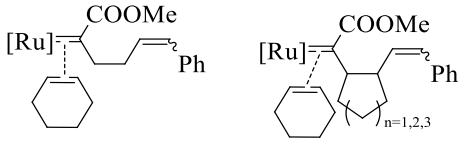

Figure 2-8. Coordination of cyclohexene with [Ru]-cyclobutene and [Ru]-bicyclic cyclobutenes.

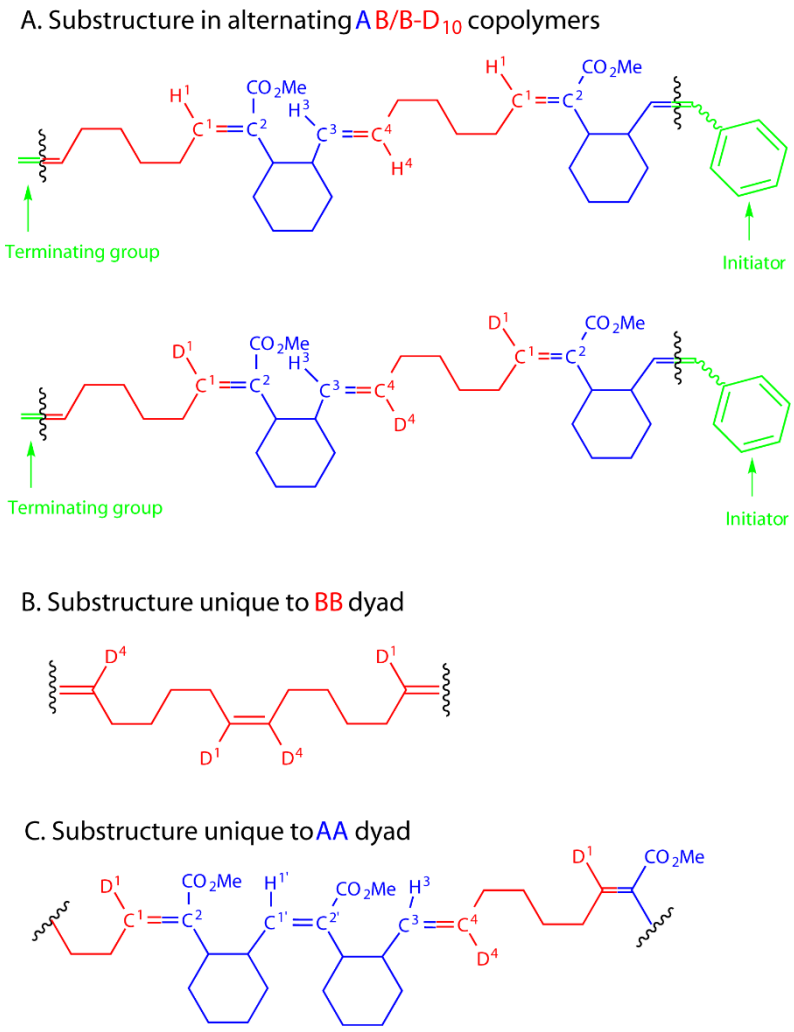

Figure 2-9. Possible substructures generated in the copolymerization of monomers **4a** (blue) with cyclohexene and cyclohexene-D_{10}, **6a-D$_{10}$** (red), respectively. Terminating group derived from ethyl vinyl ether and the initiator carbons are green.

The ^{1}H NMR spectrum of each of the polymers from AROMP of bicylic monomers with cyclohexene is consistent with an alternating backbone structure in which the olefin bearing the carbomethoxy substituent has an *E* configuration (Figure 2-9A). For example, in the spectrum of poly(**4a**-*alt*-**6a**)$_{13}$, the proton resonance for the carbomethoxy-substituted olefin (H1), which is

derived from the cyclohexene, has an identical integration to the H3 alkene resonance at 5.8 ppm derived from monomer **4a** (Figure 2-7a). Likewise, the analogous proton resonances in poly(**3**-*alt*-**6a**)$_n$ and poly(**5**-*alt*-**6a**)$_n$ have nearly identical integration values. Moreover, characterization of poly(**4a**-*alt*-**6a**)$_n$ by HSQC spectroscopy confirmed that the carbomethoxy-substituted olefin is a single stereoisomer; there is a single H1 signal, at 6.5 ppm that correlates with C1 (Figure 2-7b). Comparison of model compound chemical shifts with the H1 alkene chemical shift further confirmed the >90% of *E* configuration was obtained (Figure 2-7c).[103, 152]

Further evidence for the alternating structure was obtained for the poly*(***4a**-*alt*-**6a**)$_n$ copolymers using cyclohexene-$D_{10,}$ **6a-D$_{10}$**. ^{1}H NMR analysis of the deuterium labeled copolymer poly*(***4a**-*alt*-**6a-D$_{10}$**)$_n$ indicates a complete loss of the carbomethoxy-substituted olefin (H1) resonance at 6.5 ppm and the H4 alkene resonance at 5.3 ppm (Figure 2-7a). Complete loss of the H1 and H4 resonances upon deuteration is consistent with a rigorously alternating **AB** linear scaffold. Upon deuteration, the integrated ratio of H3 versus the methyl ester remains 1:3 suggesting that no **BB** dyads (Figure 2-9B) was formed. Likewise, the loss of H1 and H4 resonances indicates the absence of **AA** dyads (Figure 2-9C, between 7.0 - 6.5 ppm) that can form upon backbiting during the AROMP.[1] Therefore, introduction of a cyclohexyl ring fused to the cyclobutene provides access to linear, alternating copolymers.

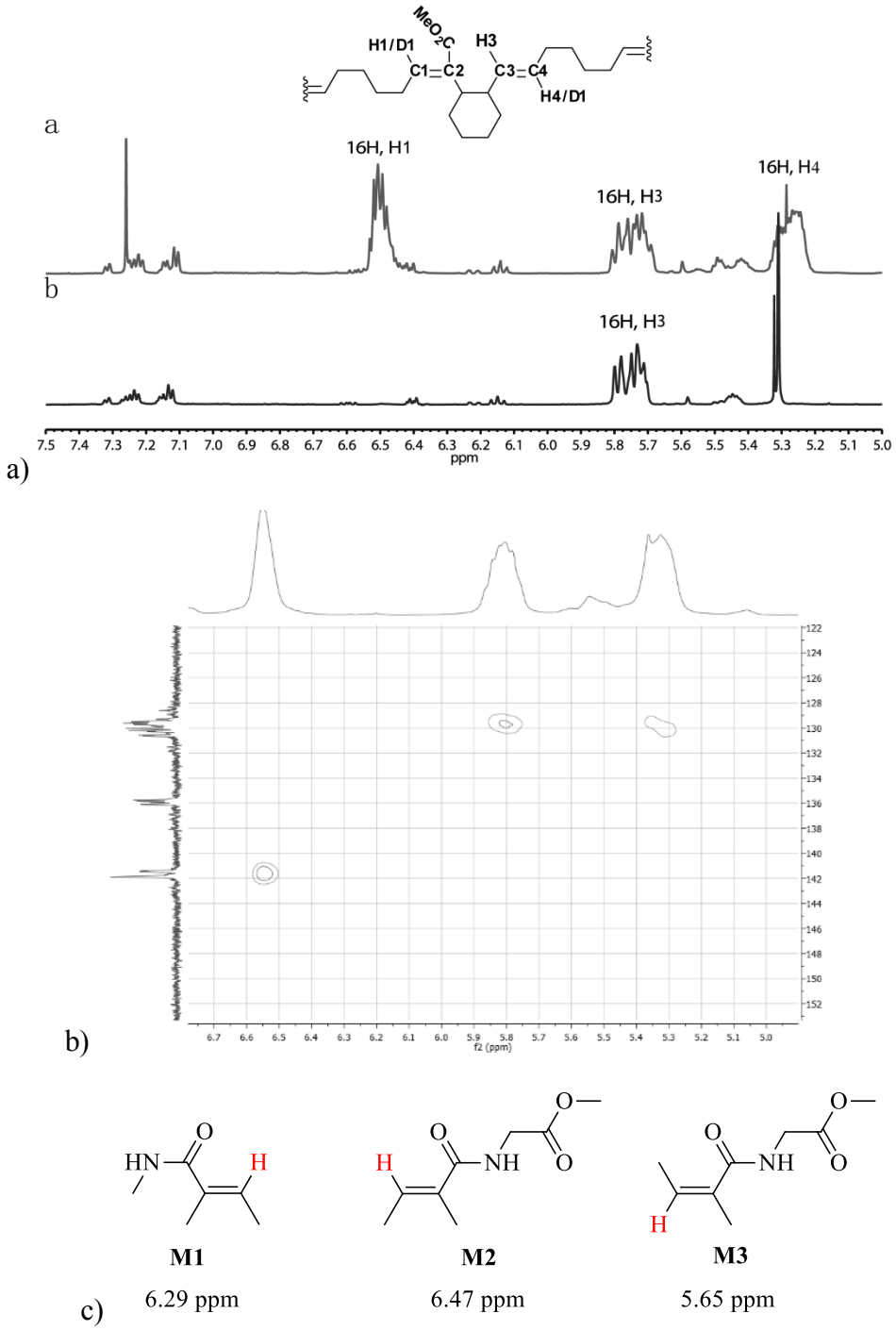

Figure 2-10. Structural analysis of poly(**4a**-*alt*-**6a**)$_n$. a) Top: ^{1}H NMR of poly(**4a**-*alt*-**6a**)$_n$. Bottom: ^{1}H NMR of poly(**4a**-*alt*-**6a**-**D$_{10}$**)$_n$. The region in which backbone olefinic hydrogen resonances of poly(**4a**-*alt*-**6a**)$_n$ appear is shown. Polymer product prepared from cyclohexene and dissolved in $CDCl_3$ with the ratio of H1:H3:H4 is 1:1:1; and polymer product prepared from

cyclohexene-D_{10} and dissolved in CD_2Cl_2 with the ratio of H1:H3:H4 is 0:1:0. poly(**4a**-*alt*-**6a**-**D_{10}**)$_n$ was dissolved in CD_2Cl_2 instead of $CDCl_3$ to allow accurate integration of the phenyl resonances. b) Alkene region of HSQC of poly(**4a**-*alt*-**6a**)$_{20}$ in CD_2Cl_2. c) Model compounds used for comparison to determine configuration of the polymer backbone.

All three monomers **3, 4a** and **5** produced rigorously alternating copolymers. However, at the same concentrations and monomer/catalyst ratios, monomers **3** and **5** both generate shorter polymers than did monomer **4a** (Table 2-1). Monomer **4a** provided provides polymers with up to 35-36 **AB** repeats. Reaction conditions of poly(**4a**-*alt*-**6a**)$_n$ were examined and the best yield was

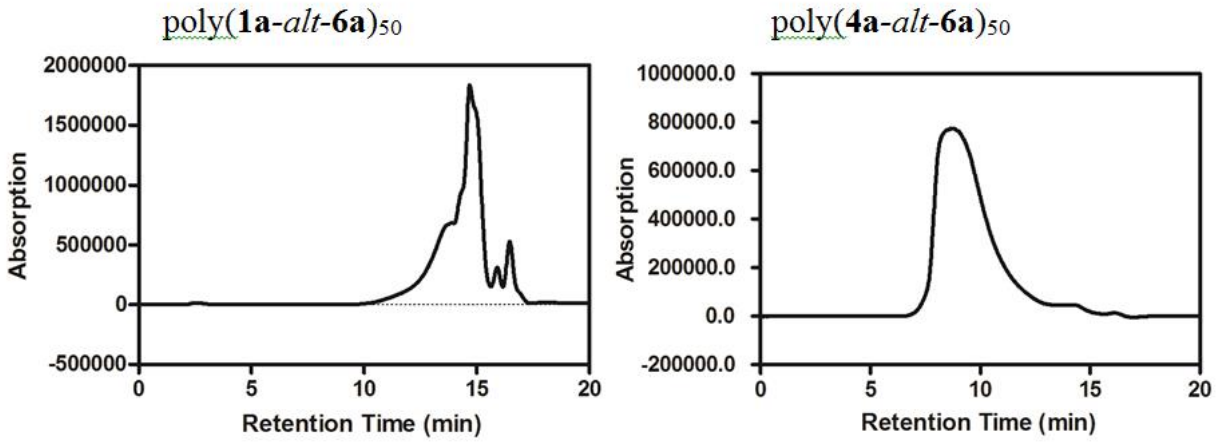

Figure 2-11. GPC traces of alternating copolymer poly(**4a**-*alt*-**6a**)$_{50}$ and the corresponding traces of poly(**1a**-*alt*-**6a**)$_{50}$, the length of the polymers were determined by the feeding ratio in AROMP.

obtained in CH_2Cl_2, at temperatures between 35-60 °C. Moreover, the GPC elution profile of poly(**4a**-*alt*-**6a**)$_n$ displayed a monomodal molecular weight distribution (Table 2-2 and Figure 2-11). This distribution is consistent with the absence of cyclic polymer. The dispersity ($Đ_M$ = 2.0 ± 0.1) of poly(**4a**-*alt*-**6a**)$_n$ are significantly smaller than that of the previously reported poly(**1a**-

alt-**6a**)$_n$, ($Đ_M$ = ~5) which display a bimodal molecular weight distribution. The molecular weight profile is consistent with the absence of intramolecular cross metathesis.

2.3.3. Intrinsic Rates of Chain Propagation.

We assumed monomer **3** would AROMP faster than **4a** and **5** monomers. However, **4a** is actually a better AROMP monomer. Therefore, we set out to explore the explanation of this aberrancy. Monomer **3** was selected in comparison with monomer **4a** in order to study their AROMP different activities in the metathesis reactions and how their structures affect the rates and the extents of polymerization. To preclude the possibility that impurities in monomer **3** inherited from synthesis deactivated the catalyst, monomer **3** was also treated with *m*-CPBA. It was utilized in AROMP and compared with monomer **3** synthesized otherwise. No difference in activity or polymer length was observed.

The result from analyzing the AROM-1 products lead us to believe that backbiting or cross metathesis occurred in the reaction. An independent experiment mixing **G4** with monomer **3** for 18 hours showed that [Ru]-**3** remains intact. Thus, the Ru enoic carbene is not reactive with itself, and side reactions must occur after cyclohexene addition. Formation of stilbene suggests that if the desired propagation pathway is kinetically less favorable, the Ru alkylidene ([Ru]-**6a**-**3**) species undergoes cross-metathesis intra- or inter-molecularly with the styrene end group of the **BA** dimer. In contrast, no regeneration of **G4** was observed in the (**4a**-*alt*-**6a**)$_1$ experiment (Figure 2-10, [Ru]+**4a**+**6a**). The [Ru]-**6a**-**4a** carbene remained stable for 2 days under the reaction conditions, consistent with our previous observations with monomer **4a** that it is able to provide a longer and backbiting-free linear alternating copolymer via AROMP.

We ascribe the differences in reactivity between oligomers derived from monomer **3** versus monomer **4a** to be due to the different dihedral angles between the *cis*-1,2 substituents of cyclopentane versus cyclohexane which are 20 - 40°, depending on the conformation, and 60°, respectively.[153-160] These dihedral angles determine the relative orientation of the two polymer chain ends as the backbone extends from the cyclic moiety. The orientation of the chain ends determines access to the [Ru]-alkylidene. If the chain ends are aligned, intramolecular cross metathesis will ensue, as is the case for AROMP of monomers **3** and **6a**. If access of the incoming monomer to [Ru]-alkylidene is hindered, the rate of propagation will be suppressed and the polymerization reaction unable to compete with cross-metathesis. Thus, despite the higher strain and inherent reactivity of monomer **3**, the resulting polymer backbone appears to hinder propagation and favor cross-metathesis, both of which lead to the premature termination of polymerization.

2.3.4. Alternating ROMP for poly(Cyclobutenes-Cyclopentene).

Cyclopentene was utilized in AROMP with bicyclic monomers to improve reaction rates (see Table 2-3). With a low ring strain of 6.8 kcal/mol, cyclopentene homopolymerizes slowly and has been used with norbornene to obtain alternating copolymers. In most cases, cyclopentene is used in a large excess relative to norbornene to overcome the reactivity difference. Therefore, we decided to use cyclopentene to replace cyclohexene and to investigate its behavior in AROMP. Alternating copolymers were formed as confirmed by ^{1}H NMR spectroscopy. However, we also observed homopolymerization of cyclopentene which dominated the reaction. Unlike AROMP using norbornenes, reaction of bicyclic monomers with **G4** is slow (refer to

ROM rate in Figure 2-2) which allows homopolymerization of cyclopentene to compete. As a result, alternating polymer blocks as well as homopolymer peaks were formed.

2.4. Summary

We screened different conditions to inhibit backbiting during formation of poly(**1a**-*alt*-**6a**)$_n$ including introduction of co-solvents, additives, catalysts and monomers with different electronic and steric effects and ring strains. We demonstrated that alternating copolymers are synthetically accessible via AROMP with bicylic carbomethoxy olefin monomers **3-5** and cyclohexene. Importantly, the AROMP-active monomers do not undergo self-metathesis regardless of monomer feed ratios or concentrations. Thus, formation of hompolymeric blocks, as is observed in other systems,[34, 111, 112, 118, 161, 162] does not occur in the **3, 4a** and **5/6a** AROMP system. Furthermore, monomer **4a** in which the cyclobutene ring is fused to a cyclohexane provides rigorously linear, alternating copolymers free of backbiting and cross metathesis. To our knowledge, this system is the first example of completely linear and alternating copolymers obtained by ruthenium-catalyzed ring-opening metathesis polymerization.

Chapter 3. Very Long, Linear Polymers from Tandem Isomerization/Alternating Ring-Opening Metathesis Polymerization (*i*-AROMP)

3.1. Introduction

Sequence-controlled polymers have the potential to provide high-density information storage [105]. In addition, the ability to define sequence offers control of folding and macroscopic properties like conductivity or rigidity.[163-165] Currently, polymer sequence is best controlled by utilizing nature's machines, which are themselves composed of sequence-controlled polymers. Although nature's approach can be coopted to introduce non-natural monomers, it is limited to biopolymer backbones, primarily polyamides and polyphosphosaccharides.[107] Therefore, synthetic chemists have sought ways to prepare more diverse structures. Iterative, stepwise synthesis is the most advanced method for controlling monomer sequence in a polymer, but lengths become limited by reaction yields and repeated purification steps. Application of chain or step growth polymerizations could overcome these challenges, but brings a new set of challenges in regulating sequence, namely ensuring that a single monomer type is incorporated at each position of the polymer.[107] ROMP has been shown to be of great potential to realize alternating sequence control.[1, 34-36, 101, 111-114, 117, 135-137] However, improvement is required for a higher accuracy of sequence alignment and/or monomer economics. Herein, we describe an efficient, synthetic, chain growth polymerization route to extremely long (MW > 100kDa) copolymers in

which the sequence of monomers is perfectly alternating, and one of the monomers bears functional groups.

Ring-opening metathesis polymerization (ROMP) is an attractive chain growth method that can be catalyzed by functional-group tolerant ruthenium complexes.[166-168] Cyclobutene-1-carboxylic acid derivatives exhibit selective reactivities in ruthenium-catalyzed ring-opening metathesis.[1, 126, 169] The ROMP of secondary amides of 1-substituted cyclobutenecarboxylic acid provides regioregular polymers that contain *E*-olefins and that have low molar-mass dispersities ($Đ_M$s) (Figure 3-1 and Table 3-1). Although neither a cyclobutenecarboxylic ester nor a cyclohexene undergoes ROMP on its own, the two copolymerize to produce precisely alternating copolymers.[1] This iterative process, enabled when the enoic Ru carbene produced in the initiation undergoes ROM with cyclohexene, provides a perfectly alternating copolymer in a single reaction. We named the process AROMP, for alternating ring-opening metathesis polymerization.

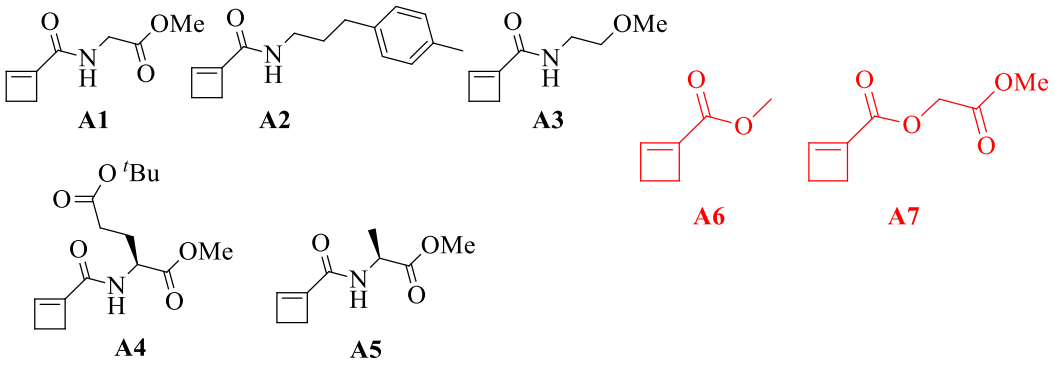

Figure 3-1. Cyclobutene monomers subjected to ROMP. Shown in black are secondary amides, and esters in red. Adapted from Song, et al.[104]

Table 3-1. ROMP results for cyclobutene monomers. The table was adapted from Song, et al.[104]

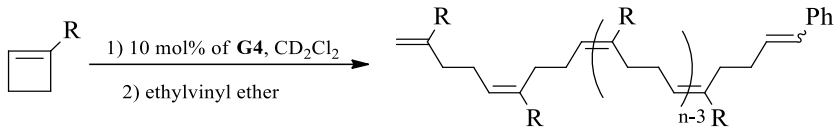

Entry	Monomer	% Conv.[a]	Rxn Time/h	t_{50}/min[b]	M_n^{Calc}	M_n[c]	M_w[d]	$Đ_M$
1	**A1**	93	3	3	1796	1835	2220	1.21
2	**A2**	97	6	3	1936	1820	2522	1.39
3	**A3**	85	3	4	1656	1349	1653	1.23
4	**A4**	94	4	3	3077	3483	4796	1.38
5	**A5**	96	6	3	2397	2222	3047	1.37
6	**A6**	10	3	∞[f]	n/a	n/a	n/a	n/a
7	**A7**	10	3	∞	n/a	n/a	n/a	n/a

General reaction conditions: CD_2Cl_2, 25 ºC, [monomer] = 0.1 M, [**G4**] = 0.01 M. [a]Determined by ^{1}H NMR spectroscopy. [b]Reaction time for 50% consumption of monomer. [c]Number-average molecular weight by GPC using polystyrene standards. [d]Weight-average molecular weight by GPC using polystyrene standards. [e]The reaction stops after 10% consumption of monomer.

The perfect alternation obtained in cyclobutene carboxylic acid/cyclohexene AROMP suggests interesting applications.[126, 170] However, the length of the resulting linear polymers is limited by intramolecular cross-metathesis (backbiting) reactions. In order to eliminate these chain shortening and cyclization reactions,[1, 139] we designed strained bicyclic olefinic esters as AROMP substrates.[169] We found that methyl bicyclo[4.2.0]oct-7-ene-7-carboxylic ester and cyclohexene provide linear, alternating copolymers without competing inter- or intramolecular cross-metathesis reactions, although their length was limited by slow propagation.

Recognizing the interesting architecture of polymers that contain cyclic moieties incorporated into their backbones, we tested the corresponding bicyclo[4.2.0]oct-7-ene-7-

carboxamides **8** (Scheme 3-1) in ROMP reactions with **G4**. We expected that they would yield regio- and stereoregular polymers with low molar-mass dispersities, as did the polymers derived from 1-substituted cyclobutenecarboxylic acid secondary amides (Scheme 3-1, **8** ⇨ poly (**8**)).

To our surprise, under ROMP conditions, amides **8** isomerized to the more stable bicyclo[4.2.0]oct-6-ene-7-carboxamide olefin **8'** (Scheme 3-1). On the other hand, amide **9** underwent minimal isomerization under the same conditions. None of the amides showed evidence of polymerization with the **G4**.

Opportunely, addition of cyclohexene **6a** to amides **8'** in the presence of catalyst **G4** (i.e. to the reaction mixtures from amides **8**) provided a reaction manifold for the isomerized amides that yields linear, alternating copolymers, poly(**8'**-*alt*-**6a**)$_n$, of great length. We now refer to this tandem reaction as *i*-AROMP for isomerization, alternating ring-opening metathesis polymerization.

3.2. Results

3.2.1. Design and Synthesis of Monomers

Synthesis of Monomers. Bicyclo[4.2.0] and [3.2.0] esters were synthesized by a modification of Snider's approach[145] using $AlCl_3$ catalyzed [2+2] cycloaddition.[169] Basic hydrolysis provided the carboxylic acids that were coupled to selected amines to yield amides **8a-8f** and **9**. Diastereomers **8f** and **8f*** were prepared from the mixture of racemic bicyclo[4.2.0]oct-7-ene-7-carboxylic acid (Figure 3-2) and (*S*)-phenylglycinol, separated, and then, individually acylated. Relative stereochemistry was not assigned to the diastereomers.

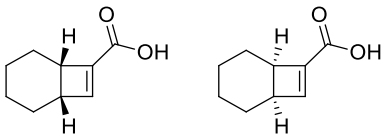

Figure 3-2. Racemate of bicyclo[3.2.0]hept-6-ene-6-carboxylic acid.

3.2.2. Attempted ROMP of Bicycloamides.

We submitted the bicyclic monomers to ROMP conditions with catalyst **G4** (Scheme 3-1). The bicyclo[4.2.0] amides underwent rapid reaction. Upon mixing amides **8a-8f** with catalyst **G4**, the olefinic proton signals at ~6.7 ppm disappeared or nearly disappeared (Figure 3-3a and b) within 15 minutes to 24 hours. However, no polymerization could be detected. In contrast, when amide **4** was stirred with catalyst **2** for 18 hours at 25 °C, only a 2% decrease in the intensity of the olefinic resonance was observed. We attributed the lack of polymerization to steric hindrance from the cyclopentyl ring as the two substitutions are closer in a cyclopentyl ring than that in a cyclohexyl ring as a result of dihedral angles.

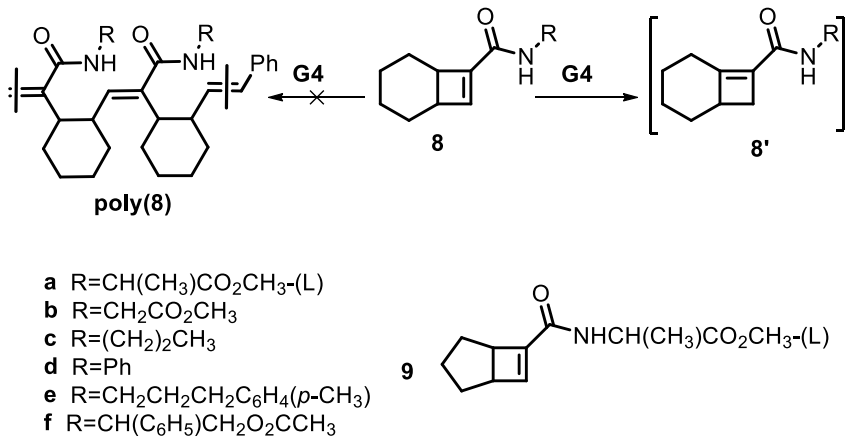

Scheme 3-1. Reaction of bicyclic cyclobutene derivatized amides and cyclohexene **6a** in the presence of **G4**.

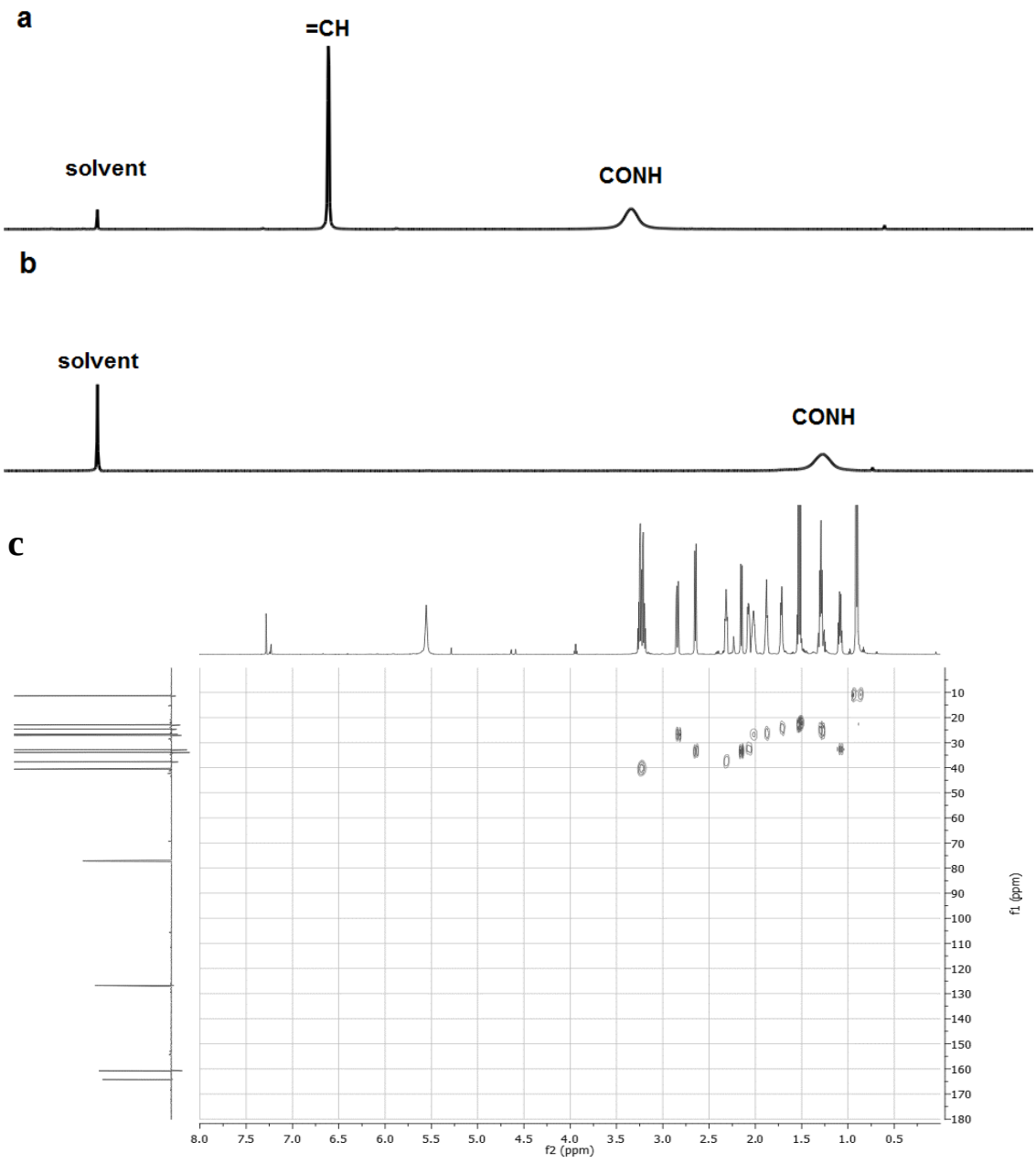

Figure 3-3. ^{1}H NMR spectra of bicyclic trisubstituted α,β-unsaturated secondary amides undergo isomerization in the presence of **G4.** a) Alkene and aromatic region of monomer **8c** in $CDCl_3$. b) Alkene and aromatic region of formation of the tetrasubstituted isomer of **8c'** with **G4** in CD_2Cl_2. Disappearance of the alkene proton, shift of the amide proton and the loss of symmetry in the upfield can be observed. c) HSQC of **8c'**.

Monomers **8c** and **8d** were selected for further study. Purification of the reaction products yielded compounds **8c'** and **8d'** with molecular masses identical to those of the starting materials. The spectroscopic signatures of **8c'** and **8d'** were distinct from **8c** and **8d** indicating that isomerization had occurred. No ring-opened products could be detected. Relative to the spectra of the starting materials, those of **8c'** and **8d'** contained an additional methylene proton signal, one less methine signal, and no olefinic proton resonance (Figure 3-3a and b). Further spectroscopic characterization by HSQC NMR spectroscopy of **8c'** indicated that it retains the bicyclic structure of **8c**, but the olefinic proton had disappeared and the double bond had migrated (Figure 3-3c). Amide **8d'** is the analogous product of double bond migration. Likewise, the crude reaction ^{1}H NMR spectra of amides **8a**, **8b**, **8e**, **8f,** and **8f*** mixed with catalyst **G4** are consistent with their respective isomerization to **8a'**, **8b'**, **8e'**, **8f'** and **8f*'**.

3.2.3. Scope of Isomerization

Cyclobutenes are sensitive to acid-catalyzed decomposition and/or reaction. In order to exclude the possibility that substrates **8** were being converted to isomers **8'** by adventitious acid, the monomers were repurified by passing through dry basic alumina and subjected to **G4**. The isomerization rates and products were unchanged. Furthermore, no isomerization was observed upon incubation of **8c** in CH_2Cl_2 at 35 °C for 16 hours in the absence of **G4**.

Typically tetrasubstituted olefins are not obtained with catalyst **G4**.[171-174] However, by analogy with the unsubstituted bicyclic olefin [4.2.0] system,[175] isomer **8'** is approximately 4-5 kcal/mol more stable than isomer **8**. Further isomerization to the bicyclo[4.2.0]oct-1(2)-ene-8-carboxamide is unfavorable because this alkene is not in conjugation with the amide. By analogy

with the smaller, unsubstituted bicyclic olefin [3.2.0] system, isomer **9** is 9-11 kcal/mol more stable than isomer **8'**,[175] and regioisomer **8'** is not formed. Thus, the **8'** regioisomers formed upon addition of catalyst **2** are the thermodynamically-preferred products of isomerization.

The isomerization of **8** with a range of amide substituents proceeds nearly quantitatively with a catalytic amount of **G4** (Table 3-2). Over the course of our experiments, we utilized four different batches of **G4**. All four preparations of **G4** catalyzed isomerization to the same extent and at the same rate.

The isomerization rate is slower for amides of substituted amines, i.e **8b** > **8a** > **8f**. In addition, inclusion of an ester in the alkyl chain of the amide reduces the isomerization rate, i.e. **8c** > **8b**. The anilide **8d** isomerizes three times faster than the unhindered alkyl amide **8c**. To investigate further the electronic influence on isomerization, a control experiment was undertaken to establish the amount of isomerization with the corresponding methyl bicyclo[4.2.0]oct-7-ene-7-carboxylate, **4a**. When subjected to catalyst **G4** (2 mol%) at 50 ºC for 2 days, the ester only underwent ROM without isomerization as judged by the chemical shift of the product ester and the disappearance of the catalyst alkylidene proton signal. Therefore, the amide moiety assists rapid equilibration of isomers of **8** in the presence of **G4.**

Table 3-2. ROMP results of bicyclic α, β-unsaturated secondary amides by catalyst **G4**.

entry	**8**	[**8**]:[**6a**][a]	time(h)	% conv[b]
1	**8a**	20:1	16	90
2	**8b**	50:1	8	95
3	**8c**	50:1	1.5	100
4	**8d**	20:1	0.3	100
5	**8e**	50:1	6	100
6	**8f**	10:1	24	70
7	**8f***	10:1	24	90
8	**4**	20:1	18	2

[a]Two stereoisomers of **8f/8f*** were isolated and subjected to ROMP respectively. [b][**G4**]=0.01M, CD_2Cl_2, 35 ºC. [c]Conversion was determined by tracking the monomers in ^{1}H NMR spectra.

3.2.4. Alternating Ring-Opening Metathesis Polymerization of *i*-Amides.

On the basis of our monitoring **1e** isomerization by ^{13}C NMR spectroscopy, we postulated that upon formation of **8'**, and that the amide-substituted carbene derived from 8' does not undergo metathesis with the remaining monomer. We reasoned, by analogy to the reaction of Ru enoic carbenes in our previous AROMP work,[1, 126, 169] that the enamide carbene might undergo AROMP with cyclohexene **6a**. Indeed, copolymer was rapidly formed upon addition of cyclohexene **6a** (Table 3-3). The AROMP monomers **8c** and **8d** with **6a**, yields a 50-**AB**-mer in approximately 2 hours which is faster than 1-cyclobutene carboxylic methyl ester/cyclohexene AROMP.[1]

Table 3-3. Alternating copolymerization of bicyclic amides and cyclohexene via ROMP by catalyst **G4**.

entry	**A**	[**A**]:[**3**]:[**2**]	time (h)	% conv[a]	$DP_{[AB]}$
1	**1c**	10:20:1	1.5	100	10
2	**1c**	50:100:1	2	100	49
3	**1c**	100:200:1	2	100	97[b]
4	**1c**	500:1000:1	6	85	424[b]
5	**1d**	50:100:1	1	100	50[c]

[a]Conversion was determined by monitoring the disappearance of the amide resonance in **8**. [b]Degree of polymerization (DP_n) was determined for the **AB** repeat by integration of polymer resonances relative to the styrene end group. [c]The DP_n could not be determined due to spectral overlap and was estimated from the feed ratio of **8d** and catalyst **G4**.

3.3. Discussion

3.3.1. ROMP/Isomerization of Amides, Identification of Culprit for Isomerization

Previous reports[176-179] of ruthenium-catalyzed alkene isomerization proposed that a Ru hydride species species[46, 63, 180-182] or a π-allyl Ru complex[63, 183-186] is responsible for alkene isomerization (Figure 3-4). The Ru hydride can form upon decomposition that occurs with extended reaction times or extreme reaction conditions.[177, 178] The rapid isomerization rates we observe are inconsistent with the formation of Ru hydride species that typically requires extended reaction times. Moreover, we never observed Ru hydride resonances at the expected upfield region between 0 and -30 ppm in the ^{1}H NMR spectra of the above reactions. Nevertheless, we tested whether 1,4-benzoquinone, which has been reported to oxidize ruthenium hydride species and prevent olefin isomerization,[187] would influence the

isomerization. However, addition of 1,4-benzoquinone did not suppress isomerization of amides **8e**. Therefore, a reduced, electron-rich species is unlikely to be responsible for isomerization.

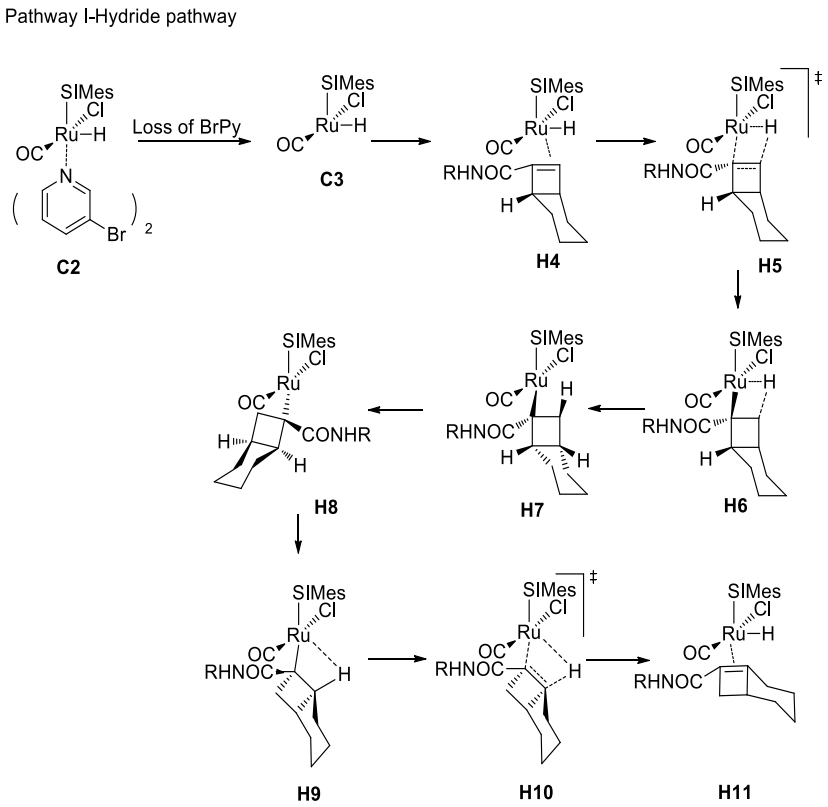

Figure 3-4. Possible hydride pathway for isomerization of bicyclo[4.2.0]oct-7-ene-7-carboxamides.

Next, we tested isomerization of **8c** with and without methanol in the presence of 10 mol% of **G4**. A coodinating solvent, such as methanol, can act as ruthenium reducing agent to enhance Ru hydride formation[183] or its coordination with Ru can suppress isomerization that proceeded via a π-allyl mechanism.[184, 188, 189] The **8c** isomerization reaction containing 8% methanol in CD_2Cl_2 proceeded much more slowly than the reaction without methanol; only 65%

isomerization was observed over 24 hours as compared to complete isomerization in 1.5 hours in the absence of methanol.

We also examined the effect of low concentrations of methanol (0.1-1 equivalent relative to catalyst **G4**). In these experiments, there was no observable effect on the isomerization rates. Moreover, we never observed Ru hydride resonances at the expected upfield region between 0 and -30 ppm in the ^{1}H NMR spectra of the above reactions.

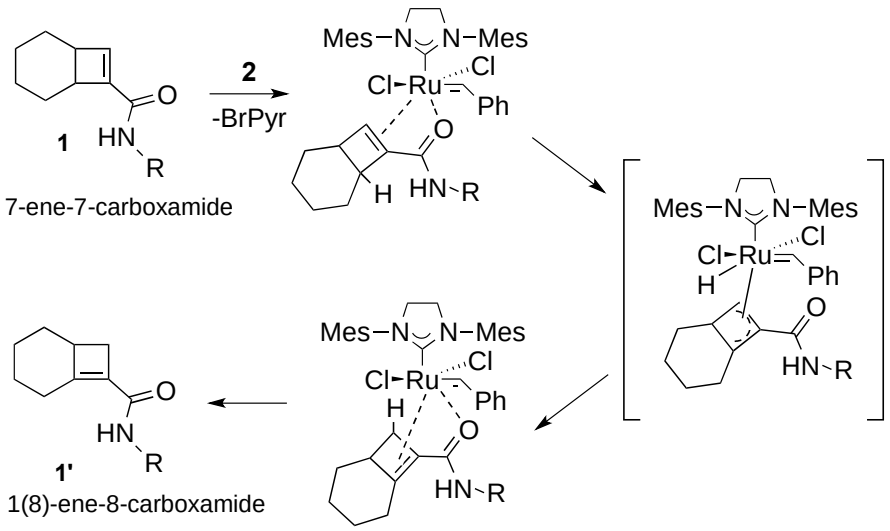

Scheme 3-2. Proposed π-allylic isomerization of amides **8** to **8'**.

Therefore, we conclude that the isomerization process does not require Ru hydride. Our observations are consistent with isomerization via a π-allyl Ru complex formed upon coordination of amide **8** with catalyst **G4** (Scheme 3-2). The conjugated amide increases the acidity of H8, and promotes oxidative addition of the allylic C8-H8 bond relative to a simple allylic system. Furthermore, dissociation of one or both pyridyl ligands to form an electron deficient Ru species will enhance coordination with **8**. Consistent with this hypothesis, addition of 50 equivalents of 3-bromopyridine to amide **8e** and catalyst **G4** to disfavor ligand dissociation

reduced the percentage of isomerization 3-fold over a 14-hour time period as compared to isomerization in the absence of exogenous 3-bromopyridine. Likewise, we found that 10 mol% of $(Cl)_2(H_2IMes)(PCy_3)Ru=CHPh$, for which PCy_3 ligand dissociation is less favored, catalyzed less than 5% isomerization of amide **8e** in 14 hours as compared to 100% conversion with 10 mol% catalyst **G4** within 1 hour under the same conditions.

Normally, the isomerization reactions were carried out under an N_2 atmosphere. We also evaluated the rate of isomerization of **8c** in the presence of air and discovered that the isomerization rate increases 1.5-fold. Over the course of our experiments, we utilized four different batches of **G4**. All four preparations of **G4** catalyzed isomerization to the same extent and at the same rate.

The timescale for **8e** isomerization was amenable to monitoring by ^{13}C NMR spectroscopy (Figure 3-5). Upon addition of **8e** to **G4** (1:1 ratio), about half of the Ru alkylidene **G4** is rapidly converted to a new Ru carbene species with a ^{13}C chemical shift at 315.7 ppm which is slightly upfield from that of the starting material at 316.4 ppm. The chemical shift of this species is consistent with that expected for Ru alkylidene coordinated to an eneamide instead of 3-bromopyridine (Scheme 3-2). The relative amount of this new species remained almost unchanged as amide **8e** was converted to **8e'** and within 90 minutes, the isomerized amide **8e'** underwent ring-opening as judged by the formation of [Ru]-CONHR at 178.5 ppm in the ^{13}C NMR spectra and the decrease of isomer and alkylidene **G4** resonances. The kinetic data taken together with the structure-activity data strongly support a mechanism in which the both the alkene and the amide carbonyl coordinate with Ru to enable equilibration of regioisomers via oxidative-addition of the activated allylic C-H bond.

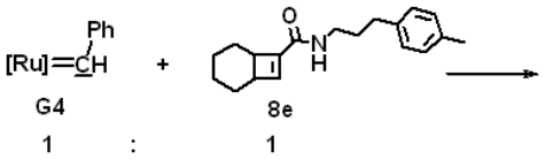

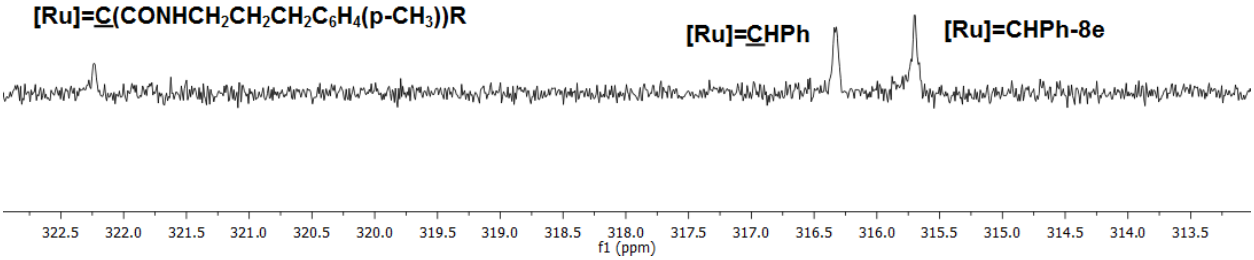

Figure 3-5. ^{13}C NMR spectrum of **8e** in the presence of alkylidene **G4** (1:1 ratio) in CD_2Cl_2 at 70-90 min after mixing.

3.3.2. Alternating Ring-Opening Metathesis Polymerization of Amides and Cyclohexene.

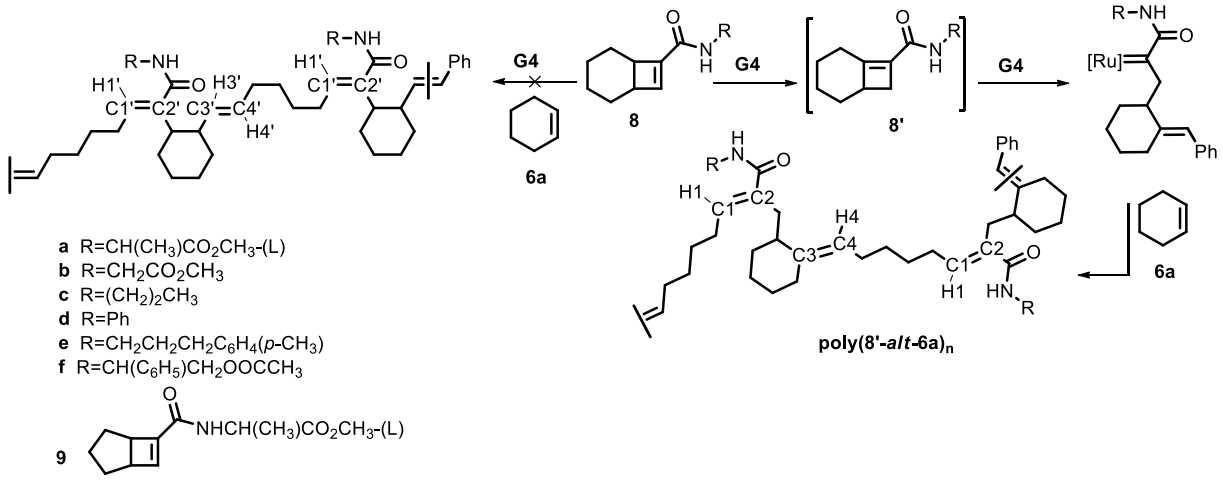

Scheme 3-3. Synthesis of alternating copolymers with bicyclic cyclobutene derivatized amides and cyclohexene **6a**.

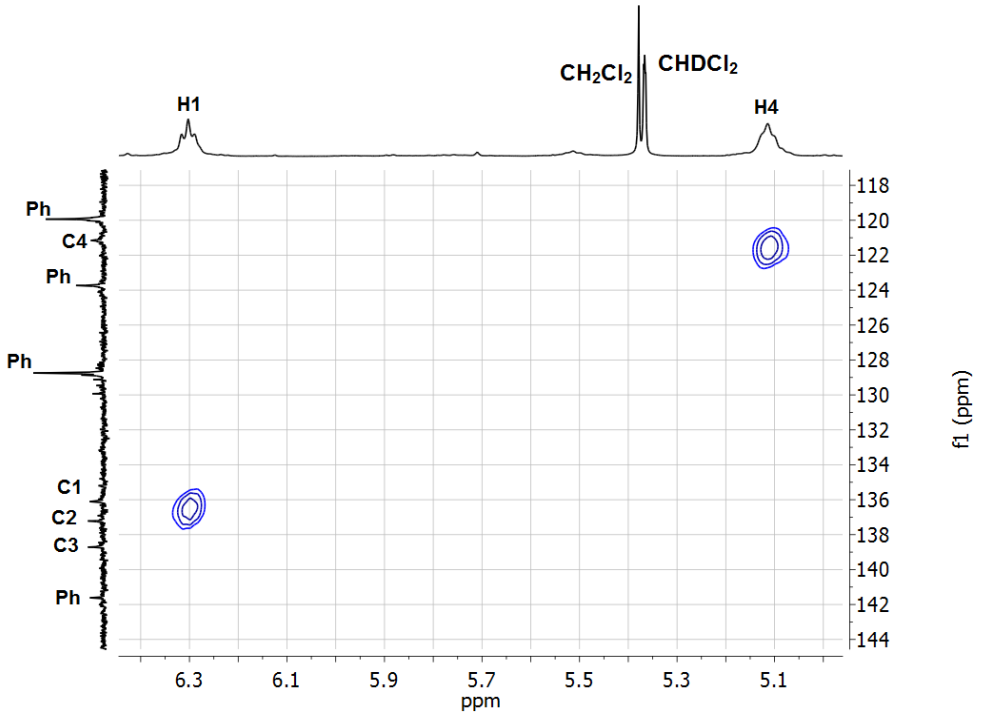

Figure 3-6. HSQC spectrum of poly(**8d'**-*alt*-**6a**)$_{20}$ in CD_2Cl_2, partial. The polymer backbone has only four alkene carbons and two alkene hydrogens corresponding to C1-C4 and H1 and H4.

^{1}H NMR spectroscopy of the copolymers obtained from mixing **8** and **6a** in the presence of **G4** displayed two alkene signals consistent with AROMP of isomer **8'**. In contrast, AROMP of the original amide **8** would have resulted in the appearance of three alkene signals see Scheme 3-2, left route). We premixed cyclohexene **6a** with catalyst **G4** before addition of amide **8c** to investigate the possibility of AROMP of the original amide. However, no polymer resonances were detected before a significant amount of amide **8c** had isomerized to amide **8c'**, in contrast, the analogous bicyclic ester readily undergoes ring-opening metathesis without isomerization.[169] Therefore, isomerization of **8c** is faster than ROM, and thus faster than ROMP or AROMP of **8c**. However, in the cases of **1a**, **1b**, **1e**, and **1f**, the rate of isomerization is slower than or similar to

the rate of ROM and mixtures of starting material, and alternating polymers of broad dispersities were obtained, thus necessitating that isomerization is complete before addition of cyclohexene **3**. The AROMP products of amides **1c** and **1d** were selected for further characterization owing to their fast isomerization and polymerization.

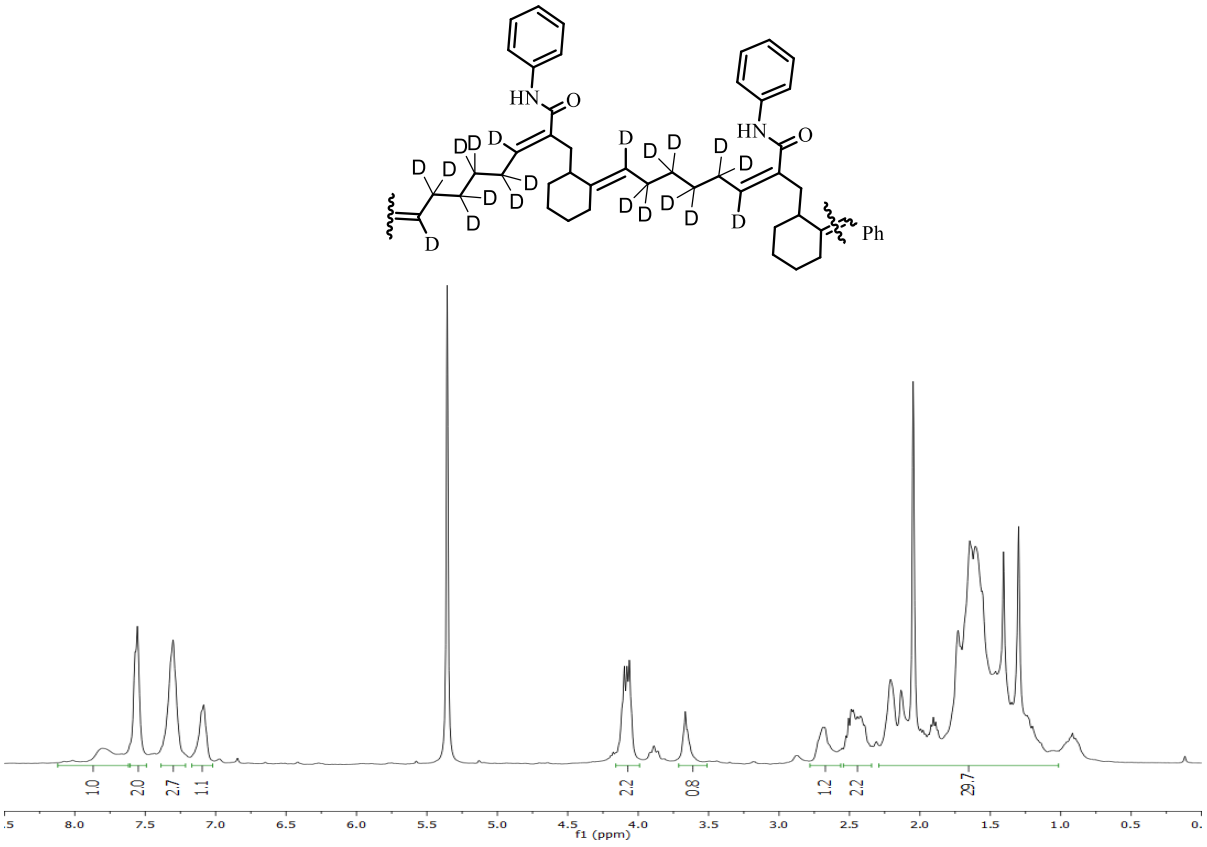

Figure 3-7. Isotopic labeling experiment of poly(**8d'**-*alt*-**6a**)$_{10}$**.**

Characterization of the poly(**8d'**-*alt*-**6a**)$_{20}$ by ^{1}H NMR, ^{13}C NMR, APT and HSQC spectroscopy revealed that the polymer backbone has four alkene carbons and two alkene hydrogens corresponding to C1-C4 and H1 and H4 (Scheme 3-2). HSQC spectroscopy confirmed that the amide substituted olefin is a single stereoisomer; there is a single H1 signal, at 6.29 ppm that correlates with C1 at 136 ppm (Figure 3-6). The alkene is of *E* configuration based

on comparison of the H1 alkene chemical shift with model compounds.[103, 152] A single H4 signal at 5.11 ppm correlates with C4 at 121 ppm. Due to peak broadening in the polymer, we could not determine if the C3-C4 alkene was stereoregular or not.

Integration of the poly(**8'**-*alt*-**6a**)$_n$ alkene signals relative to side chain signals demonstrated that an equal incorporation of the two monomers had occurred. Further evidence for the equal incorporation of monomers **8d'** and **6a** was obtained using cyclohexene-D_{10}. The ^{1}H NMR spectra of the deuterium labeled copolymer poly(**8d'**-*alt*-**6a-D$_{10}$**)$_{10}$ show a complete loss of the alkene resonances at 6.3 ppm and 5.1 ppm as expected for a 1:1 ratio of **A** and **B** monomers (Figure 3-7). An **AA** or **BB** dyad is formed upon backbiting. Additional alkene proton resonances in the 5 ppm region of the ^{1}H NMR spectrum which would indicate formation of **BB** dyad were not observed. In the *i*-AROMP product, the **AA** dyad does not possess an alkene proton. Therefore, we inspected the ^{13}C NMR spectra of poly(**8d'**-*alt*-**6a**)$_{10}$ and poly(**8c'**-*alt*-**6a**)$_{424}$ for the presence of **AA** dyad alkene resonances, specifically, a C3' resonance between 160-145 ppm, and found none (Figure 3-8).

We explored the utility of alternating copolymerization by testing the maximal length poly(**8c'**-*alt*-**6a**)$_n$ that could be prepared. When cyclohexene **6a** was added directly to a completed isomerization reaction, poly(**8c'**-*alt*-**6a**)$_n$ was obtained (Table 3-3), however the molecular weights exceeded those expected from the monomer:catalyst ratio due to loss of catalyst during isomerization. Therefore, in order to facilitate characterization of polymers greater than 100 **AB** dyads, and to maximize their purity and to minimize their dispersity, **8c'** was isolated before initiation of the AROMP reaction and fresh catalyst added. For example, when amide **8c'** was mixed with catalyst **G4** in a ratio of 500:1 with 1000 equivalents of

cyclohexene **6a,** we obtained alternating copolymer with a narrow molecular weight distribution ($Đ_M$ = 1.26) and more than 400 **AB** dyads were incorporated (Fig. 3-9).

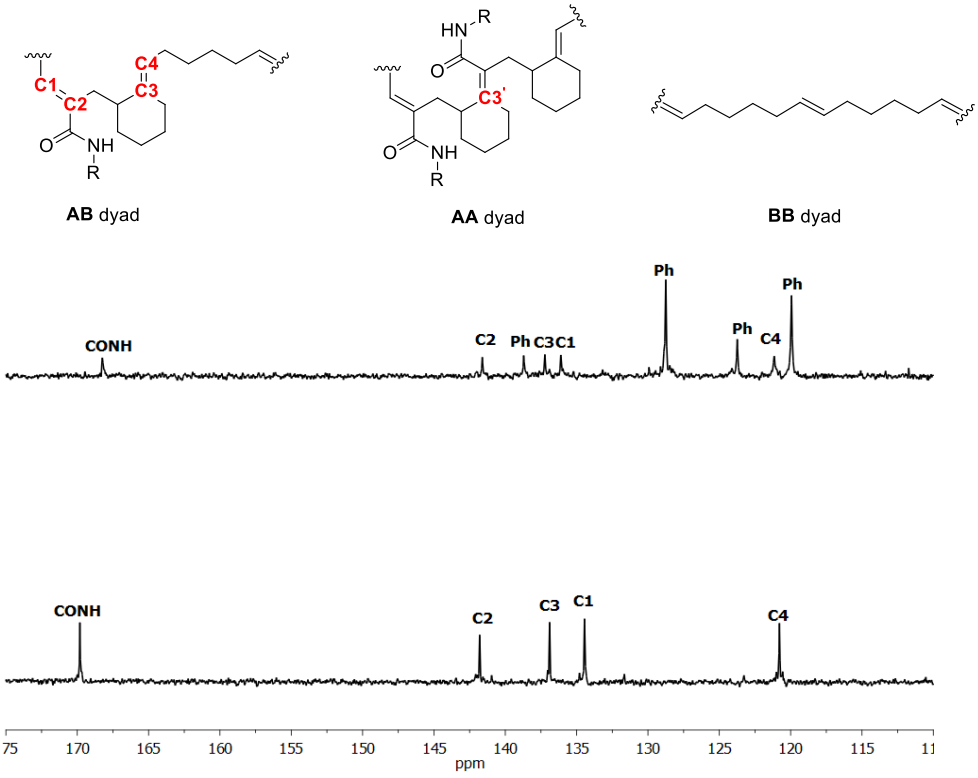

Figure 3-8. Partial ^{13}C NMR spectra of *i*-AROMP polymers illustrate the absence of **AA** dyad or **BB** dyad ^{13}C resonances, top spectrum poly(**8d'**-*alt*-**6a**)$_{50}$, bottom spectrum poly(**8c'**-*alt*-**6a**)$_{424}$.

Given the unique polymer backbone generated in the *i*-AROMP reaction, the thermostability and rigidity of poly(**8c'**-*alt*-**6a**)$_n$ was evaluated by TGA and differential scanning calorimetry (DSC) in air to gain insight into its physical properties. The T_g of poly(**8c'**-*alt*-**6a**)$_{97}$ is 86 ºC ± 0.7 ºC and it has a T_{d10} = 130 ºC (5 wt%). Decomposition of poly(**8c'**-*alt*-**6a**)$_{424}$ occurred before the glass transition could be achieved. The high rigidity of these room

temperature glasses are most likely due to the incorporation of both an unsaturated amide and an alkylidene cyclohexane in the poymer backbone.

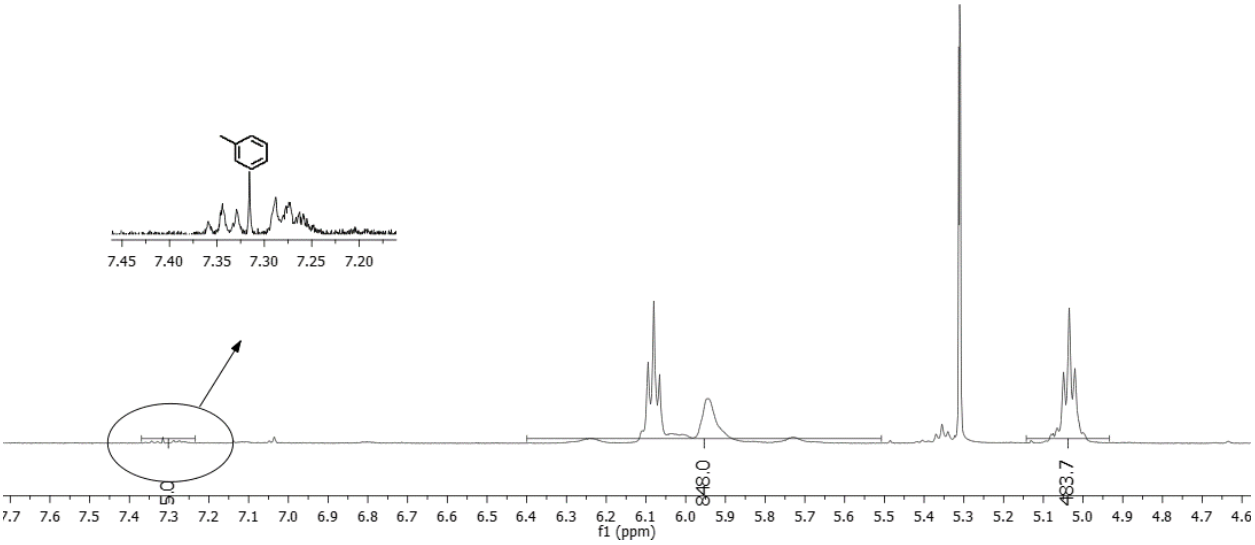

Figure 3-9. Alternating copolymers of **8c** and cyclohexene **6a** in the present of **G4** in a ratio of 500:1000:1 yields poly(**8c'**-*alt*-**6a**)$_{424}$. Two sets of alkene signals were obtained corresponding to H1 and H4 in Scheme 3-3.

3.4. Summary

Bicyclo[4.2.0]oct-7-ene-7-carboxamides of primary amines are quantitatively isomerized to bicyclo[4.2.0]oct-1(8)-ene-8-carboxamides in the presence of catalyst **G4**. Moreover, reaction of compound **8d** to give **8d'**, which is complete within 15 minutes, is by far the fastest ruthenium-catalyzed olefin isomerization reported to date. This isomerization of an internal olefin in a bicyclic system provides a facile approach to synthesize tetra-substituted bicyclo[4.2.0]oct-1(8)-ene-8-carboxamides.

Most notably, bicyclic tetra-substituted α, β-unsaturated amides are excellent AROMP substrates for the preparation of extremely long, alternating copolymers. Isomerized unsaturated amides **8c'** and **8d'** undergo alternating ROMP with cyclohexene more rapidly than previously studied bicyclo[4.2.0]oct-7-ene-7-carboxylic esters or 1-cyclobutenecarboxylic acid esters. The *i*-AROMP reaction is compatible with a variety of amides that provide functional group handles. This remarkable cascade, isomerization followed by alternating ring-opening cross metathesis of **A** and ring-opening cross metathesis of **B,** provides an efficient entry to well-controlled architectures, enables the production of linear and extremely long (greater than 400 **AB** units) alternating polymers, and unlocks the prospect of employing functionalized alternating copolymers in multiple applications.

Chapter 4. Alternating ROMP Copolymers Containing Charge-Transfer Units*

*The work presented here has been published. As indicated in the text, some experiments were performed by Joy Romulus at NYU.

4.1. Introduction

Nature's uniquely sequenced polymers assume well-defined structures that are held together by noncovalent interactions such as hydrogen bonding, ionic, aromatic, hydrophobic, and van der Waals interactions.[164, 190] These structures enable biopolymers to carry out sophisticated functions such as catalysis, specific binding, or directed flow of electrons.[165] Emulation of nature's affinity to engineer systems with precise structure-to-function relationships will provide new functional materials for potential applications such as synthetic enzymes.[165, 191]

Alternating copolymers, in particular, provide high precision over incorporation of two different monomers into a polymer sequence. The preparation of alternating copolymers has been achieved via a variety of polymerization techniques including ring-opening metathesis polymerization (ROMP),[192] alkene polymerization,[193] and radical polymerization.[129, 194] Despite the well-established implementation of ROMP that affords well-defined polymers, there are only a few reports using ROMP to obtain alternating copolymers.[34, 36, 115] This is likely due to the challenge in choosing monomer pairs with alternating affinities for the living metal alkylidene

and also to appropriate catalyst selection. Employment of norbornene (NB)/cyclopentene (CPE) or NB/cyclooctene (COE) monomer pairs in alternating-ROMP has been reported.[195-197] These methods rely on the slow homopolymerization of CPE or COE in combination with a significant excess of one of these monomers to obtain a high level of alternation.[36, 115] Such strategies are chemically inefficient and risk generating homopolymer blocks of the monomer in excess.

Synthetic foldamers contains non-covalent interactions and they can fold into a conformationally ordered state in solution, which mimic the ability of biopolymers.[164] The system composed primarily of aromatic rings which utilizes donor-acceptor interactions was first described by Iverson and Lokey.[163] They have demonstrated the ability of donor-acceptor interactions to drive polymers to fold into specific secondary structures, such as a pleated structure.

Donor-acceptor pair dialkoxynaphthalene (DAN) and pyromellitic dianhydride (PDI) units allows for directed noncovalent interactions and charge transfer and are currently used in making foldamers (Figure 4-1a).[161] This functional pair exhibits a charge-transfer absorbance (~ 460 nm in chloroform) when the aromatic units are properly aligned in a face-t-face geometry.[198] The charge-transfer unit provides an effective spectroscopic handle to characterize the conformational arrangement of these aromatic groups in solution.[163, 199, 200] Previously Weck and coworkers reported the first alternating ROMP copolymers synthesized from NB/COE monomers that were functionalized with DAN/PDI (Figure 4-1b). However, it requires a significant excess amount of one of the monomers for a high level of alternation,[36, 115, 136] which is chemically inefficient and risks generating homopolymer of the monomer in excess. Indeed, they inevitably attached a homopolymer tail end on each polymer (Figure 4-1c).

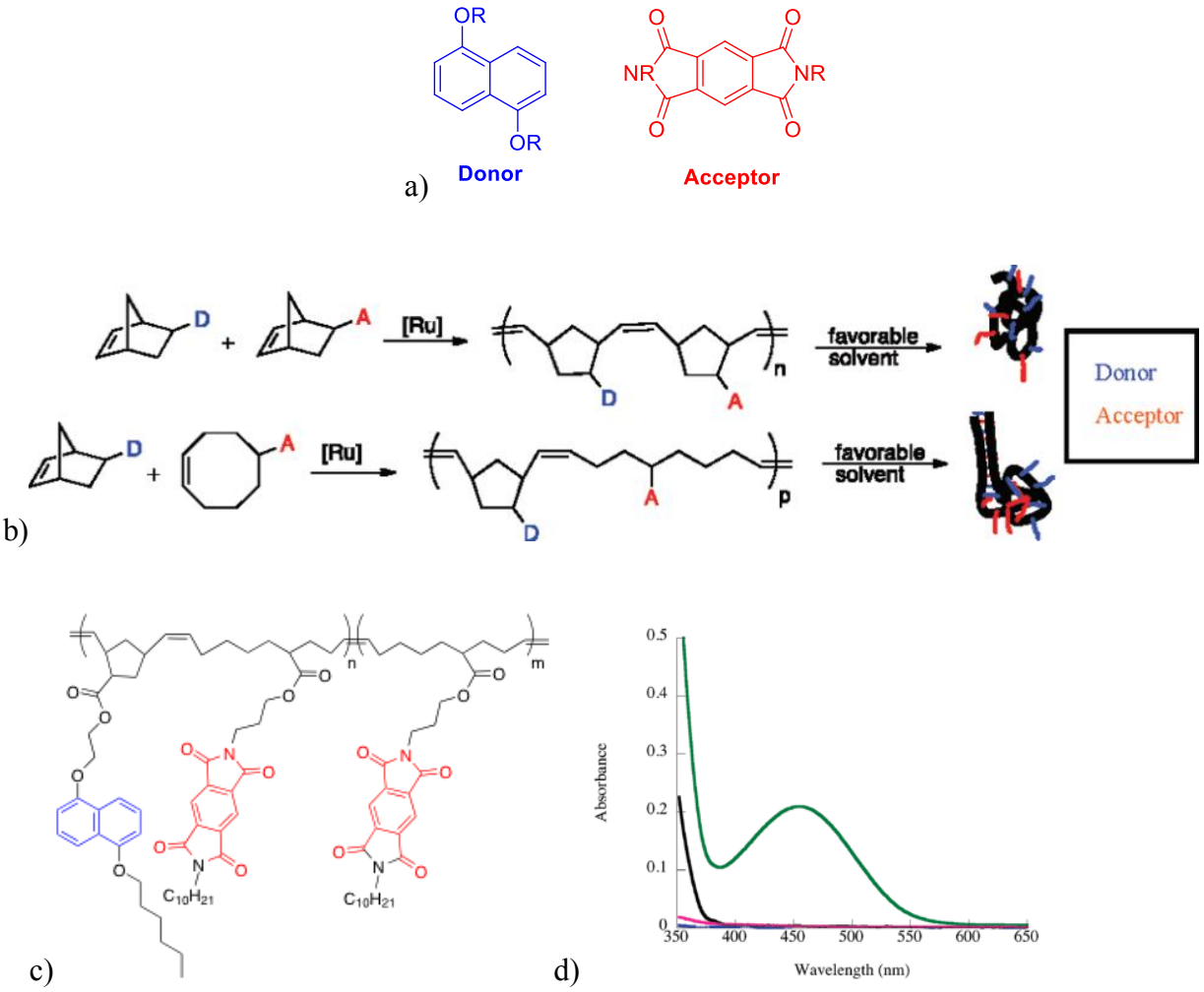

Figure 4-1. Alternating copolymerization via ROMP of side chain functionalized NB and COE. a) Dialkoxynaphthalene (DAN) and pyromellitic dianhydride (PDI) side chains used as a donor-acceptor pair. b) Alternating ROMP copolymers synthesized from NB/COE monomers functionalized with dialkoxynaphthalene (DAN) and pyromellitic dianhydride (PDI) units, respectively. c) Alternating copolymers by norbornene (NB) and cyclooctene (COE) with a homopolymer tail. d) Comparison of absorption of monomers, mixed monomers (1:1), mixed homopolymers (40mers; 1:1), random copolymer (40-mer), and blocky copolymer (120-mer). The green trace is the random copolymer spectrum which exhibited a charge-transfer absorbance signal at ~460 nm. This figure was adapted from Romulus, et al.[161]

4.2. Results and Discussion

We demonstrated that CB derivatives substituted at the 1-position, that have a similar strain energy to NB,[201, 202] undergo ruthenium-catalyzed ROMP.[103] Introduction of an ester functional group at the 1-position leads to a loss of homopolymerization ROMP ability.[103, 104] In contrast to CBE, the strain energy of CH is close to zero and is not a suitable monomer for ROMP. However, CH was found to react with the enoic carbene generated from the ring-opened CBE.[1] In turn, the regenerated Ru alkylidene reacts with an equivalent of CBE. This alternating reactivity of the ruthenium catalyst provides alternating copolymers irrespective of the monomer feed ratio. The alternating copolymers, however, were found to display a bimodal molecular weight distribution due to intramolecular cross metathesis, i.e., "backbiting".

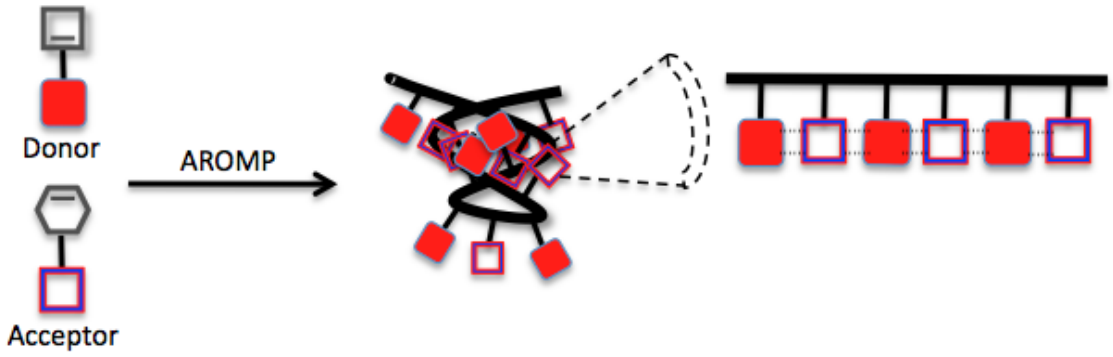

Figure 4-2. Proposed structure of charge-transfer units containing alternating copolymers. [Reprinted with permission from Romulus, et al;[126] copyright 2013, Macromolecular Letters]

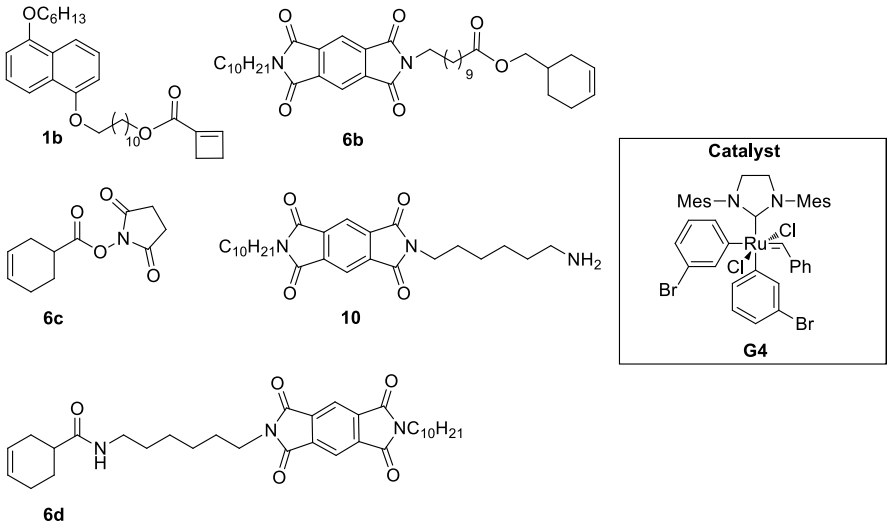

Figure 4-3. Chemical structures of monomers and catalyst (box) applied for AROMP. [Adapted with permission from Romulus, et al;[126] copyright 2013, Macromolecular Letters]

In this research, we hypothesized that introduction of steric hindrance by the bulky side chains on the polymer backbone will prevent backbiting and the placement of charge-transfer units in an alternating fashion will increase quantum efficiency and the absorption of the charge-transfer band (Figure 4-2).[161] We attached the bulky DAN and PDI units to cyclobutene and cyclohexene, respectively, and synthesized target molecules (Figure 4-3). The syntheses of the side chains and the side chain attached monomers are described in Chapter 7.

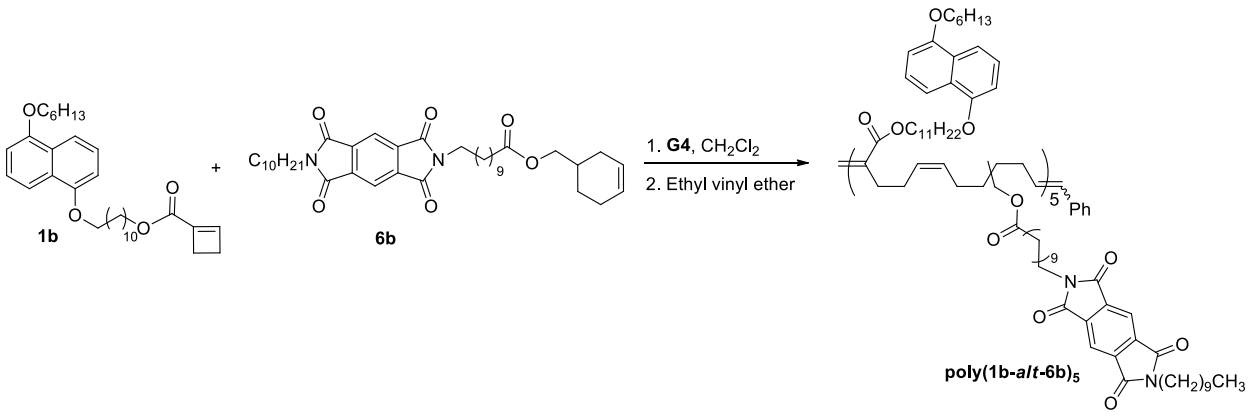

Scheme 4-1. Original synthetic scheme of poly(**1b**-*alt*-**6b**)$_5$, route 1. [Reprinted with permission from Romulus, et al;[126] copyright 2013, Macromolecular Letters]

Based on previous studies,[1] synthetic route 1 (Scheme 4-1) was first investigated for the alternating copolymerization of the DAN and PDI functionalized CBE and CH monomers, respectively. This route successfully afforded poly(**1b**-*alt*-**6b**)$_5$ as determined by feeding ratio in AROMP since determination by ^{1}H NMR was not viable as a result of peak overlap. We observed a perfectly alternating ring-opening metathesis polymerization (AROMP) between cyclobutene (CB) and CH. Both ^{1}H NMR spectroscopy and gel permeation chromatography (GPC) analysis indicated backbiting-free alternating copolymers. The previously reported studies on poly(**1a**-*alt*-**6a**)$_n$ revealed a triplet peak in the ^{1}H NMR spectrum between 7.0-6.8 ppm corresponding to concentration-independent intramolecular backbiting of the enoic ruthenium carbene on the unhindered disubstituted alkenes in the polymer backbone (Figure 4-4a). As a result, molar mass dispersity of unfunctionalized poly(**1a**-*alt*-**6a**)$_n$ were larger than 2 and a significant fraction of the polymer was cyclic. In our case, poly(**1b**-*alt*-**6b**)$_{10}$ did not show any proton resonance signals due to backbiting, had $Đ_M$s lower than 1.3, and displayed a monomodal distribution (Figure 4-4b). Herein we addressed both, the limitation of the NB/COE ROMP, i.e.

the formation of COE homoblocks, as well as the intramolecular cross metathesis of current AROMP by utilizing CBE/CH monomers containing the DAN-PDI pair to achieve perfectly alternating copolymers.

We hypothesize that backbiting is inhibited by the increased steric hindrance at the enoic carbene and disubstituted alkene in combination with the restricted flexibility of the polymer backbone upon modification with larger substituents. As a consequence, longer AROMP copolymers were obtained than previously reported.

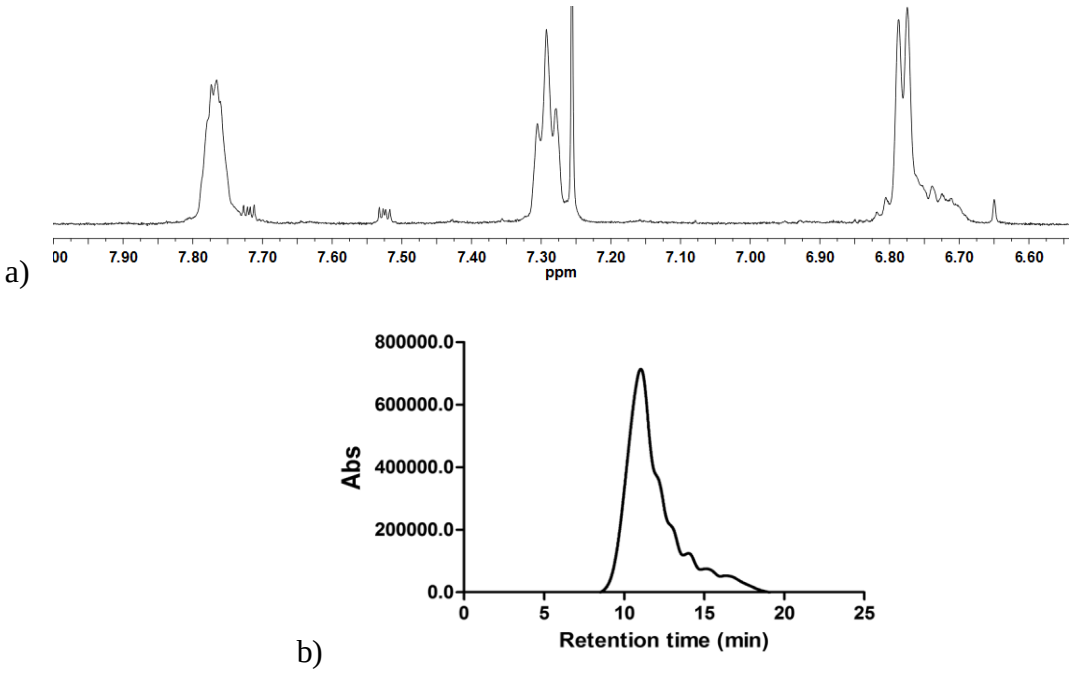

Figure 4-4. Analysis of alternating copolymers supports backbiting-free polymers poly(**1b**-*alt*-**6b**)$_5$. a) ^{1}H NMR spectrum of poly(**1b**-*alt*-**6b**)$_5$, the triplet from cyclic polymers disappeared around 6.9 ppm. b) Monomodal distribution of GPC trace of poly(**1b**-*alt*-**6b**)$_5$. [Adapted with permission from Romulus, et al;[126] copyright 2013, Macromolecular Letters]

However, longer polymerization times were required due to the significant steric hindrance presented by the side chain units in AROMP of side chain functionalized monomers. This resulted in a decrease in the rate of polymerization inhibiting the formation of higher molecular weight polymers.

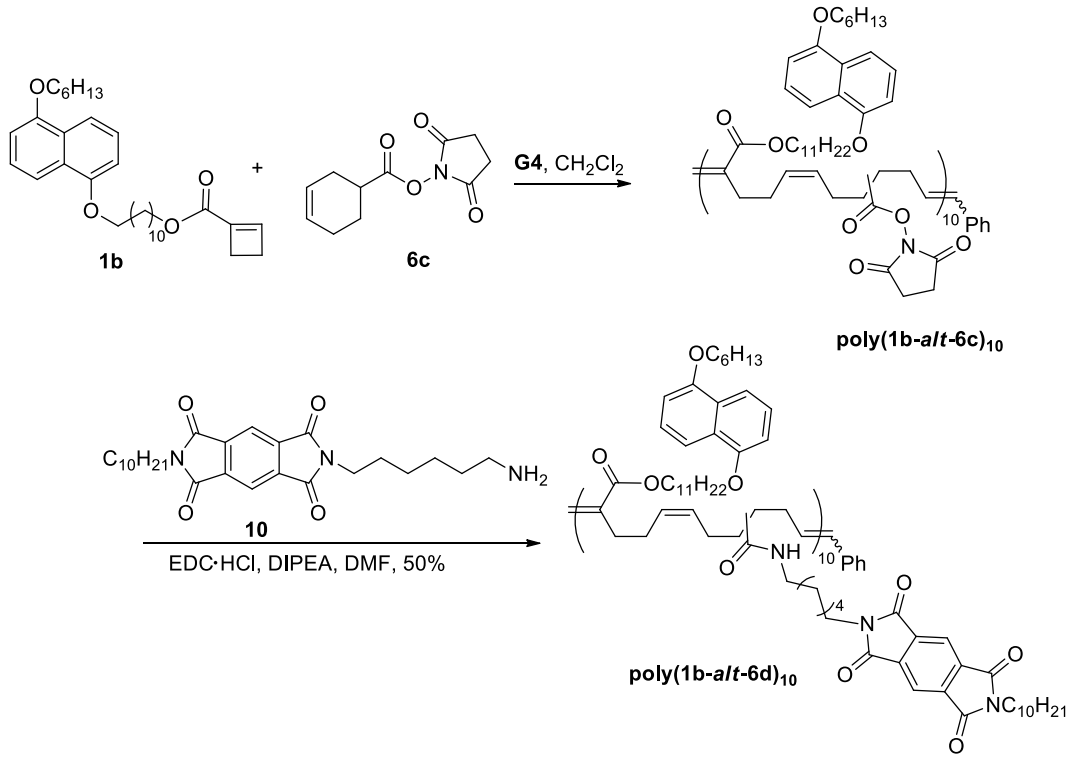

Scheme 4-2. Revised synthetic scheme for the preparation of poly(**1b**-*alt*-**6d**)$_{10}$ using a post polymerization functionalization step. [Reprinted with permission from Romulus, et al;[126] copyright 2013, Macromolecular Letters]

To minimize steric hindrance and to achieve a higher degree of polymerization, a revised synthetic route was applied using DAN-CBE, **1b** and a cyclohexene functionalized with N-hydroxysuccinimide (NHS), **6c** for AROMP (Scheme 4-2). The NHS group is less bulky than the PDI, and is not reactive during the polymerization. The PDI ester can then be formed via a post-

polymerization functionalization strategy to generate poly(**1b**-*alt*-**6d**)$_{10}$. This modified route not only allowed for a higher degree of polymerization, but also provided an alternative strategy for the incorporation of the PDI moiety. poly(**1b**-*alt*-**6d**)$_{10}$ was subjected to ^{1}H NMR and GPC analysis, and was identified to be backbiting-free as well.

We demonstrated that the alternating placement of the charge-transfer units along a single polymer chain provides insight into the polymer structure. UV-Vis spectroscopy was utilized to investigate the charge-transfer between the side chains of the alternating copolymers in solution. (UV analysis was performed by Dr. Joy Romulus). The UV-Vis spectrum of poly(**1b**-*alt*-**6d**)$_{10}$ (3 mM in chloroform) shows a charge-transfer absorbance at the characteristic wavelength (Figure 4-5a – light blue trace) indicating that the side chains are able to favorably orient to transfer energy in this system. A concentration study from 3 mM to 100 μM was carried out to determine if these interactions occur inter- or intramolecularly over the concentration rage examined. As shown in Figure 4-6a, the charge-transfer absorbance signal was persistent even at low concentrations. Moreover, the absorbance followed Beer-Lambert behavior based on the concentration of polymer (Figure 4-5b), which demonstrated that the charge-transfer is intramolecular. Additionally, the aromatic signals in the ^{1}H NMR spectrum of poly(**1b**-*alt*-**6d**)$_{10}$ are shifted upfield in comparison to the individual monomers (Figure 4-6). These shifts further indicate the pi-pi stacking of the donor-acceptor aromatic units, and are consistent with similar shifts previously reported for partially-folded polymers.[163]

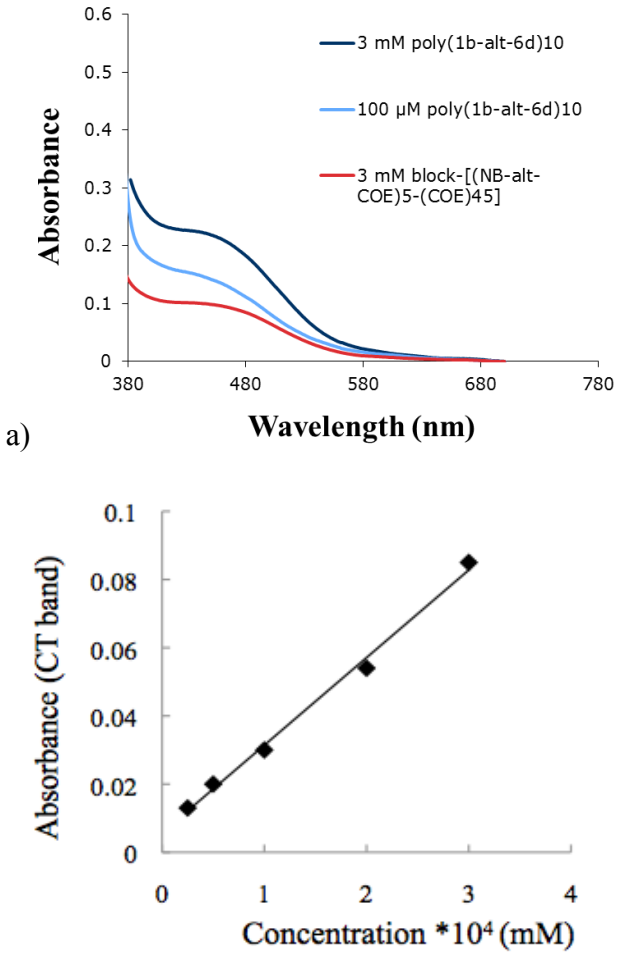

Figure 4-5. Partial UV-Vis spectra of the charge-transfer region in chloroform. a) Comparison of alternating copolymers. Blue trace = 3 mM poly(**1b**-*alt*-**6d**)$_{10}$, red trace = 100 µM poly(**1b**-*alt*-**6d**)$_{10}$, green trace = 3 mM poly(NB-*alt*-COE)-block-poly(COE). b) Plot of charge-transfer absorbance versus concentration of poly(**1b**-*alt*-**6d**)$_{10}$. (Performed by Dr. Joy Romulus) [Reprinted with permission from Romulus, et al;[126] copyright 2013, Macromolecular Letters]

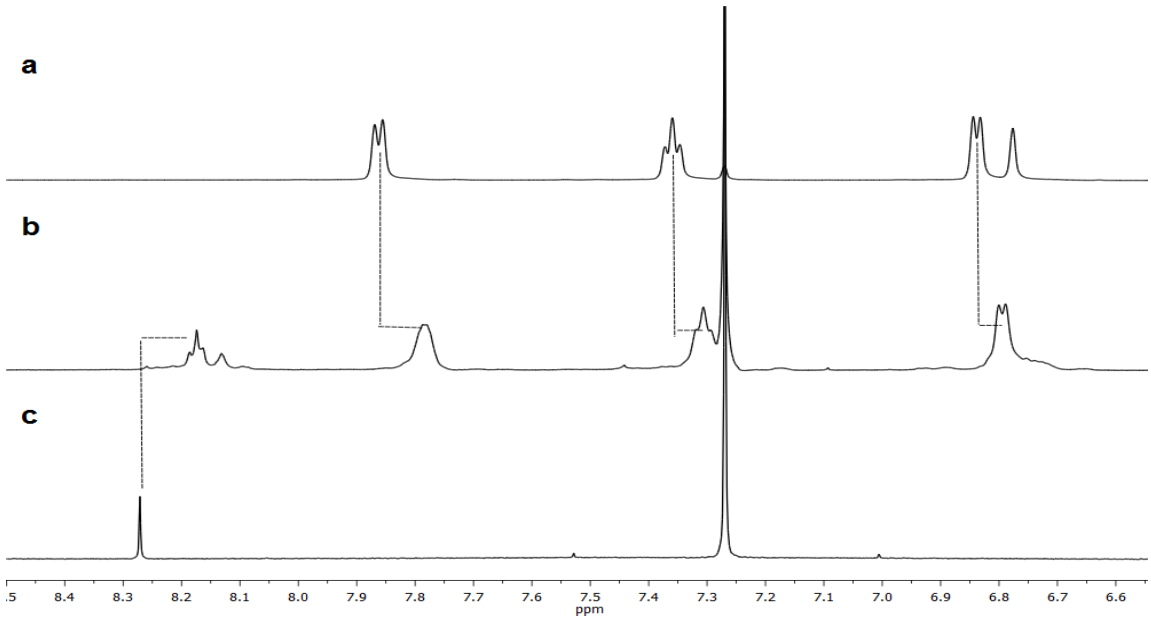

Figure 4-6. Aromatic and alkene region of ^{1}H NMR spectra of a) Monomer **1b**; b) poly(**1b**-*alt*-**6b**)$_5$; and c) Monomer **6b**. [Reprinted with permission from Romulus, et al;[126] copyright 2013, Macromolecular Letters]

We compared the charge-transfer absorbance of the functionalized poly(**1a**-*alt*-**6a**)'s to the previously reported functionalized poly(NB-*alt*-COE)-*b*-COE. As shown in Figure 4-6a, poly(**1b**-*alt*-**6d**)$_{10}$ exhibits a higher charge-transfer absorbance intensity in comparison to the NB/COE polymers at the same concentration, which indicates that the new poly(**1b**-*alt*-**6d**)$_{10}$ polymers more favorably align the aromatic units of the donor and acceptor moieties.

4.3. Conclusion

In conclusion, we have demonstrated the AROMP of CBE and CH monomers containing bulky DAN/PDI side chains. We attribute inhibition of backbiting to the steric hindrance provided by bulky side chains around the carbene and the polymer alkenes. UV-Vis

spectroscopic analysis shows a charge-transfer absorbance signal for the perfectly alternating copolymers signifying the alignment of the side chains. The new polymers demonstrate an enhancement of charge-transfer in comparison to previously studied polymers, indicating that the sequence specificity in alternating CBE-CH copolymers provides efficient energy transfer. These results will guide the direction of future monomer designs to provide backbiting-free AROMP and towards efficient materials for charge-transfer. Precise control of monomer sequence presents a viable handle towards regulating polymer assembly; a step towards advanced material properties.

Chapter 5. Orthogonally Functionalized Alternating Copolymers via Alternating Ring-Opening Metathesis Polymerization.

5.1. Introduction

Positioning functional groups onto polymers with precise control has been a great challenge in polymer chemistry. It generally requires laborious stepwise addition or sequence-controlled polymerization. In most cases sequence control still lacks rigorous fidelity in that monomer incorporation is not well-controlled. Alternating ring-opening metathesis polymerization (AROMP) offers a useful synthetic approach for preparing alternating copolymers (Scheme 5-1).[1, 169, 203]

While exploring 1-substituted cyclobutenes, Lee and Song discovered that ROMP of secondary amides of cyclobutenecarboxylic acid provides regioregular polymers with an *E*-configuration and low molar-mass dispersities ($Đ_M$s). However, 1-cyclobutenecarboxylic acid tertiary amides and 1-cyclobutenecarboxylic acid esters undergo only one single ring-opening metathesis cycle (ROM) without polymerization.[104] The esters were utilized for AROMP by mixing them with cyclohexene in the presence of catalyst **G4**. Copolymers with perfectly alternating monomers were obtained.[1] However, the molecular weight homogeneity of the copolymers is limited by cross metathesis reactions that lead to undesired polymer dispersities and cyclic polymers. The side products are practically impossible to separate and limit yields.

To inhibit backbiting, we designed new cyclobutene derivatives with bicyclic structures in chapter 2 that yield rings in the polymeric backbone upon metathesis.[203] The new monomers form alternating copolymers. Specifically, methyl bicyclo[4.2.0]oct-7-ene-7-carboxylate afforded rigorously linear alternating copolymers without any evidence of backbiting. Based on the discoveries above, we explored the applications of the new polymers.

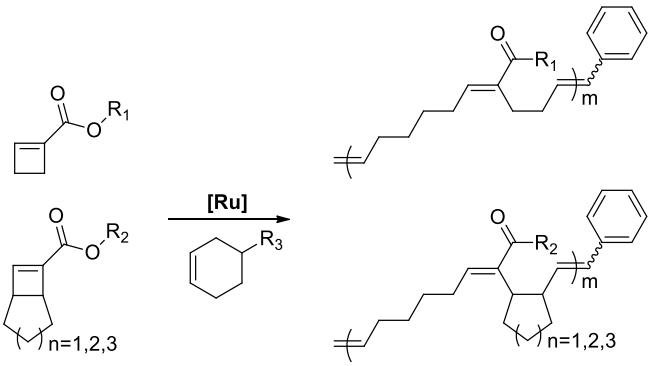

R_1=Me, Ph
R_2=Me, Perfluorophenyl
R_3=H, Me, CHO, COONHC, Perfluorophenyl

Scheme 5-1. Alternating copolymer synthesis by alternating ring-opening metathesis polymerization (AROMP).[1, 169]

One of the advantages of our alternating copolymers over other polymers such as random or block copolymers is the distance between AB subunits is on the nanometer scale and provide precise positioning. These parameters suggested that our polymers would provide a good framework for efficient energy transfer which requires the donor and accepter to be in very close proximity.

Förster/fluorescence resonance energy transfer (FRET) is a phenomenon that occurs between a fluorescence donor and a fluorescence acceptor. For FRET to occur, the two

molecules should be within a maximum distance of 100 Å (depending on specific pairs). In the process of FRET, the excited-state energy of a donor is transferred to an acceptor molecule. When the emission spectrum of the donor overlaps with the excitation spectrum of the acceptor (Figure 5-1),[204] the acceptor molecule emits light at its characteristic wavelength which is always longer than the emission wavelength of the donor.

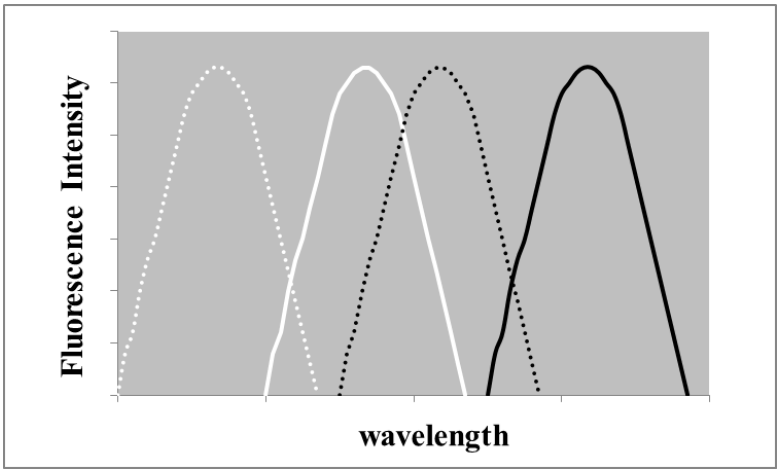

Figure 5-1. Illustration of excitation and emission curves of fluorescence donor and acceptor that FRET. Excitation (dotted lines) and emission (solid lines) spectra of an idealized fluorescence donor (D, white lines) and fluorescence acceptor (A, black lines) pair. Wavelength and intensity values are in arbitrary units. Adapted from De Angelis.[204]

In this project, we utilized an alkyl bromide functionalized bicyclo[4.2.0]oct-7-ene-7-carboxylate and an aldehyde-containing cyclohexene as the AROMP pair. This combination provided a facile approach to prepare long and completely alternating copolymers with orthogonal functional groups. Post-polymerization modification of the alkyl bromide with an azide group allows click-chemistry modification and the aldehyde can be coupled to a hydrazide. Both bromide and aldehyde are compatible with AROMP and allow introduction of

functionalities which are not compatible with AROMP reactions. In this work, we introduce alkyne-attached tryptophan and hydrazide-attached dansyl as a fluorophore FRET pair and observe the fluorescence. This example for well-controlled architecture enables the prospect of employing alternating copolymers in materials applications such as energy transfer devices.

5.2. Results and Discussion

5.2.1. Design of Orthogonal Functionalities.

Alkyl bromides have been shown to be compatible with the activity of ruthenium catalysts.[149] The bromide can be readily converted to other functional groups by substitution. Therefore, we attached an alkyl bromide to the bicyclo[4.2.0]oct-7-ene-7-carboxylate monomer. A two-carbon linker was introduced between the bromide and the ester to prevent any electronic effects the bromide might have on the metathesis reaction of the conjugated alkene (Scheme 5-2). Moreover, **4e** was prepared and its AROMP ability as monomer **A** with cyclohexene **6a** as monomer **B** in the presence of **G4** was tested. We observed complete conversion of **4e** within 6 hours in an experiment to synthesis **AB** 20-mer, and the ^{1}H NMR spectrum of the product showed that alternating copolymers with targeted length were obtained. The triplet at around 6.9 ppm in ^{1}H NMR which is characteristic in AA repeat was not observed, therefore, the polymers are linear.

Next, we investigated modified cyclohexenes as AROMP monomers. We tested the ability of cyclohexene conjugated to different functional groups, including a hydroxyl group, a carboxylic acid and esters, to undergo AROMP with **4a** as monomer **A** in the presence of **G4** in CD_2Cl_2. All of the above cyclohexene derivatives failed to produce polymers. We attribute the

failure to the sp^3 hybridized oxygen which coordinates with the ruthenium alkylidene.[205, 206] Therefore, an sp^3 containing species should be avoided in AROMP.

We considered the possibility of using azide. However, azide has been reported to be incompatible with ruthenium catalysts.[207, 208] Aldehydes have been used in ROMP, but they have never been used in AROMP.[128, 209] Therefore, we mixed aldehyde-modified cyclohexene **6e** and methyl bicyclo[4.2.0]oct-7-ene-7-carboxylate in the presence of **G4**; alternating copolymers were produced.

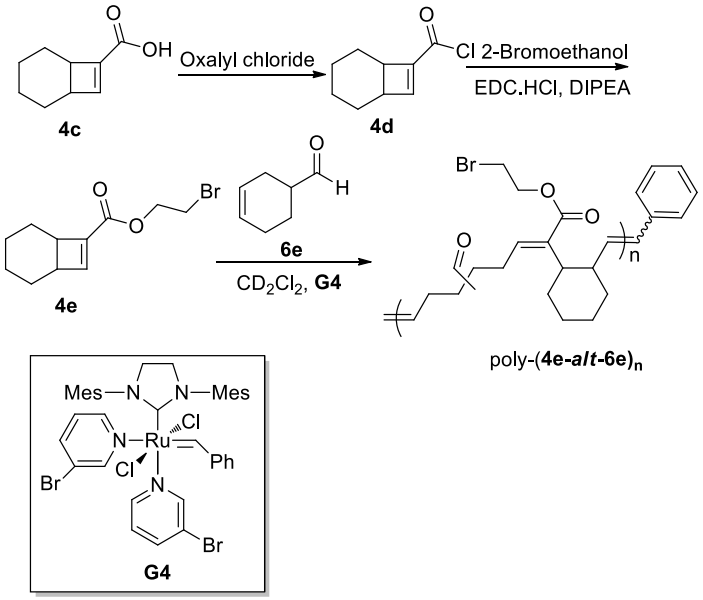

Scheme 5-2. Alternating copolymers with orthogonal functional groups synthesized by alternating ring-opening metathesis polymerization (AROMP).

5.2.2. Selection of FRET Pair.

The distance between the two orthogonal functional groups conjugated to the alternating copolymers was predicted by ChemBio 3D to be around 10 Å. This distance is far smaller than

R_0 of most FRET pairs, where R_0 is the Förster distance for the donor and acceptor pair, i.e. the distance at which the energy transfer efficiency is 50%.[210, 211] The fluorophores that we select should be inert to the post-polymerization modification procedures, and they should also be soluble in solvents for characterization. The wavelength of maximum absorption (λ_{max}) of tryptophan is at 284 nm and it has an emission maximum at 330 nm in THF. Dansyl hydrazide has λ_{max} of absorption at 335 nm which overlaps with the emission curve of tryptophan. The dansyl fluorophore emits at around 507 nm. Moreover, they are both inexpensive fluorophores. Therefore, they were used for the demonstration of FRET in AROMP polymers.

5.2.3. Alternating Ring-Opening Metathesis Polymerization and Post Polymerization Modifications.

After establishing the abilities of both **4e** and **6e** to undergo AROMP separately, we subjected them to AROMP together and poly(**4e**-*alt*-**6e**)$_{27}$ was obtained (Scheme 5-2). The bromide was first converted to an azide by mixing poly(**4e**-*alt*-**6e**)$_{27}$ with NaN_3 in DMF at 60 °C for 3 hours. poly(**4e'**-*alt*-**6e**)$_{27}$ was obtained after workup. ^{1}H NMR of poly(**4e'**-*alt*-**6e**)$_{27}$ showed no significant difference from that of poly(**4e**-*alt*-**6e**)$_{27}$. Therefore, the IR spectroscopy was utilized and the distinctive N_3 vibration signal at 2104 cm^{-1} for poly(**4e'**-*alt*-**6e**)$_{27}$ was observed.

The alternating copolymer poly(**4e'**-*alt*-**6e**)$_{27}$ was further modified as shown in Scheme 5-3 to conjugate the dansyl hydrazide (DH) and to form poly(**4e'**-*alt*-**6e-DH**)$_{27}$. Although it was coupled with Boc-Trp-alkyne to form poly(**4e'**-**Trp**-*alt*-**6e**)$_{27}$. Or both fluorophores were introduced in a one-pot reaction to provide poly(**4e'**-**Trp**-*alt*-**6e-DH**)$_{27}$. The IR spectrum of poly(**4e'**-**Trp**-*alt*-**6e**)$_{27}$ and poly(**4e'**-**Trp**-*alt*-**6e-DH**)$_{27}$ were obtained to determine the percent conversion of the click reaction, and no azide peak was found (See Appendix). ^{1}HNMR

spectroscopy was also used to monitor the conjugation of dansyl fluorophore and the aldehyde resonance disappeared completely after the reaction. All polymers were analyzed by GPC after purification with LH-20, an organic phase gel filtration column, eluted with THF.

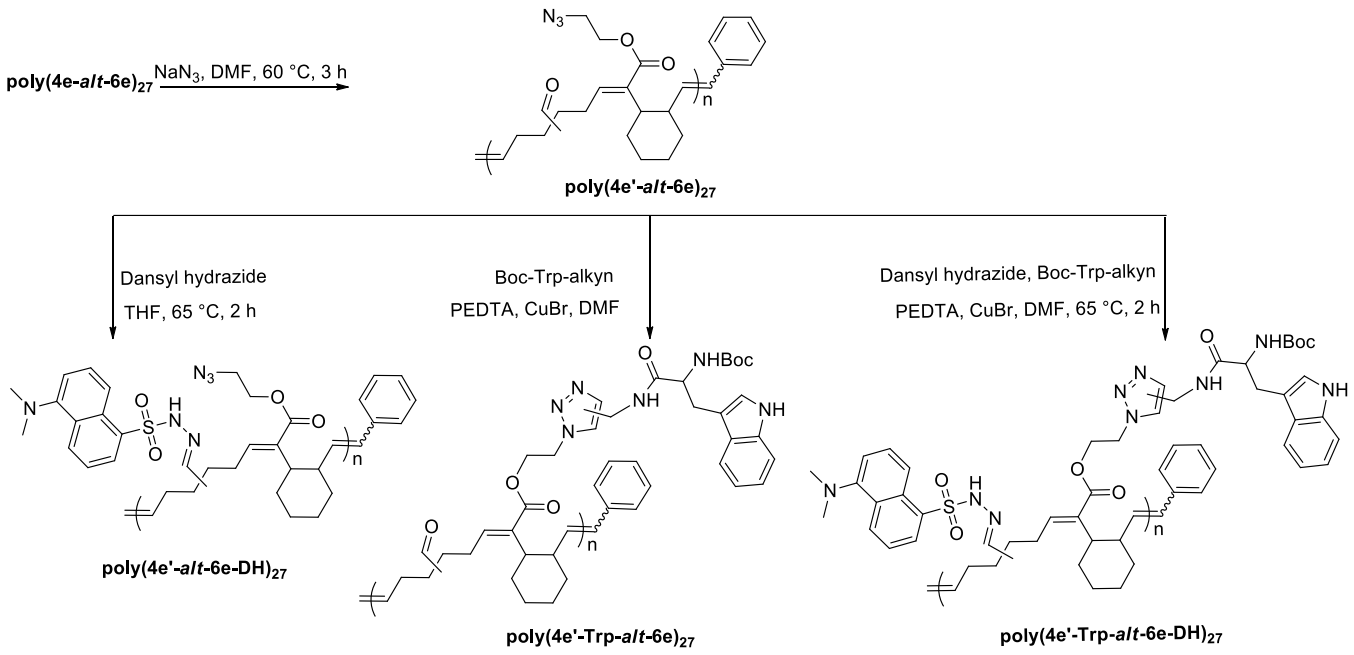

Scheme 5-3. Post polymerization modifications of alternating copolymers poly(**4e**-*alt*-**6e**)$_{27}$.

5.2.4. Characterization of Fluorescent Copolymers.

The fluorescence spectra of all polymers in Scheme 5-2 were obtained to investigate the degree of FRET effect for the polymers conjugated to both tryptophan and dansyl fluorophores. The emission spectra of poly(**4e'**-*alt*-**6e-DH**)$_{27}$ (1.2 μM in THF) with excitation at the characteristic wavelengths of tryptophan (284 nm, red dotted trace) and dansyl fluorophore (335 nm, red solid trace), respectively, were obtained. Figure 5-2a shows the emission spectra of the

donor, dansyl fluorophore, which has an emission maximum at 506~507 nm. Notably, poly(**4e'-*alt*-6e-DH**)$_{27}$ showed a low emission with excitation at 284 nm.

poly(**4e'-Trp-*alt*-6e-DH**)$_{27}$ (1.2 μM in THF) was also excited at 284 nm (blue dotted trace) and 335 nm (blue solid trace) separately. The emission spectrum of poly(**4e'-Trp-*alt*-6e-DH**)$_{27}$ obtained by exciting at 335 nm completely overlaps with that of poly(**4e'-*alt*-6e-DH**)$_{27}$. The emission spectrum of poly(**4e'-Trp-*alt*-6e-DH**)$_{27}$ with excitation at 284 nm (blue dotted trace) displays a much higher emission in comparison to the corresponding emission of poly(**4e'-*alt*-6e-DH**)$_{27}$ (red dotted trace). This result demonstrates that excitation of the tryptophan fluorophore results in energy transfer to excite the dansyl fluorophore when the two fluorophores are placed in very close proximity as a consequence of being attached to the alternating copolymers (Figure 5-2a).

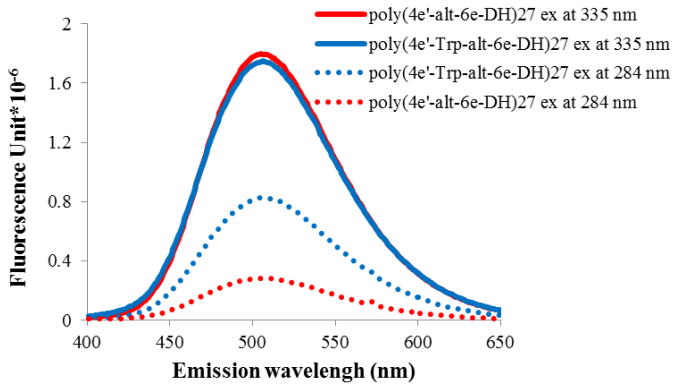

a)

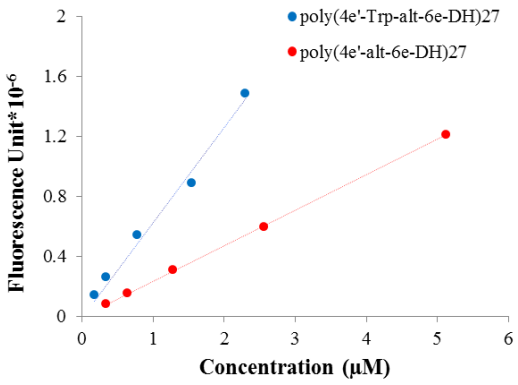

b)

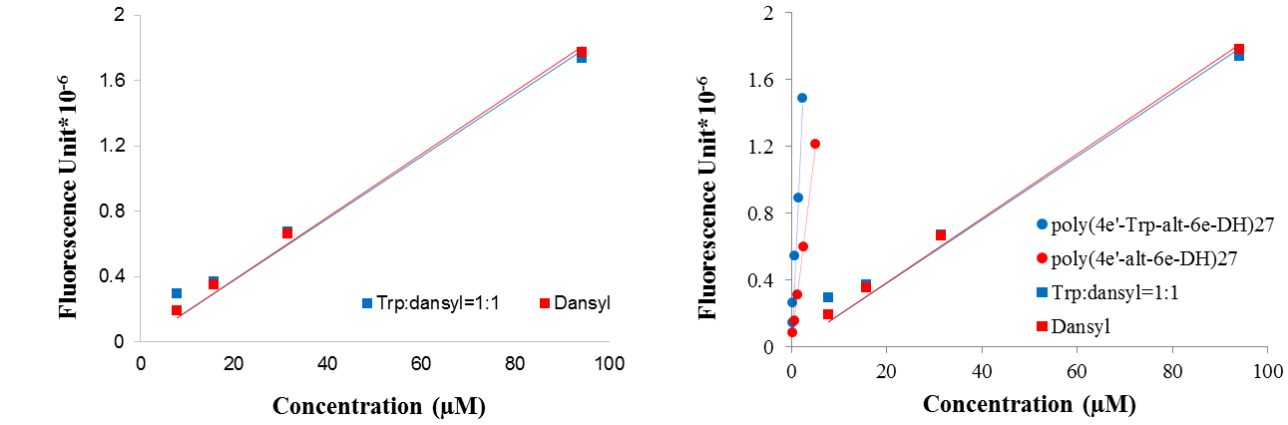

c)

d)

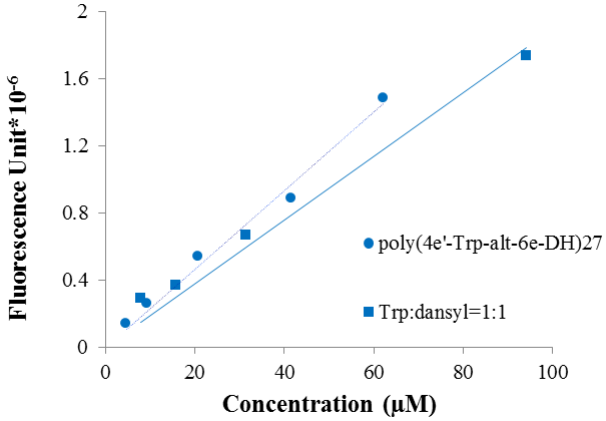

e)

Figure 5-2. Emission of dansyl fluorophore in poly(**4e'**-*alt*-**6e-DH**)$_{27}$ and poly(**4e'-Trp**-*alt*-**6e-DH**)$_{27}$ in THF. a) Comparison of emission of poly(**4e'**-*alt*-**6e-DH**)$_{27}$ and poly(**4e'-Trp**-*alt*-**6e-DH**)$_{27}$ at 1.2 µM. Blue solid trace = emission of poly(**4e'-Trp**-*alt*-**6e-DH**)$_{27}$ with excitation at 335 nm, blue dotted trace = emission of poly(**4e'-Trp**-*alt*-**6e-DH**)$_{27}$ with excitation at 284 nm, red solid trace = emission of poly(**4e'**-*alt*-**6e-DH**)$_{27}$ with excitation at 335 nm and red dotted trace = emission of poly(**4e'**-*alt*-**6e-DH**)$_{27}$ with excitation at 284 nm. b) Plots of FRET emission versus concentration of poly(**4e'**-*alt*-**6e-DH**)$_{27}$ (y=236429x, R^2=0.9998) and poly(**4e'-Trp**-*alt*-**6e-DH**)$_{27}$ at 284 nm (y=633282x, R^2=0.9877). c) Plots of FRET emission of dansyl hydrazide and Boc-Trp-alkyne mixture in a ratio of 1:1 (y=18968x, R^2=0.9746) in comparison to dansyl

hydrazide emission (y=19212, R^2=0.9941) with excitation at 284 nm. d) Comparison of FRET emission of dansyl fluorophores with excitation at 284 nm between polymers and monomers. e) Fluorescence of each AB dyad in comparison to the mixture of the two fluorophores with excitation at 284 nm.

Concentration studies were carried out to determine if these interactions occur inter- or intramolecular. The fluorescence signal of poly(**4e'-Trp**-*alt*-**6e-DH**)$_{27}$ was persistent even at low concentrations and it is 2-fold higher than that of poly(**4e'**-*alt*-**6e-DH**)$_{27}$ as a result of FRET. Moreover, the emission of the dansyl fluorophore in poly(**4e'-Trp**-*alt*-**6e-DH**)$_{27}$ followed Beer-Lambert behavior at concentrations between 0.2 and 3 μM (Figure 5-2b), which demonstrated that FRET is intramolecular and not due to chain-chain transfer. At higher concentrations, the polymers tend to precipitate.

The concentration dependence of fluorophores without the backbone was also evaluated (Figure 5-2c). The mixture of two fluorophores showed no emission difference in comparison to the solution with dansyl fluorophore alone with excitation at 284 nm. These results further demonstrate the presence of FRET when the two fluorophores are positioned in an alternating copolymeric backbone.

Since each poly(**4e'-Trp**-*alt*-**6e-DH**)$_{27}$ strand contains approximately 27 AB repeating dyads, we analyzed the dependence of the FRET for each pair ($y = 23455x$, $R^2 = 0.9877$) in comparison to that of the mixture of two fluorophores ($y = 18968x$, $R^2 = 0.9746$) with excitation at 284 nm (Figure 5-2e) in order to evaluate the efficiency of FRET under such circumstances. We expected a more significant difference. However, poly(**4e'-Trp**-*alt*-**6e-DH**)$_{27}$ has only 25%

higher signal relative to the mixture of the two fluorophores. Tryptophan, as a donor, was reported to have small quantum efficiency (E). When we were selecting the FRET pair, this limitation was overlooked because E depends on the distance between the two fluorophores with an inverse 6th power and the distance in our case is much smaller than that in regular applications. Another effect we think might contribute to the low quantum yield is the degree of rotational freedom within the polymer. The dansyl fluorophore is attached to the ring-opened cyclohexene which is flexible, and the linker between the triazole and the bicyclic ester can also increase the rotational freedom of the tryptophan. However, the 3D structure of the polymers is yet unknown. The structure might limit the rotation of those bonds related to the conformations of the fluorophores. Therefore, in our future work, we will study the effect of linkers and explore FRET pairs with higher quantum yields.

During the fluorescence analysis, we observed the emission of the dansyl fluorophore with excitation at 284 nm, even without the presence of the tryptophan fluorophore. We tested other excitation wavelengths close to 284 nm, searching for the optimum wavelength to diminish the unwanted fluorescent signal. As shown in Figure 5-3, we varied the excitation wavelength from 276 to 297 nm. We observed an emission signal at 507 nm in all of the spectra (Figure 5-3). When excited at wavelengths below 284 nm, all spectra are identical, indicating that the signal is not from direct excitation of the dansyl fluorophore and these wavelengths do not fall in the excitation spectrum of the dansyl fluorophore. The grey curve in Figure 5-4 indicated that the backbone has absorption at the characteristic wavelength of dansyl fluorophore, therefore, the fluorescent we collected at 507 nm from excitation at 335nm is lower than expected, and it also explains why the poly(dansyl) has a lower fluorescence than the monomer. Therefore, the future work of this direction is to replace the FRET pair Trp-danysl with a pair that excites and emits at

a higher wavelength, so the backbone won't interfere with the observation. Fortunately, poly(**4e'**-*alt*-**6e-DH**)$_{27}$ and dansyl hydrazide (Figure 5-2b and c) signals are weaker than the real FRET signal from poly(**4e'-Trp**-*alt*-**6e-DH**)$_{27}$ and we are still able to determine the occurrence of FRET.

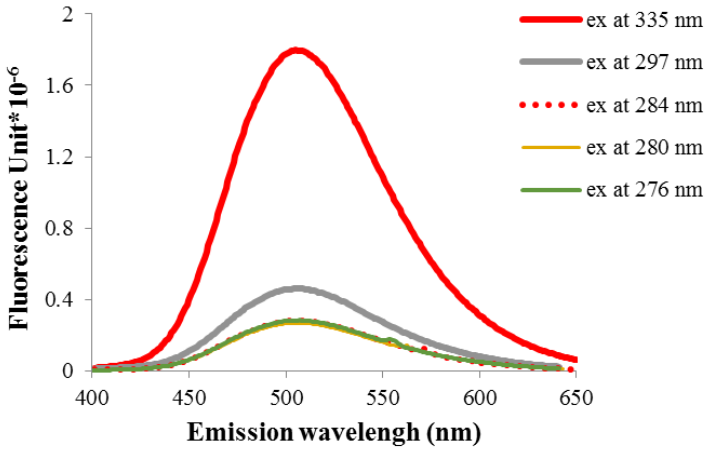

Figure 5-3. Emission of poly(**4e'**-*alt*-**6e-DH**)$_{27}$ excited at different wavelengths.

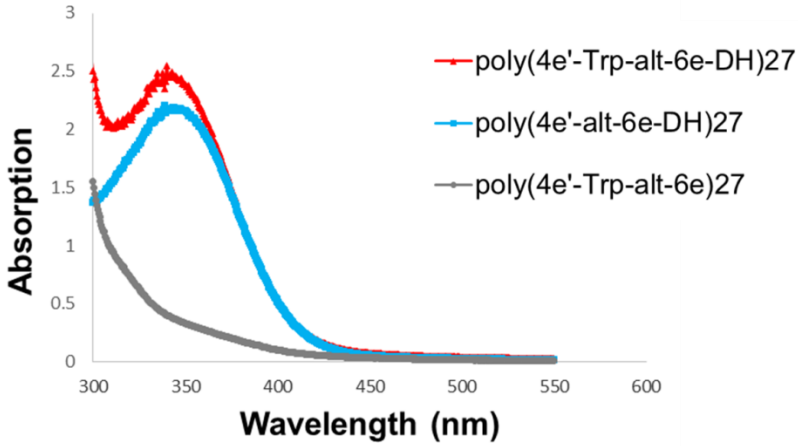

Figure 5-4. UV spectra of all three polymers.

5.3. Conclusion

Alkyl bromide bicyclo[4.2.0]oct-7-ene-7-carboxylate and cyclohexene substituted with aldehyde have been used to prepare alternating copolymers. These orthogonal functionalities provide an efficient route for post-polymerization modification with functional groups that are not compatible with AROMP. Two moieties that interact with each other when in close proximity are easily introduced without affecting the polymer backbone. To demonstrate the utility of this approach, a tryptophan and dansyl fluorophore pair was conjugated onto the bromide/aldehyde derivatized polymers. FRET was observed between fluorophores confirming the substitution, and illustrating the use of the polymer backbone for functional group presentation. These results will guide the direction of future polymer applications towards advanced material properties.

Chapter 6. Future Directions

6.1. Introduction

The ultimate goal of the research which focuses on the synthesis of alternating copolymers is to serve the biochemical and material sciences. With the success of inhibiting backbiting and of obtaining linear and long alternating copolymers, the future direction is to functionalize the polymers. Our collaboration with Dr. Joy Romulus at NYU on the project of alternating copolymers containing charge-transfer units encouraged us to further explore the application of our polymers in energy-transfer material development.

As introduced in Chapter 4, an **AB** 10-mer was obtained which displayed higher charge-transfer efficiency than polymers synthesized otherwise.[126] However, they are too short to be utilized. Moreover, the post polymerization modification of replacing N-hydroxysuccinimide (NHS) is not efficient as it is only 50%. Further experiments have been designed to improve the rate of polymerization and post polymerization efficiency.

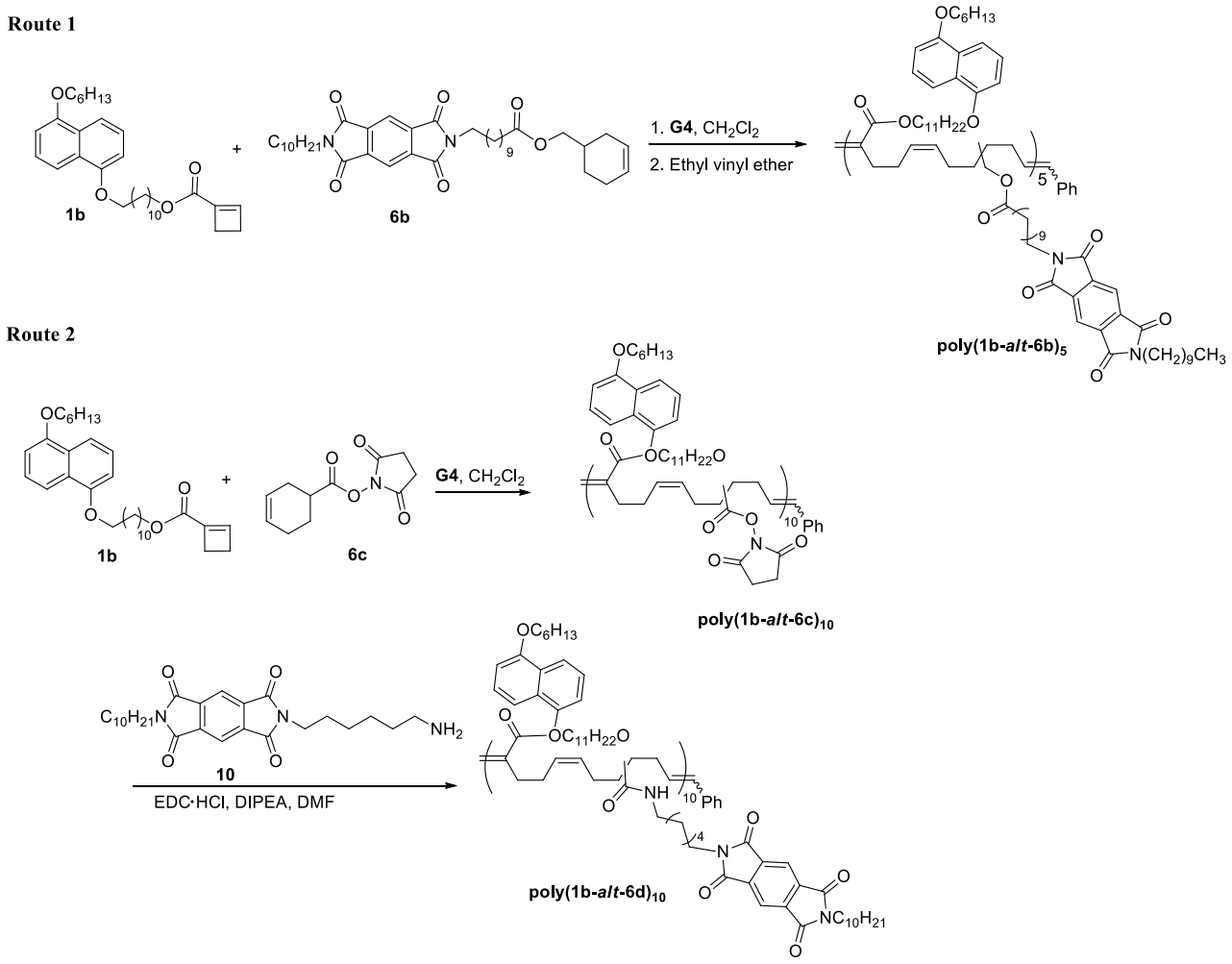

Scheme 6-1. Synthetic scheme of poly(**1b**-*alt*-**6b**)$_n$. [Adapted with permission from Romulus, et al;[126] copyright 2013, Macromolecular Letters]

It takes 8 hours for AROMP with **1b** and **6b** to reach an **AB** 5-mer following route 1 (Scheme 6-1); with optimized route 2, it still takes 6 hours to obtain an **AB** 10-mer. Substituting the side chain on cyclobutene with a less bulky functional group will lead to backbiting and a high molar-mass dispersity. Therefore, the need for a new backbone is vital for further progress.

6.2. Exploration of Backbones.

1) Utilization of a bivalent initiator would double the lengths of the alternating polymers by propagating in two directions. The key of this strategy is the equivalence of the initiator. To obtain linear alternating copolymer, rigorously one equivalent of this bivalent initiator should be used. Otherwise, a dendrimer like structure would be obtained.

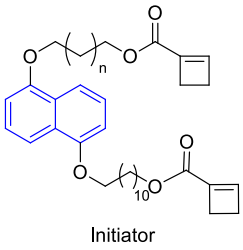

Figure 6-1. Bivalent initiator.

2) Lee, et al demonstrated that ROMP of cyclobutene secondary amides is highly regioselective and stereoselective and provides head-to-tail ordered polymers.[103] If we attach both donor and acceptor to cyclobutene amide, it should provide strictly alternating donor/acceptors.

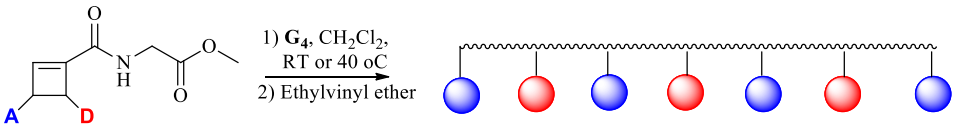

Scheme 6-2. Proposed ROMP of cyclobutene secondary amide containing alternating functionalities.

One of the major concerns of this strategy is the synthesis of the monomer. The bulky side chains might be able to be attached to the carbon neighbors. A linkage might be able to help. Also, the amide coupled with both side chains will be not quite soluble in ROMP solvents such as CH_2Cl_2 or $CHCl_3$. Therefore, side chains should be introduced post-polymerization.

3) We can also utilize the recently developed bicyclic tetrasubstituted α, β-unsaturated secondary amides which AROMP at comparable rates to the ROMP of cyclobutene secondary amides and construct linear and extremely long alternating copolymers.

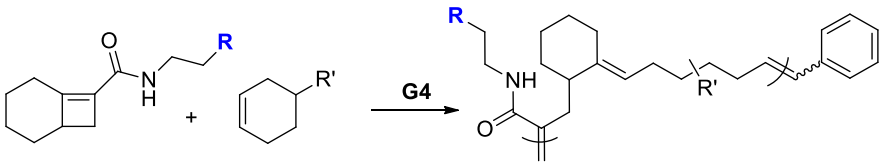

Scheme 6-3. Synthesis of alternating copolymers using bicyclo[4.2.0]oct-6-ene-7-carboxamides and cyclohexene with functional groups.

6.3. Improve Rate of Post Polymerization Modification.

The yield of amide side chain PDI exchanging with NHS is only 50%. We hypothesize that steric hindrance posed by the polymer backbone and other side chains prevents access to the side chain by the NHS ester. A linker introduced between NHS and cyclohexene may help.

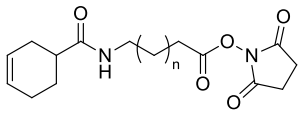

Figure 6-2. Optimization of NHS-cyclohexene.

We can also utilize the orthogonal functionalization introduced in Chapter 5 to attach an alkyl bromide and an aldehyde to AROMP monomers.

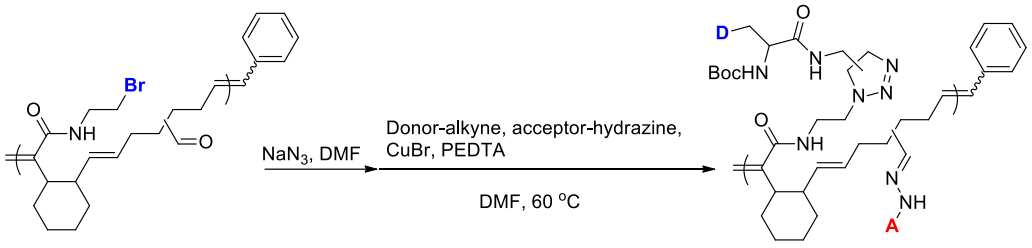

Scheme 6-4. Post polymerization modifications to introduce charge-transfer units.

Chapter 7. Experimental Methods

Materials and General Procedures.

All metathesis reactions were performed under an N_2 atmosphere. Solvents, e.g. THF, CH_2Cl_2, DMF and benzene, were purified with Pure Process Technology (PPT). Deuterated solvents for all metathesis reactions were degassed and filtered through basic alumina before use. [$(H_2IMes)(PCy_3)(Cl)_2Ru$=CHPh] **G3** and ethyl 1-bromocyclobutane carboxylate were purchased from Aldrich. Cyclohexene-D_{10} was purchased from CDN Isotope Inc. The synthesis of Grubbs III catalyst, [$(H_2IMes)(3\text{-Br-Pyr})_2Cl_2Ru$=CHPh] **G4**, was performed according to the procedure of Love, J.A. *et al*.[91] A fresh stock solution of the Grubbs III catalyst (0.02 M for AROMP or 0.03 M for ROM, AROM-1 and AROM-2) and fresh stock solutions of monomers **3** and **4a** (0.17 – 1.0 M for AROMP, depending on the desired length, or 0.03 M for ROM, AROM-1 and AROM-2) were prepared in CD_2Cl_2 for each of the NMR experiments. 11-((5-(Hexyloxy)naphthalen-1-yl)oxy)undecan-1-ol, cyclohex-3-en-1-ylmethyl 3-aminopropanoate and 2-(6-aminohexyl)-6-decylpyrrolo[3,4-f]isoindole-1,3,5,7(2H,6H)-tetraone were obtained from collaborator J. Romulus.[126] Dansyl hydrazide was purchased from Fisher Scientific. Mallinckrodt silica gel 60 (230-400 mesh) was used for column chromatography. Analytical thin layer chromatography (TLC) was performed on precoated silica gel plates ($60F_{254}$), flash chromatography on silica gel-60 (230-400 mesh), and Combi-Flash chromatography on RediSep normal phase silica columns (silica gel-60, 230-400 mesh). Varian Inova400, Inova500, Inova600 and Bruker Nanobay 400, Avance III 500, Avance III 700, Avance III-HD 850 MHz NMR instruments were used for analysis. Chemical shifts were calibrated from residual

undeuterated solvents; they are denoted in ppm (δ). The degree of polymerization (DP) of linear polymers was assessed by ^{1}H NMR integration of polymer alkene protons relative to that of the phenyl end group. Molecular weights and molar-mass dispersities were estimated by gel permeation chromatography with UV detection, THF as the eluent, and a flow rate of 0.700 mL/min on an American Polymer Standards column (Phenogel 5 μ MXL GPC column, Phenomenex). All GPCs were calibrated with poly(styrene) standards with molecular weight ranging from 2,000 – 50,0000 at 30 °C. Fluorescent experiments were performed on an Applied Phototechnology fluorescence spectrophotometer. The excitation and emission slits were set at 8 nm, and a 1.5 cm^3 cuvette was used.

Monomer Synthesis

11-(5-(Hexyloxy)naphthalen-1-yloxy)undecyl cyclobut-1-enecarboxylate, 1b.

Cyclobut-1-enecarboxylic acid was prepared according to the procedure for the preparation of 3,3-dimethylcylobutene carboxylic acid as described by Campbell et al[212] and modified as previously reported.[1] To a solution of cyclobut-1-enecarboxylic acid (190 mg, 1.94 mmol) and dicyclohexylcarbodiimide (DCC) (417 mg, 2.04 mmol) in CH_2Cl_2 (10 mL) stirred at 0 °C for 30 minutes, 11-((5-(hexyloxy)naphthalen-1-yl)oxy)undecan-1-ol (400 mg, 0.97 mmol) and a catalytic amount of dimethylaminopyridine (DMAP) were added. The mixture was allowed to warm to room temperature over 12 h. CH_2Cl_2 was evaporated under reduced pressure and the crude product was purified by flash chromatography (1:1/Hexanes:CH_2Cl_2) to afford **1** in 35% yield: ^{1}H NMR (600 MHz, $CDCl_3$) δ 7.86 (d, J = 8.2 Hz, 2H), 7.36 (t, J = 7.6 Hz, 2H), 6.84 (d, J = 7.2 Hz, 2H), 6.80 (s, 1H), 4.10 (m, 6H), 2.74 (s, 1H), 2.47 (s, 1H), 1.93 (d, J = 6.3 Hz, 2H), 1.67 (d, J = 6.4 Hz, 1H), 1.58 (d, J = 5.7 Hz, 2H), 1.36 (d, J = 45.9 Hz, 8H), 0.94 (s, 2H). ^{13}C

NMR (126 MHz, $CDCl_3$) δ 162.3, 154.6, 154.6, 146.1, 146.1, 138.8, 126.7, 124.9, 113.9, 113.9, 105.1, 68.0, 64.2, 64.2, 33.9, 32.7, 31.6, 29.5, 29.4, 29.4, 29.4, 29.3, 29.2, 29.0, 28.7, 28.6, 25.9, 25.8, 22.6, 14.0.

Bicyclo[2.2.1]hept-2-ene-2-carboxylic Acid.[141, 213]

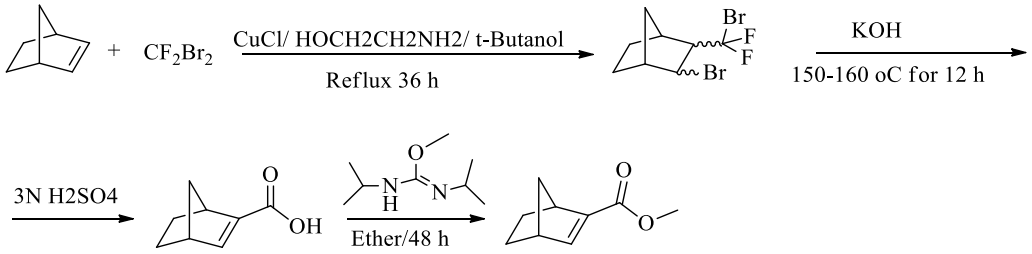

A modification of the 3-step procedure of Elsheimer was followed.[141] **Safety Warning:** CF_2Br_2 has a very low boiling point and addition of CF_2Br_2 to norbornene is very exothermic. Therefore, for a large-scale reaction, this procedure should be done carefully behind a safety shield.

2-Bromo-3-(bromodifluoromethyl)bicyclo[2.2.1]heptanes. To a mixture of norbornene (6.10 g, 65 mmol), CuCl (0.99 g, 1 mmol), ethanolamine (3.00 g, 50 mmol), and tert-butyl alcohol (7.40 g, 100 mmol) in a 50-mL flask, CF_2Br_2 was slowly added (27.30 g, 130 mmol). The resulting mixture was protected from light and stirred at reflux (80-85 °C) for 48 h. Then it was cooled and diluted with deionized water (50 mL) and Et_2O (25 mL). The Et_2O layer was washed with H_2O (5 × 25 mL), and dried over anhydrous Na_2SO_4. After filtration, the extract was concentrated and the residue was purified by flash column chromatography to yield a mixture of exo- and endo-bicyclo[2.2.1]heptanes as a colorless oil (16.75 g, 87%): ^{1}H NMR (500 MHz, $CDCl_3$) δ 4.09 (d, J = 10 Hz, 1H), 2.78 (td, J = 15 Hz, 10 Hz, 1H), 2.71 (s, 1H), 2.68 (d, J = 10 Hz, 1H), 2.12 (d, J = 10 Hz, 1H), 1.76 (m, 1H), 1.64 (m, 1H), 1.40-1.20 (m, 3H).

Bicyclo[2.2.1]hept-2-ene-2-carboxylic acid. In a screw-top vial under an N_2 atmosphere, KOH (5.89 g, 10.5 mmol) was dissolved in deionized H_2O (4 mL). 2-Bromo-3-(bromodifluoromethyl)bicyclo[2.2.1]heptanes (0.776 g, 2.66 mmol) was added to the solution and the mixture was heated at 130 °C in a microwave reactor at 20 bar for 2 h. Then the solution was cooled and washed with $CHCl_3$ (2 × 4 mL), and the pH of the basic extract was adjusted to 2 with 3N aq HCl. The aqueous mixture was extracted with $CHCl_3$ (3 × 4 mL) and the combined $CHCl_3$ solution was dried over anhydrous Na_2SO_4 and concentrated *in vacuo* to give a brown oil. Purification by flash column chromatography (95:5/CH_2Cl_2:MeOH) yielded bicyclo[2.2.1]hept-2-ene-2-carboxylic acid as a colorless oil (160 mg, 50%).

Methyl bicyclo[2.2.1]hept-2-ene-2-carboxylate, **2**. The procedure of Mathias was followed.[213] Bicyclo[2.2.1]hept-2-ene-2-carboxylic acid (40 mg, 0.29 mmol) was treated with *N,N*-diisopropyl-*O*-methylisourea (180 mg, 1.16 mmol) in dry ether (5 mL) and stirred for 48 h. The urea byproduct precipitated at -20 ^oC and it was removed by filtration. Removal of the solvent afforded a yellow oil which was purified by flash column chromatography (90:10/hexane:CH_2Cl_2) to yield ester **2** (26 mg, 58%): ^1H NMR (400 MHz, CD_2Cl_2) δ 6.91 (d, J = 2.8 Hz, 1H), 3.72 (s, 3H), 3.26 (s, 1H), 3.02 (s, 1H), 1.75 (m, 2H), 1.48 (d, J = 8.4 Hz, 1H), 1.20 (d, J = 8.4 Hz, 1H). ^{13}C NMR (100 MHz, $CDCl_3$) δ 164.9, 146.6, 140.5, 51.0, 48.0, 43.4, 41.8, 24.5, 24.4.

General procedure for the synthesis of bicyclo[n.2.0] monomers.

These monomers were prepared according to Snider's approach;[145] the purification of monomer **4** was modified as noted. To a 50-mL flask with anhydrous $AlCl_3$ powder under an N_2 atmosphere was added dry benzene and methyl propiolate. The mixture was stirred until a

homogeneous yellow solution formed. Cycloalkene was added and the resulting mixture was stirred for 7 days. The reaction mixture was cooled in an ice bath and quenched with saturated NH_4Cl solution. The precipitate was removed by filtering the resulting mixture through a pad of Celite. The filtrate was extracted with three portions of Et_2O and the combined Et_2O extract was washed with brine and dried over anhydrous $MgSO_4$. The solvent was removed *in vacuo* and the crude product was subjected to flash column chromatography.

Methyl bicyclo[3.2.0]hept-6-ene-6-carboxylate, **3.**

$AlCl_3$ (160 mg, 1.21 mmol, 0.5 equiv), methyl propiolate (204 mg, 2.42 mmol) and cyclopentene (170 μL, 2.90 mmol, 1.2 equiv) were stirred for 7 days in dry benzene (50 mL). Flash column chromatography of the crude product (30:70/hexane:CH_2Cl_2) yielded ester **3** (175 mg, 48% yield): ^{1}H NMR (400 MHz, acetone-D_6): δ 6.62 (br s, 1H), 3.69 (s, 3H), 3.33 (br dd, J = 3.2 Hz, J' = 7.6 Hz, 1H), 3.06 (br dd, J = 3.6 Hz, 8.0 Hz, 1H), 1.78-1.21 (m, 6H). ^{13}C NMR (100 MHz, $CDCl_3$) δ 162.5, 147.5, 138.2, 51.1, 46.9, 44.5, 25.5, 25.4, 22.9.

Bicyclo[3.2.0]hept-6-ene-6-carboxylic acid.

3 (500 mg, 3.29 mmol) in THF (5 mL) was cooled in an ice bath, 2N KOH (20 mL) was added, and the solution was stirred for 30 min. The ice bath was removed and the reaction mixture was allowed to warm to 25 ^{o}C and stirred for another 4 h. THF was evaporated and the aqueous solution was acidified with 2N HCl to pH 2. The solution was extracted with CH_2Cl_2 (3 × 20 mL) and the combined CH_2Cl_2 solution was dried over anhydrous $MgSO_4$. The solvent was removed after filtration and the product bicyclo[3.2.0]hept-6-ene-6-carboxylic acid (350 mg, 80%)was used without further purification.

Methyl bicyclo[4.2.0]oct-7-ene-7-carboxylate, **4a.**

$AlCl_3$ (227 mg, 1.72 mmol, 0.86 equiv), methyl propiolate (168 mg, 2.00 mmol) and cyclohexene (263 μL, 2.60 mmol, 1.30 equiv) were stirred for 7 days in dry benzene (5 mL), and yielded a mixture of compound **4a** and isomer methyl (*E*)-3-(cyclohex-1-enyl)propenoate in a ratio of 1:0.11~0.23. The mixture was treated with *m*-chloroperoxybenzoic acid (*m*-CPBA) to epoxidize the isomer byproduct followed by flash column chromatography (30:70/hexane:CH_2Cl_2) to provide bicyclic ester **4a** (210 mg, 65% yield): ^{1}H NMR (400 MHz, acetone-D_6): δ 6.89 (d, J = 1.2 Hz, 1H), 3.71 (s, 3H), 3.07-3.04 (m, 1H), 2.80-2.77 (m, 1H), 2.00-1.30 (m, 8H). ^{13}C NMR (100 MHz, $CDCl_3$) δ 162.4, 150.1, 141.4, 50.7, 39.8, 38.1, 23.5, 23.3, 18.6, 18.0.

Bicyclo[4.2.0]oct-7-ene-7-carboxylic acid.

4a (2.00 g, 12.0 mmol) in THF (5 mL) was cooled in an ice bath, 2N KOH (20 mL) was added, and the solution was stirred for 30 min. The ice bath was removed and the reaction mixture was allowed to warm to 25 ^{o}C and stirred for another 4 h. THF was evaporated and the aqueous solution was acidified with 2N HCl to pH 2. The solution was extracted with CH_2Cl_2 (3 × 20 mL) and the combined CH_2Cl_2 solution was dried over anhydrous $MgSO_4$. The solvent was removed after filtration and the product bicyclo[4.2.0]oct-7-ene-7-carboxylic acid (1.74 g, 95%) was used without further purification.

2-Bromoethyl bicyclo[4.2.0]oct-7-ene-7-carboxylate, **4e**.

Bicyclo[4.2.0]oct-7-ene-7-carboxylic acid (500 mg, 3.3 mmol) was dissolved in 5 mL of CH_2Cl_2 and was cooled in an ice bath when oxalyl chloride (5 mL) was added. The reaction was stirred for 30 min followed by evaporation to yield bicyclo[4.2.0]oct-7-ene-7-carbonyl chloride as off white oil. 2-Bromoethanol (1.2 mg, 10 mmol), EDC•HCl (630 mg, 3.3 mmol), DIPEA (425 mg,

3.3 mmol) were mixed with the acyl chloride oil in 20 mL of CH_2Cl_2. The mixture was stirred for 16 h and was washed with 5% $NaHCO_3$ (3×), 1N HCl (3×) and brine (2×) sequentially and dried over anhydrous $MgSO_4$. The solvent was filtered and removed by evaporation. The crude was subjected to flash silica chromatography (30:70/hexane:CH_2Cl_2) to yield **4e** (590 mg, 70%): ^{1}H NMR (500 MHz, CD_2Cl_2): δ 6.91 (d, J = 1.1 Hz, 1H), 4.46 (m, 2H), 3.60 (t, J = 6.1 Hz, 2H), 3.04 (dd, J = 10.3 Hz, J = 5.6 Hz, 1H), 2.77 (td, J = 5.6 Hz, J = 1.1 Hz, 1H), 1.74 (m, 3H), 1.55-1.38 (m, 5H). ^{13}C NMR (100 MHz, $CDCl_3$) δ 161.4, 151.6, 141.0, 63.0, 40.0, 38.4, 28.6, 23.4, 18.8, 18.2. HRMS (ESI) calcd. for $C_{11}H_{15}BrO_2$ $[M+H]^+$ 258.0255, found 258.0248.

Methyl bicyclo[5.2.0]non-8-ene-8-carboxylate, **5.**

$AlCl_3$ (1.00 g, 7.56 mmol, 0.5 equiv), methyl propiolate (1.27 g, 15.2 mmol) and cycloheptene (2.16 mL, 18.2 mmol, 1.2 equiv) were stirred for 7 days in dry benzene (50 mL). Flash column chromatography of the crude product (30:70/hexane:CH_2Cl_2) yielded **5** (1.40 g, 50% yield): ^{1}H NMR (400 MHz, $CDCl_3$): δ 6.70 (d, J = 1 Hz, 1H), 3.61 (s, 3H), 2.99 (m, 1H), 2.77 (m, 1H), 1.77-1.21 (m, 10H). ^{13}C NMR (100MHz, $CDCl_3$) δ 162.6, 148.9, 140.5, 50.6, 46.9, 45.4, 31.6, 29.1, 28.6, 27.9, 27.7.

2,5-Dioxopyrrolidin-1-yl cyclohex-3-enecarboxylate, **6c**.

3-Cyclohexene-1-carboxylic acid (100 mg, 0.79 mmol), N-hydroxysuccinimide (100 mg, 0.87 mmol), and ethyl, dimethylaminopropyl carbodiimide hydrochloride (EDC•HCl) (182 mg, 0.95 mmol) were dissolved in CH_2Cl_2 and cooled in an ice bath. Then DIEA was added to adjust the pH to 8-9. The reaction was stirred for 16 h and washed with 5% Na_2CO_3 (50 mL). The organic phase was dried and condensed, followed by flash chromatography, eluted with 100% CH_2Cl_2 to yield 6c as a white solid in 80% yield: ^{1}H NMR (600 MHz, $CDCl_3$) δ 5.88 – 5.44 (m, 2H), 3.01 –

2.80 (m, 1H), 2.76 (s, 4H), 2.42 – 2.22 (m, 2H), 2.17 – 1.92 (m, 3H), 1.90 – 1.62 (m, 1H). ^{13}C NMR ($CDCl_3$) δ 170.6, 169.2, 126.6, 124.0, 36.6, 26.9, 25.4, 24.6, 23.6.

General procedure for the synthesis of bicyclo[n.2.0]alkene amides.

To bicyclo[n.2.0]alkene carboxylic acid, EDC•HCl and the amine in a 50-mL flask was added dry CH_2Cl_2 and cooled in an ice bath. DIPEA was added to adjust pH to 8~9. The mixture was stirred for 8 h until all of the acid has been consumed. Workup was accomplished by wash with 5% $NaHCO_3$ (3×), 1N HCl (3×), and brine (2×) sequentially and dried over anhydrous $MgSO_4$ and the solvent was filtered and removed in vacuo. The crude product was subjected to flash silica chromatography.

Methyl 2-(bicyclo[4.2.0]oct-7-enecarboxamido)propanoate, **8a.**

Bicyclo[4.2.0]oct-7-ene-7-carboxylic acid (100 mg, 0.66 mmol), HCl•Ala-OMe (104 mg, 0.72 mmol) and EDC•HCl (139 mg, 0.72 mmol) were dissolved in CH_2Cl_2 and cooled in an ice bath. DIPEA was then added and the general procedure followed. Chromatography (97:3/CH_2Cl_2:MeOH) yielded amide **8a**, (146 mg, 80%). ^{1}H NMR (600 MHz, $CDCl_3$): δ 6.70 (d, J = 6.7 Hz, 1H, =CH), 6.19 (d, J = 5.6 Hz, 1H, CONH), 4.61 (qd, J = 7.2, 2.6 Hz, 1H, side chain CH), 3.71 (s, 3H, OCH_3), 3.05 (m, 1H, CH), 2.74 (m, 1H, CH), 1.79 (m, 1H, CH_2), 1.69 (m, 2H, CH_2), 1.52 (m, 3H, CH_2), 1.39 (m, 5H, CH_2 and CH_3). ^{13}C NMR (126 MHz, $CDCl_3$): δ 173.5 (COOR), 162.1 (CONH), 145.2 (=CH), 144.1 (=CH), 52.4 (OCH_3), 47.5 (side chain CH), 39.3 (CH), 37.6 (CH), 23.8 (CH_2), 23.6 (CH_2), 18.7 (CH_2), 18.5 (CH_2), 18.2 (CH_3). Apparent peak doublets that arise from the presence of two diastereomers were reported as a single chemical shift. HRMS (ESI) calcd. for $C_{13}H_{19}NO_3$ $[M+H]^+$ 238.1438, found 238.1429.

Methyl 2-(bicyclo[4.2.0]oct-7-enecarboxamido)acetate, **8b.**

Bicyclo[4.2.0]oct-7-ene-7-carboxylic acid (100 mg, 0.66 mmol), HCl•Gly-OMe (87 mg, 0.69 mmol) and EDC•HCl (139 mg, 0.72 mmol) were dissolved in CH_2Cl_2 and cooled in an ice bath. DIPEA was then added and the general procedure followed. Chromatography (97:3/CH_2Cl_2:MeOH) yielded amide **8b**, (146 mg, 80%). ^{1}H NMR (400 MHz, $CDCl_3$): δ 6.71 (s, 1H, =CH), 6.36 (s, 1H, CONH), 4.03 (m, 2H, side chain CH_2), 3.70 (s, 3H, OCH_3), 3.02 (dd, *J* = 10.4, 5.3 Hz, 1H, CH), 2.74 (dd, *J* = 9.7, 4.8 Hz, 1H, CH), 1.77 (m, 1H, CH_2), 1.67 (m, 2H, CH_2), 1.52 (m, 3H, CH_2), 1.37 (m, 2H, CH_2). ^{13}C NMR (101 MHz, $CDCl_3$): δ 170.3 (COOR), 162.6 (CONH), 145.1 (=CH), 143.9 (=CH), 52.1 (OCH_3), 40.5 (side chain CH_2), 39.3 (CH), 37.6 (CH), 23.6 (CH_2), 23.5 (CH_2), 18.5 (CH_2), 18.1 (CH_2). HRMS (ESI) calcd. for $C_{12}H_{17}NO_3$ $[M+H]^+$ 224.1281, found 224.1273.

N-Propylbicyclo[4.2.0]oct-7-ene-7-carboxamide, **8c.**

Bicyclo[4.2.0]oct-7-ene-7-carboxylic acid (300 mg, 2.0 mmol), propylamine (130 mg, 2.2 mmol) and EDC•HCl (421 mg, 2.2 mmol) were dissolved in CH_2Cl_2 and cooled in an ice bath. DIPEA was then added and the general procedure followed. Chromatography (97:3/CH_2Cl_2:MeOH) yielded amide **8c**, (307 mg, 80%). ^{1}H NMR (400 MHz, $CDCl_3$): δ 6.71 (s, 1H, =CH), 6.36 (s, 1H, CONH), 4.03 (m, 2H, side chain CH_2), 3.70 (s, 3H, OCH_3), 3.02 (dd, *J* = 10.4, 5.3 Hz, 1H, CH), 2.74 (dd, *J* = 9.7, 4.8 Hz, 1H, CH), 1.77 (m, 1H, CH_2), 1.67 (m, 2H, CH_2), 1.52 (m, 3H, CH_2), 1.37 (m, 2H, CH_2). ^{13}C NMR (101 MHz, $CDCl_3$): δ 170.3 (COOR), 162.6 (CONH), 145.1 (=CH), 143.9 (=CH), 52.1 (OCH_3), 40.5 (side chain CH_2), 39.3 (CH), 37.6 (CH), 23.6 (CH_2), 23.5 (CH_2), 18.5 (CH_2), 18.1 (CH_2). HRMS (ESI) calcd. for $C_{12}H_{17}NO_3$ $[M+H]^+$ 224.1281, found 224.1273.

N-Phenylbicyclo[4.2.0]oct-7ene-7-carboxamide, **8d**.

Bicyclo[4.2.0]oct-7-ene-7-carboxylic acid (300 mg, 2.0 mmol), aniline (204 mg, 2.2 mmol) and EDC•HCl (421 mg, 2.2 mmol) were dissolved in CH_2Cl_2 and cooled in an ice bath. DIPEA was then added and the general procedure followed. Chromatography (98:2/CH_2Cl_2:MeOH) yielded amide **8d**, (170 mg, 40%). ^{1}H NMR (500 MHz, $CDCl_3$): δ 7.58 (d, *J* = 7.8 Hz, 2H, Ph), 7.36 (s, 1H, CONH), 7.31 (t, *J* = 7.9 Hz, 2H, Ph), 7.10 (t, *J* = 7.4 Hz, 1H, Ph), 6.83 (s, 1H, =CH), 3.15 (dd, *J* = 10.5, 5.5 Hz, 1H, CH), 2.82 (q, *J* = 5.1 Hz, 1H, CH), 1.89 (m, 1H), 1.78 (m, 2H), 1.60 (m, 3H), 1.46 (m, 2H). ^{13}C NMR (126 MHz, $CDCl_3$): δ 160.6 (CONH), 145.4 (=CH), 145.0 (=CH), 137.6 (Ph), 129.0 (Ph), 129.0 (Ph), 124.2 (Ph), 124.2 (Ph), 119.6 (Ph), 39.6 (CH), 37.6 (CH), 24.0 (CH_2), 23.7 (CH_2), 18.8 (CH_2), 18.3 (CH_2). HRMS (ESI) calcd. for $C_{15}H_{17}NO$ $[M+H]^+$ 228.1383, found 228.1382.

N-(3-*p*-Tolylpropyl)bicycle[4.2.0]oct-7-ene-7-carboxamide, **8e**.

Bicyclo[4.2.0]oct-7-ene-7-carboxylic acid (97 mg, 0.64 mmol), 3-*p*-tolylpropan-1-amine (100 mg, 0.67 mmol) and EDC•HCl (129 mg, 0.67 mmol) were dissolved in CH_2Cl_2 and cooled in ice bath. DIPEA was then added and the general procedure followed. Chromatography (97:3/CH_2Cl_2:MeOH) yielded amide **8e**, (147 mg, 85%). ^{1}H NMR (600 MHz, $CDCl_3$): δ 7.17 – 6.97 (m, 4H, Ph), 6.65 (s, 1H, =CH), 5.66 (m, 1H, CONH), 3.35 (m, 2H, side chain CH_2), 2.97 (dd, *J* = 10.5, 5.6 Hz, 1H, CH), 2.75 (q, *J* = 5.1 Hz, 1H, CH), 2.62 (t, *J* = 7.6 Hz, 2H, side chain CH_2), 2.30 (s, 3H, CH_3), 1.84 (m, 2H, side chain CH_2), 1.78 (m, 2H, CH_2), 1.65 (m, 1H, CH_2), 1.55 (m, 3H, CH_2), 1.42 (m, 2H, CH_2). ^{13}C NMR (101 MHz, $CDCl_3$): δ 162.7 (CONH), 144.7 (=CH), 143.7 (=CH), 138.3 (Ph), 135.3 (Ph), 129.0 (Ph), 129.0 (Ph), 128.1 (Ph), 128.1 (Ph), 39.2 (side chain CH_2), 38.6 (CH), 37.4 (CH), 32.9 (side chain CH_2), 31.2 (side chain CH_2), 23.9

(CH_2), 23.7 (CH_2), 20.8 (side chain CH_3), 18.6 (CH_2), 18.2 (CH_2). HRMS (ESI) calcd. for $C_{19}H_{25}NO$ $[M+H]^+$ 284.2009, found 284.2005.

2-(Bicycle[4.2.0]oct-7-ene-carboxamido)-(R)-2-phenylethyl propionate, **8f/8f***.

Bicyclo[4.2.0]oct-7-ene-7-carboxylic acid (200 mg, 2.0 mmol), (S)-2-phenylglycinol (400 mg, 2.2 mmol), and EDC•HCl (281 mg, 2.2 mmol) were allowed to react and subjected to work up as described. The crude product was developed on silica TLC plates with 20:1/CH_2Cl_2:MeOH and two partially separated spots were observed with R_f values = 0.32 and 0.25. Chromatography (97:3/CH_2Cl_2:MeOH) yielded two diastereomers: **A** (60 mg, 11%) and **A*** (50 mg, 9%). Each diastereomer (50 mg, 0.18 mmol) was mixed with acetic anhydride (20.7 mg, 0.203 mmol) and TEA (20.5 mg, 0.203 mmol) in anhydrous CH_2Cl_2, and the mixture was stirred for 16 h. After concentrating *in vacuo,* the reaction mixture was subjected to flash chromatography (97:3/CH_2Cl_2:MeOH) to yield amide **1f** (41 mg, 62%) from the higher R_f alcohol **A**. ^{1}H NMR (500 MHz, $CDCl_3$): δ 7.42-7.23 (m, 5H, Ph), 6.75 (s, 1H, =CH), 6.20 (d, *J* = 7.8 Hz, 1H, CONH), 5.35 (td, *J* = 7.8, 5.0 Hz, 1H, CH), 4.50 (dd, *J* = 11.5, 7.7 Hz, 1H, CH_2O), 4.26 (dd, *J* = 11.5, 4.6 Hz, 1H, OCH_2), 3.06 (q, *J* = 5.5 Hz, 1H, CH), 2.78 (q, *J* = 4.9 Hz, 1H, CH), 2.04 (s, 3H, CH_3), 1.83 (m, 1H, CH_2), 1.76 – 1.68 (m, 2H, CH_2), 1.58 (m, 3H, CH_2), 1.44 (m, 2H, CH_2). ^{13}C NMR (126 MHz, $CDCl_3$): δ 171.2 (COOR), 162.2 (CONH), 145.1 (=CH), 144.3 (=CH), 138.2 (Ph), 128.7 (Ph), 128.7 (Ph), 127.9 (Ph), 126.6 (Ph), 126.6 (Ph), 65.8 (OCH_2), 52.1 (side chain CH), 39.4 (CH), 37.6 (CH), 23.8 (CH_2), 23.7 (CH_2), 20.7 (CH_3), 18.7 (CH_2), 18.3 (CH_2). HRMS (ESI) calcd. for $C_{20}H_{25}NO_3$ $[M+H]^+$ 314.1751, found 314.1749. Amide **8f*** (45 mg, 66%) was obtained from the lower R_f alcohol **A***. ^{1}H NMR (500 MHz, $CDCl_3$): δ 7.42 – 7.23 (m, 5H, Ph), 6.76 (s, 1H, =CH), 6.27 (d, *J* = 7.2 Hz, 1H, CONH), 5.35 (td, *J* = 7.8, 4.6 Hz, 1H, CH), 4.54

(dd, J = 11.5, 7.7 Hz, 1H, CH_2O), 4.27 (dd, J = 11.5, 4.5 Hz, 1H, OCH_2), 3.07 (dd, J = 10.5, 5.6 Hz, 1H, CH), 2.81 (dd, J = 9.9, 4.9 Hz, 1H, CH), 2.03 (s, 3H, CH_3), 1.87 (m, 1H, CH_2), 1.75 (m, 2H, CH_2), 1.59 (m, 3H, CH_2), 1.46 (m, 2H, CH_2). ^{13}C NMR (126 MHz, $CDCl_3$): δ 171.5 (COOR), 162.2 (CONH), 144.8 (=CH), 144.4 (=CH), 138.3 (Ph), 128.8 (Ph), 128.8 (Ph), 127.9 (Ph), 126.5 (Ph), 126.5 (Ph), 66.1 (OCH_2), 52.3 (side chain CH), 39.4 (CH), 37.7 (CH), 24.0 (CH_2), 23.7 (CH_2), 20.8 (CH_3), 18.7 (CH_2), 18.3 (CH_2). HRMS (ESI) calcd. for $C_{20}H_{25}NO_3$ $[M+H]^+$ 314.1751, found 314.1742.

Methyl 2-(bicyclo[3.2.0]hept-6-enecarboxamido)propanoate, **9**.

Bicyclo[3.2.0]hept-6-ene-6-carboxylic acid (138 mg, 1 mmol), HCl•Ala-OMe (157 mg, 1.1 mmol) and EDC•HCl (210 mg, 1.1 mmol) were dissolved in CH_2Cl_2 and cooled in an ice bath. DIPEA was then added and the general procedure followed. Chromatography (97:3/CH_2Cl_2:MeOH) yielded amide **9** (157 mg, 75%). ^{1}H NMR (600 MHz, $CDCl_3$): δ 6.49 (d, J = 5.0 Hz, 1H, =CH), 6.21 (s, 1H, CONH), 4.64 (m, 1H, CH), 3.75 (s, 3H, OCH_3), 3.32 (s, 1H, CH), 3.02 (d, J = 7.2 Hz, 1H, CH), 1.78-1.70 (m, 1H), 1.68-1.60 (m, 2H, CH_2), 1.57-1.54 (m, 1H, CH_2), 1.40 (d, J = 7.1 Hz, 3H, CH_3), 1.30-1.23 (m, 2H, CH_2). ^{13}C NMR (101 MHz, $CDCl_3$): δ 173.5 (COOR), 161.6 (CONH), 142.1 (=CH), 140.6 (=CH), 52.4 (OCH_3), 47.4 (side chain CH), 45.8 (CH), 43.9 (CH), 25.6 (CH_2), 25.4 (CH_3), 23.0 (CH_2), 23.1 (CH_2), 18.6 (CH_2), 18.6 (CH_2). Apparent peak doublets that arise from the presence of two diastereomers were reported as a single chemical shift. HRMS (ESI) calcd. for $C_{12}H_{17}NO_3$ $[M+H]^+$ 224.1281, found 224.1278.

General procedure for isomerization of amides.

Under an N_2 atmosphere, a solution of the original amide and catalyst **G4** was prepared in the indicated solvent (600 μL) in an NMR tube and NMR spectra were acquired at 35 ℃. At the end of the isomerization reaction (after complete consumption or no further isomerization of amide as judged by the change of the olefinic proton resonance), each reaction was terminated with ethyl vinyl ether (100 μL) and stirred for 30 min. The solvent was evaporated and each of the residues was purified by silica chromatography with CH_2Cl_2:MeOH to isolate the isomerized amide.

Methyl 2-(bicyclo[4.2.0]oct-6-enecarboxamido)propanoate, **8a'**.

Amide **8a** (28.4 mg, 0.12 mmol) and **G4** (5.3 mg, 0.006 mmol) were mixed in CD_2Cl_2 in an NMR tube, ^{1}H NMR spectrum was acquired in 16 h and followed by termination with ethyl vinyl ether. 90% of amide **8a** was isomerized to yield **8a'**. Partial ^{1}H NMR of the crude **8a'** (600 MHz, $CDCl_3$): δ 6.75 (s, 0.1H, =CH), 6.13 (s, 0.1H, CONH), 5.98 (s, 0.9H, CONH), 4.64 (m, 1H, CH). (Partial ^{1}H NMR spectroscopic data are reported due to incomplete isomerization and significant upfield overlap of **8a** with the new peaks from **8a'**.)

Methyl 2-(bicyclo[4.2.0]oct-6-enecarboxamido)acetate, **8b'**.

Amide **10** (66.8 mg, 0.30 mmol) and **G4** (5.3 mg, 0.006 mmol) were mixed in CD_2Cl_2 in an NMR tube, ^{1}H NMR spectrum was acquired in 100 min and followed by termination with ethyl vinyl ether. The mixture was concentrated and isomerization product **8b'** was isolated by chromatography, yield 17 mg, 92% (100:1/CH_2Cl_2:MeOH). ^{1}H NMR of the crude **8b'** (500 MHz, $CDCl_3$): δ 5.98 (s, 0.9H, CONH), 4.11 (d, J =5.3 Hz, 2H, side chain CH_2), 3.78 (s, 3H,

OCH_3), 2.87 (dd, J =13.4, 2.7 Hz, 1H, CH_2), 2.75 (dt, J =12.0, 3.8 Hz, 1H, CH_2), 2.37 (m, 1H, CH), 2.23 (m, 1H, CH_2), 2.10 (m, 2H, CH_2), 1.93 (m, 1H, CH_2), 1.75 (m, 1H, CH_2), 1.34 (m, 2H, CH_2), 1.12 (m, 1H, CH_2).

N-Propylbicyclo[4.2.0]oct-6-ene-7-carboxamide, **8c'.**

Amide **8c** (57.8 mg, 0.30 mmol) and **G4** (5.3 mg, 0.006 mmol) were mixed in CD_2Cl_2 in an NMR tube, ^{1}H NMR spectrum was acquired in 6 h for a complete isomerization and followed by termination with ethyl vinyl ether. The mixture was concentrated and isomerization product **8c'** was isolated by chromatography, yield 49.0 mg, 85% (100:1/CH_2Cl_2:MeOH). ^{1}H NMR (500 MHz, $CDCl_3$) δ 5.50 (s, 1H, CONH), 3.21 (m, 2H, side chain CH_2), 2.81 (dd, J =13.4, 2.7 Hz, 1Hz, CH_2), 2.65 (dt, J = 12.0, 3.8 Hz, 1H, CH_2), 2.31 (m, 1H, CH), 2.15 (m, 1H, CH_2), 2.04 (m, 2H, CH_2), 1.89 (m, 1H, CH_2), 1.69 (m, 2H, side chain CH_2), 1.51 (m, 2H, CH_2), 1.27 (m, 2H, CH_2), 0.91(t, J =7.5 Hz, 3H, CH_3). ^{13}C NMR (126 MHz, CD_2Cl_2): δ 164.1 (CONH), 161.7 (=C), 126.7 (=CCONH), 40.4 (side chain CH_2), 37.6 (CH), 33.9 (CH_2), 32.8 (CH_2), 27.1 (CH_2), 26.6 (CH_2), 24.5 (CH_2), 22.9 (side chain CH_2), 11.3 (CH_3). HRMS (ESI) calcd. for $C_{12}H_{19}NO$ $[M+H]^+$ 194.1539, found 194.1535. $\lambda_{max.}$ 224 nm was consistent with the $\lambda_{max.}$ 223 nm previously reported for bicyclo[4,2,0]oct-1(8)-ene-8-carboxyamide. [214]

Isomerization of **8c** with MeOH.

A 0.01 M solution of catalyst **G4** in CD_2Cl_2 was divided into two aliquots, one with 50 μL MeOH (in large excess relative to **G4**) and one without MeOH both were stirred for 2 h. Monomer **8c** (10 equiv) was added and the kinetics of isomerization were monitored by ^{1}H NMR spectroscopy.

N-Phenylbicyclo[4.2.0]oct-6-ene-7-carboxamide, **8d'**.

Amide **8d** (23.1 mg, 0.12 mmol) and **G4** (5.3 mg, 0.006 mmol) were mixed in CD_2Cl_2 in an NMR tube, ^{1}H NMR spectrum was acquired in 20 min for a complete isomerization and followed by termination with ethyl vinyl ether. ^{1}H NMR (500 MHz, CD_2Cl_2) of **8d'**: δ 7.61 (d, *J* = 7.8 Hz, 2H, Ph), 7.37 (t, *J* = 7.6 Hz, 2H, Ph), 7.20 (s, 1H, CONH), 7.13 (t, *J* = 7.4 Hz, 1H, Ph), 2.98 (dd, *J* =13.4, 2.7 Hz, 1Hz, CH_2), 2.84 (dt, *J* = 12.0, 3.8 Hz, 1H, CH_2), 2.49 (m, 1H, CH_2), 2.35 (m, 1H, CH_2), 2.20 (m, 2H, CH_2), 2.00 (m, 1H, CH_2), 1.81 (m, 1H, CH_2), 1.44 (m, 2H, CH_2), 1.21 (m, 1H, CH_2).

N-(3-*p*-Tolylpropyl)bicyclo[4.2.0]oct-6-ene-7-carboxamide, **8e'**.

Amide **8e** (68.0 mg, 0.30 mmol) and **G4** (5.3 mg, 0.006 mmol) were mixed in CD_2Cl_2 in an NMR tube, ^{1}H NMR spectrum was acquired in 22 h for a complete isomerization and followed by termination with ethyl vinyl ether. ^{1}H NMR (600 MHz, CD_2Cl_2) of crude **8e'**: δ 7.20 – 7.02 (m, 4H, Ph), 5.64 (s, 1H, CONH), 3.3 (m, 2H, side chain CH_2), 2.85 (m, 1H, CH_2), 2.63 (m, 3H, ring CH_2 and side chain CH_2), 2.33 (m, 4H, ring CH and side chain CH_2), 2.13 (m, 2H, side chain CH_2), 2.03 (m, 1H, CH_2), 1.93 (m, 1H, CH_2), 1.84 (m, 2H, CH_2), 1.76 (m, 1H, CH_2), 1.32 (m, 2H, CH_2), 1.11 (m, 1H, CH_2).

Isomerization of **8e** monitored with ^{13}C NMR.

Amide **8e** (19.2 mg, 0.067 mmol) and catalyst **G4** (60.0 mg, 0.067 mmol) were mixed in CD_2Cl_2 in an NMR tube and the reaction was monitored with ^{13}C NMR at 35 °C.

Isomerization of **8e** with 1,4-benzoquinone.

A 0.02 M solution of catalyst **G4** in CD_2Cl_2 was divided into two aliquots, one with 1,4-benzoquinone (5 equiv relative to **G4**) and one without 1,4-benzoquinone. Monomer **8e** (10 equiv) was added to both aliquots and the extent of isomerization was evaluated by ^{1}H NMR spectroscopy.

Isomerization of **8e** in the presence of exogenous 3-bromopyridine.

A 0.005 M solution of catalyst **G4** in CD_2Cl_2 was divided into two aliquots, one with 50 equiv of 3-bromopyridine and one without. Monomer **8e** (10 equiv) was added to both aliquots and the kinetics of isomerization were monitored by ^{1}H NMR spectroscopy.

Isomerization of **8e** in the presence of air.

A 0.01 M solution of catalyst **G4** in CD_2Cl_2 was divided into two aliquots, one with 1 mL of air and one without. Monomer **8e** (10 equiv) was added and the kinetics of isomerization were monitored by ^{1}H NMR spectroscopy.

(*R*)-2-(Bicyclo[4.2.0]oct-6-enecarboxamido)-2-phenylethyl propionate, **8f'/8f*'**.

Amide **8f or 8f*** (16.1 mg, 0.06 mmol) and **G4** (5.3 mg, 0.006 mmol) were mixed in CD_2Cl_2 in an NMR tube, ^{1}H NMR spectra were acquired in 24 h and followed by termination with ethyl vinyl ether, conversion were 70% and 90%, respectively. Partial ^{1}H NMR of the crude **8f*'** (600 MHz, CD_2Cl_2): δ 6.71 (s, 0.2H, =CH), 6.36 – 6.26 (m, 0.3H, CONH), 6.11 (d, J = 6.9 Hz, 0.7H, CONH). (Partial ^{1}H NMR spectroscopic data are reported due to incomplete isomerization and significant upfield overlap of **8f/8f*** with the new peaks from **8f'/8f*'**.)

Methyl 2-(bicyclo[3.2.0]hept-5-enecarboxamido)propanoate, **9'**.

Amide **9** (26.7 mg, 0.12 mmol) and **G4** (5.3 mg, 0.006 mmol) were mixed in CD_2Cl_2 in an NMR tube for 18 h. Only a 2% of decrease in the intensity of the olefinic resonance of amide **9** was observed.

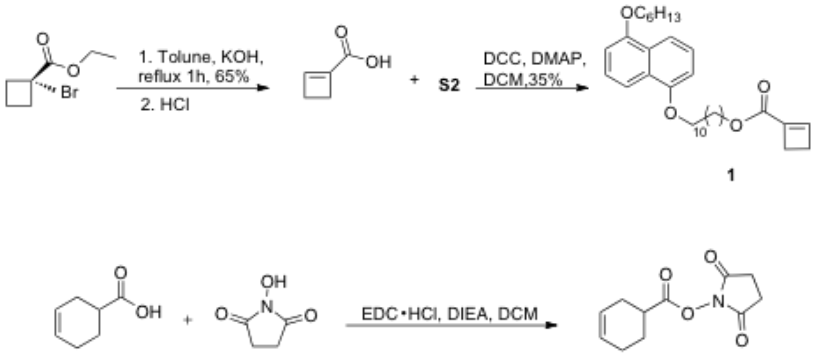

Boc-Trp-OH.

Tryptophan (1.00 g, 4.90 mmol) was dissolved in saturated $NaHCO_3$ aqueous solution and cooled in an ice bath. Boc anhydride (2.14 g, 9.80 mmol) was dissolved THF and added dropwise into the tryptophan solution and the reaction was stirred for 10 h. The organic solvent was removed by evaporation and the remaining aqueous solution was washed with CH_2Cl_2 (3×20 mL). The water layer was acidified with 1N HCl to pH=2 and was extracted with CH_2Cl_2 (3×20 mL). The organic layer was dried over $MgSO_4$. The solvent was filtered and removed by evaporation to yield Boc-Trp-OH as a white solid. It was recrystallized in ethyl acetate with hexane and used without further purification.

Boc-Trp-alkyne.

BocTrp-OH (500 mg, 1.64 mmol), propagylamine (82.1 mg, 1.49 mmol), EDC•HCl (347 mg, 1.80 mmol) and DIPEA (233 mg, 1.80 mmol) were mixed in THF. The reaction was stirred for

10 h and THF was removed by evaporation. The residue was dissolved in CH_2Cl_2 and washed sequentially with 5% $NaHCO_3$ (3×), 1N HCl (3×) and brine (2×) and dried over anhydrous $MgSO_4$. The solvent was filtered and removed by evaporation and the crude was subjected to flash silica chromatography (2% MeOH in CH_2Cl_2) to yield Boc-Trp-alkyne (390 mg, 78%). ^{1}H NMR (700 MHz, $CDCl_3$) δ 8.28 (s, 1H), 7.66 (d, J = 7.5 Hz, 1H), 7.38 (d, J = 8.1 Hz, 1H), 7.25 – 7.20 (m, 1H), 7.18 – 7.13 (m, 1H), 7.06 (s, 1H), 6.12 (s, 1H), 5.18 (s, 1H), 4.48 (s, 1H), 3.93 (s, 2H), 3.32 (s, 1H), 3.21 (s, 1H), 2.17 (s, 1H), 1.44 (s, 9H). ^{13}C NMR (176 MHz, $CDCl_3$) δ 171.5, 155.5, 136.2, 127.5, 123.3, 122.3, 119.8, 118.8, 111.3, 110.4, 80.3 79.16, 71.5, 55.0, 29.1, 28.3. ESI (M/Z) $[M+H]^+$ 341.2.

Polymer Synthesis

General procedure for NMR scale AROMP reactions of bicyclic ester and cyclohexene.

All kinetic experiments were performed at least twice, and preparative polymerization experiments were performed three times. Under an N_2 atmosphere, a solution of monomer **A** (cyclobutene derivative) in CD_2Cl_2 (300 μL) was added to the NMR tube. Then 300 μL of Grubbs III stock solution (C = 0.02 M) was added to the NMR tube. After complete mixing of the solution, NMR spectra were acquired at 25 °C until the catalyst had reacted with monomer **A** as determined by the disappearance of its alkylidene proton signal. Monomer **B** (cyclohexene **6a**) was added to the NMR tube. After no further propagation occurred, the reaction was quenched with ethyl vinyl ether and stirred for 1 h. Solvent was evaporated, and polymer was purified by chromatography over silica gel (97:3/CH_2Cl_2:acetone). Yield was determined by assuming 100% conversion of monomer **A**.

NMR AROMP of **2** and **6a**.

Monomer **2** (8.3 mg, 60 μmol, 10 equiv) and **G4** (5.3 mg, 6.0 μmol, 1 equiv) were mixed in CD_2Cl_2. The reaction was followed by ^1H NMR spectroscopy at 25 °C for 5 h before the temperature was elevated to 50 °C. Cyclohexene **6a** (12 μL, 120 μmol, 20 equiv) was added. No change in the alkylidene peak of the catalyst was observed within 300 min.

NMR AROMP of **3** and **6**a, poly(**3**-*alt*-**6a**)$_{13}$.

Monomer **3** (23.8 mg, 150 μmol, 25 equiv) and **G4** (5.3 mg, 6.0 μmol, 1 equiv) were mixed. Cyclohexene **6a** (24.5 mg, 30 μL, 50 equiv) was added 30 min later as determined by ^1H NMR. The NMR tube was spun for 19 h at 25 °C. Flash column chromatography (97:3/CH_2Cl_2:acetone) of the crude product yielded poly(**3**-*alt*-**6a**)$_{13}$ (15 mg, 43%). ^1H NMR (600 MHz, CD_2Cl_2): δ 7.35-7.14 (m, 5H), 6.60 (m, 13H), 5.32 (m, 27H), 3.68-3.60 (m, 54H), 3.20-3.10 (m, 14H), 2.0-2.3 (m, 10H), 2.60-1.00 (m, 267H).

NMR AROMP of 3 and 6-d_{10}, poly(3-*alt*-6-d_{10})$_6$.

Monomer **3** (9.5 mg, 50 μmol, 10 equiv) and **G4** (5.3 mg, 6.0 μmol, 1 equiv) were mixed. Cyclohexene **6a-d$_{10}$** (9.8 mg, 12 μL, 20 equiv) was added 30 min later. The NMR tube was spun for 8 h at 25 °C. The crude product was purified by flash column chromatography (97:3/CH_2Cl_2:acetone) to yield poly(**3**-*alt*-**6a-d$_{10}$**)$_6$ (4.8 mg, 40%). ^1H NMR (600 MHz, CD_2Cl_2): δ 7.35-7.14 (m, 5H), 7.02 (dd, J = 8.1, 5.7 Hz, 1H), 5.32 (m, 6H), 3.68-3.60 (m, 22H), 3.20-1.00 (m, 80H).

Alternating ring-opening polymerization of monomer **4a** and **6a** was carried out at different temperatures ranging from 25-60 °C to optimize reaction conditions.

NMR AROMP of **4a** and **6a**, poly(**4a**-*alt*-**6a**)$_{17}$.

Monomer **4a** (19.9 mg, 0.12 mmol, 20 equiv) and **G4** (5.3 mg, 6.0 μmol, 1 equiv) were mixed in CD_2Cl_2. Cyclohexene **6a** (19.7 mg, 24 μL, 40 equiv) was added over 50 min. The NMR tube was spun for 10 h at 25 °C to reach 90% consumption of monomer **4a**. The product was purified by flash column chromatography (97:3/CH_2Cl_2:acetone) to yield poly(**4a**-*alt*-**6a**)$_{17}$ (16 mg, 53%). ^{1}H NMR (600 MHz, CD_2Cl_2): δ 7.35-7.14 (m, 5H), 6.52 (m, 16H), 5.79 (m, 15H), 5.31 (m, 26H), 3.69-3.59 (m, 45H), 2.60 (m, 23H), 2.25 (m, 60H), 2.00-1.22 (m, 266H). ^{13}C NMR (100MHz, $CDCl_3$) δ 169.4, 142.4, 141.9, 136.3, 131.2, 130.7, 130.6, 130.4, 130.2, 130.2, 130.0, 129.1, 128.4, 51.5, 51.5, 51.4, 43.9, 42.8, 37.3, 28.7, 28.1, 21.8, 21.7.

NMR AROMP of **4a** and **6a**, poly(**4a**-*alt*-**6a**)$_{16}$.

Monomer **4a** (19.9 mg, 0.12 mmol, 20 equiv) and **G4** (5.3 mg, 6.0 μmol, 1 equiv) were mixed in CD_2Cl_2 and cyclohexene **6a** (19.7 mg, 24.2 μL, 40 equiv) was added in 50 min. The NMR tube was spun for 6 h at 35 °C to reach >95% consumption of monomer **4a**. The product was purified by flash column chromatography (97:3/CH_2Cl_2:acetone) to yield poly(**4a**-*alt*-**6a**)$_{16}$ (20 mg, 65%). ^{1}H NMR (600 MHz, $CDCl_3$): δ 7.35-7.14 (m, 6H), 6.52 (m, 16H), 5.79 (m, 15H), 5.50 (m, 1H), 5.31 (m, 17H), 3.69-3.59 (m, 47H), 2.78 (m, 23H), 2.10 (m, 64H), 1.98-1.20 (m, 263H).

NMR AROMP of **4a** and **6a**, poly(**4a**-*alt*-**6a-D$_{10}$**)$_{15}$.

Monomer **4a** (19.9 mg, 0.12 mmol, 20 equiv) and **G4** (5.3 mg, 6.0 μmol, 1 equiv) were mixed in CD_2Cl_2. After 50 min, cyclohexene-D_{10} **6a-D$_{10}$** (19.7 mg, 24.2 μL, 40 equiv) was added. The NMR tube was spun for 6 h at 35 °C to reach >95% consumption of monomer **4a**. The product was purified by flash column chromatography (97:3/CH_2Cl_2:acetone) to yield poly(**4a**-*alt*-**6a**-

D$_{10}$)$_{15}$ (18 mg, 60%). ^{1}H NMR (600 MHz, CD_2Cl_2): δ 7.35-7.4 (m, 5H), 5.78 (m, 15H), 5.42 (m, 2H), 3.70-3.60 (m, 45H), 2.82 (m, 23H), 2.25 (m, 27H), 1.78-1.20 (m, 164H).

NMR AROMP of **4a** and **6a**, poly(**4a**-*alt*-**6a**)$_{34}$.

Monomer **4a** (49.7 mg, 300 μmol, 50 equiv) and **G4** (5.3 mg, 6.0 μmol, 1 equiv) were mixed in CD_2Cl_2 and cyclohexene **6a** (49.2 mg, 60.6 μL, 100 equiv) was added in 30 min. The NMR tube was spun for 2 h at 50 °C to reach 68% conversion. The product was purified by flash column chromatography (97:3/CH_2Cl_2:acetone) to yield poly(**4a**-*alt*-**6a**)$_{34}$ (34 mg, 60%). Partial ^{1}H NMR of crude poly(**4**-*alt*-**6**)$_{34}$: (600 MHz, CD_2Cl_2): δ 7.35-7.14 (m, 5H), 6.89 (d, J = 1.2 Hz, 8H), 6.50 (m, 34H), 5.79 (m, 32H), 5.28 (m, 41H), 3.70-3.60 (m, 150H), 3.07-3.04 (m, 10H). (Partial ^{1}H NMR spectroscopic data are reported due to incomplete polymerization and significant overlap upfield of **4** and **6** with the new peaks from the polymer.)

NMR AROMP of **4a** and **6a**, poly(**4a**-*alt*-**6a**)$_{36}$.

Monomer **4a** (49.7 mg, 300 μmol, 50 equiv) and **G4** (5.3 mg, 6.0 μmol, 1 equiv) were mixed in CD_2Cl_2. Cyclohexene **6a** (49.2 mg, 60.6 μL, 100 equiv) was added after 30 min. The NMR tube was spun for 2 h at 60 °C to reach 72% conversion. The product was purified by flash column chromatography (97:3/CH_2Cl_2:acetone) to yield poly(**4a**-*alt*-**6a**)$_{36}$ (36 mg, 65%). ^{1}H NMR (600 MHz, CD_2Cl_2): δ 7.35-7.14 (m, 5H), 6.50 (m, 36H), 5.79 (m, 34H), 5.28 (m, 55H), 3.70-3.60 (m, 129H), 2.75 (m, 53H), 2.30-2.10 (m, 142H), 1.95-1.20 (m, 589H).

NMR AROMP of **5** and **6a**, poly(**5**-*alt*-**6a**)$_{10}$.

Monomer **5** (54.8 mg, 0.30 mmol, 50 equiv) and **G4** (5.30 mg, 6.00 μmol, 1 equiv) were mixed in CD_2Cl_2 and cyclohexene **6a** (49.0 mg, 60 μL, 100 equiv) was added in 50 min. The NMR tube was spun for 72 h at 35 °C until no further propagation was observed. The product was purified

by flash column chromatography (97:3/CH_2Cl_2:acetone) to yield poly(**5**-*alt*-**6a**)$_{10}$ (11 mg, 14%). ^{1}H NMR (600 MHz, CD_2Cl_2): δ 7.35-7.12 (m, 5H), 6.58 (m, 10H), 5.42 (m, 19H), 5.28 (m, 10H), 3.70-3.60 (m, 36H), 3.10-3.00 (m, 10H), 2.77-1.95 (m, 254H).

General procedure for ring-opening metathesis.

Under an N_2 atmosphere, a solution of monomer **A** (cyclobutene derivatives, **1a**, **3**, **4a** and **5**, C=0.03 M) in CD_2Cl_2 (300 μL) was added to an NMR tube. Then a stock solution of **G4** was prepared in CD_2Cl_2 (C=0.03 M) and 300 μL of the solution was added to the NMR tube. After complete mixing of the solution, the reaction was closely monitored by ^{1}H NMR or ^{13}C NMR spectroscopy.

Procedure for alternating ring-opening metathesis (AROM-1, BA dimer synthesis).

A solution of monomer **A** (**3** or **4a**, C=0.03 M) in CD_2Cl_2 (300 μL, 18.86 μmol) was added to an NMR tube that had been flushed with N_2. Then a stock solution of **G4** was prepared in CD_2Cl_2 (C=0.03 M) and 300 μL of the solution was added to the NMR tube. After complete mixing of the solution, the reaction was followed by ^{1}H NMR or ^{13}C NMR spectroscopy until >90% of the catalyst (10-12 h) was consumed as determined by disappearance of the Ru alkylidene proton or carbon resonance of the Grubbs III catalyst at 19.1 ppm or 316.1 ppm, then cyclohexene **6a** was added in 10-fold excess, and the reaction was monitored until the Ru alkylidene proton resonance at 19.0 ppm disappeared. The reaction was terminated with ethyl vinyl ether and the crude mixture was subjected to silica chromatography (100% CH_2Cl_2). Partially purified fractions were characterized by mass spectroscopy, ^{1}H NMR, ^{13}C NMR and HSQC spectroscopy. Fraction I was a white solid identified as *E*-stilbene, ^{1}H NMR (850 MHz, CD_2Cl_2): δ 7.53 (dd, *J* = 8.1, 0.9 Hz, 2H), 7.36 (t, *J* = 7.7 Hz, 2H), 7.28 – 7.23 (m, 2H), 7.13 (s, 1H). ^{13}C NMR (214

MHz, CD_2Cl_2) δ 137.9, 129.2, 129.1, 128.2, 127.0. ESI (M/Z) $[M+H]^+$ 180.1. Fraction II contained Ph-(**3**-*alt*-**6a**)$_1$-Ph as the major component. Fraction III contained *cyc*-(**3**-*alt*-**6a**)$_1$ as the major component.

Procedure for sequential alternating ring-opening metathesis (AROM-2, BA'BA tetramer synthesis).

A solution of monomer **A** (**3** or **4a**, C=0.03 M) in CD_2Cl_2 (300 μL, 18.86 μmol) was added to an NMR tube that had been flushed with N_2. Then a stock solution of **G4** was prepared in CD_2Cl_2 (C=0.03 M) and 300 μL of the solution was added to the NMR tube. After complete mixing of the solution, the reaction was followed by ^{1}H NMR spectroscopy until >90% of the catalyst (10-12 h) was consumed as determined by disappearance of the Ru alkylidene proton of the **G4** at 19.1 ppm, then cyclohexene **6a** was added in 10-fold excess. Generation of [Ru]-**B**-**A** was monitored by the appearance of a multiplet resonance at 19.0 ppm. When the formation of [Ru]-**B-A** was complete as judged by the integrated intensity of the resonance, one equivalent of monomer **A'** was added to form [Ru]-**A'**-**B**-**A** and then [Ru]-**B**-**A'**-**B**-**A**. The reaction was monitored until the Ru alkylidene proton resonance at 19.0 ppm disappeared or the intensity was constant. Then the reaction was terminated with ethyl vinyl ether.

General procedure for NMR scale AROMP reactions of bicyclic amides and cyclohexene.

Under an N_2 atmosphere, amide **8** and **G4** were mixed in CD_2Cl_2 and NMR spectra were acquired at 35 °C unless indicated otherwise. Cyclohexene **6a** was added after the amide was completely converted to its tetrasubstituted isomer as judged by the disappearance of the olefinic proton resonance around 6.7 ppm. This procedure was used for the preparation of polymers with up to 50 **AB** repeats. To ensure narrow dispersities, in the preparation of longer alternating

polymers, the isomer **8'** was isolated and mixed with fresh **G4** in CD_2Cl_2. Cyclohexene **6a** was added after **G4** completely initiated as determined by the disappearance of the Ru alkylidene resonance at 19.1 ppm in the ^1H NMR spectrum. When the propagation stopped or the isomerized amide disappeared as judged by a complete shift of the amide N-H resonance from 5.9 to 5.4 ppm, the reaction was quenched with ethyl vinyl ether and stirred for 30 min. The solvent was evaporated, and alternating copolymer was purified by chromatography (95:5/CH_2Cl_2:MeOH).

NMR AROMP of poly(**8c'**-*alt*-**6a**)$_{10}$.

Amide **8c** (11.6 mg, 0.06 mmol) and catalyst **G4** (5.3 mg, 0.006 mmol) were mixed in CD_2Cl_2 in an NMR tube. Upon completion of isomerization, **6a** (9.8 mg, 0.12 mmol) was added and after 1.5 h, amide **8c'** was completely consumed. ^1H NMR (500 MHz, CD_2Cl_2): δ 7.45 – 7.21 (m, 5H, Ph), 6.40 – 5.57 (m, 20H, =CH and CONH), 5.09 (m, 10H, =CH), 3.31 – 3.16 (m, 26H, CH_2), 2.68 – 1.09 (m, 342H), 0.95 (t, J = 7.4 Hz, 38H, CH_3).

NMR AROMP of poly(**8c'**-*alt*-**6a**)$_{50}$.

Amide **8c** (11.6 mg, 0.06 mmol) and catalyst **G4** (1.1 mg, 1.20 μmol) were mixed in CD_2Cl_2 in an NMR tube. Upon completion of isomerization, **6a** (9.8 mg, 0.12 mmol) was added and after 2 h, amide **8c'** was completely consumed. ^1H NMR (500 MHz, CD_2Cl_2): δ 7.45 – 7.27 (m, 5H, Ph), 6.40 – 5.57 (m, 97H, =CH and CONH), 5.09 (m, 49H), 3.24 (m, 105H, CH_2), 2.58 (m, 46H), 2.39 (m, 44H), 2.29 – 1.90 (m, 363H), 1.80 – 1.17 (m, 700H), 1.04 – 0.87 (m, 160H, CH_3).

NMR AROMP of poly(**8c'**-*alt*-**6a**)$_{100}$.

Amide **8c'** (23.2 mg, 0.12 mmol) and **G4** (1.1 mg, 1.20 μmol) were mixed in CD_2Cl_2 in an NMR tube. **6a** (19.6 mg, 0.24 mmol) was added when catalyst had fully reacted. ^1H NMR spectrum

was acquired in 2 h for a complete consumption of amide **8c'** and followed by termination with ethyl vinyl ether. ^{1}H NMR (500 MHz, CD_2Cl_2) δ 7.45 – 7.27 (m, 5H, Ph), 6.40 – 5.57 (m, 186H, =CH and CONH), 5.09 (m, 98H, =CH), 3.24 (m, 199H, CH_2), 2.58 (m, 98H), 2.39 (m, 84H), 2.29 – 1.90 (m, 697H), 1.75-1.17 (m, 1259H), 1.04 – 0.87 (m, 311H). M_n^{calc} = 28104. M_n^{GPC} = 20526. M_w^{GPC} = 28366. $Đ_M$ = 1.38.

NMR AROMP of poly(**8c'**-*alt*-**6a**)$_{424}$.

Amide **8c'** (23.2 mg, 0.12 mmol) and **G4** (0.22 mg, 0.24 μmol) were mixed in CD_2Cl_2 in an NMR tube. Cyclohexene **6a** (19.6 mg, 0.24 mmol) was added when catalyst had fully reacted. ^{1}H NMR spectrum was acquired in 6 h for a complete consumption of amide **8c'** and followed by termination with ethyl vinyl ether. ^{1}H NMR (500 MHz, CD_2Cl_2) δ 7.36 (m, 5H, Ph), 6.44 – 5.65 (m, 741H, =CH and CONH), 5.22 – 4.99 (m, 424H, =CH), 3.33 – 3.13 (m, 871H, CH_2), 2.55 (m, 447H), 2.48 – 2.33 (m, 390H), 2.33 – 1.87 (m, 3115H), 1.80 – 1.15 (m, 6126H), 1.06 – 0.82 (m, 1522H). ^{13}C NMR (126 MHz, CD_2Cl_2): δ 169.8, 141.8, 136.9, 134.4, 120.8, 43.7, 41.3, 33.1, 30.0, 30.0, 28.8, 28.3, 28.1, 26.9, 23.0, 11.3. M_n^{calc} = 118824. M_n^{GPC} = 28783. M_w^{GPC} = 36185. $Đ_M$ = 1.26.

NMR AROMP of poly(**1d'**-*alt*-**3-D$_{10}$**)$_{10}$. Amide **8d** (13.7 mg, 0.06 mmol) and catalyst **G4** (5.3 mg, 6.0 μmol) were mixed in CD_2Cl_2 in an NMR tube. Monomer **6a-D$_{10}$** (9.8 mg, 0.12 mmol) was added upon completion of isomerization. And after 1 h, amide **8d'** was completely consumed. ^{1}H NMR (500 MHz, CD_2Cl_2): δ 7.89 (s, 10H, CONH), 7.59 (m, 20H, Ph), 7.38 – 7.26 (m, 20H, Ph), 7.10 (m, 10H, Ph), 3.67 (m, 10H), 2.63 (m, 10H), 2.4 (m, 20H), 2.15 (m, 20H), 2.08 (m, 10H), 1.67 – 1.23 (m, 203H).

NMR AROMP of poly(**8d'**-*alt*-**6a**)$_{50}$

Amide **8d** (13.7 mg, 0.06 mmol) and **G4** (1.1 mg, 1.20 μmol) were mixed in CD_2Cl_2 in an NMR tube. Monomer **6a** (9.8 mg, 0.12 mmol) was added upon completion of isomerization. And after 1 h, amide **8d'** was completely consumed. ^{1}H NMR (500 MHz, CD_2Cl_2): δ δ 7.89 (s, 43H, CONH), 7.59 (m, 118H, Ph), 7.38 – 7.26 (m, 143H, Ph), 7.10 (m, 65H, Ph), 6.30 (m, 46H, =CH), 5.11 (m, 50H, =CH), 3.67 (m, 39H), 2.77 – 1.23 (m, 1359H). M_n^{calc} = 15554. M_n^{GPC} = 10099. M_w^{GPC} = 16042. $Đ_M$ = 1.59.

Alternating ROMP copolymer with charge-transfer units.

poly(**1b**-*alt*-**6b**)$_5$.

The reaction was monitored by ^{1}H NMR. The NMR tube was evacuated under high vacuum for 15 min, and then was purged with N_2 gas for another 15 min. Under an N_2 atmosphere, a solution of monomer **1b (**29.6 mg**,** 0.060 mmol**)** in CD_2Cl_2 (300 μL) was added to the NMR tube. Then a solution of **G4** (5.3 mg, 6.0 μmol) in CD_2Cl_2 (300 μL) was added to the NMR tube. After complete mixing of the solution, the NMR tube was spun for 60 min at an elevated temperature 37 °C until the precatalyst had reacted as can be observed by disappearance of ruthenium alkylidene proton at 19 ppm. Monomer **6b** (19.5 mg, 0.030 mmol) in CD_2Cl_2 (100 μL) was added to the NMR tube. The reaction was quenched in 8 h with ethyl vinyl ether (50 μL) and the resulting solution was stirred for another 1 h. The mixture was condensed to give a dark brown oil which was further purified by column chromatography (100:1/CH_2Cl_2:MeOH) to yield an orange solid in 55% yield. ^{1}H NMR (600 MHz, $CDCl_3$) δ 8.26 – 7.92 (m, 8H), 7.83-7.74 (m, 10H), 7.42 – 7.20 (m, 10H), 6.93 – 6.62 (m, 15H), 5.66 – 5.17 (m, 8H), 4.30 – 3.91 (m, 41H),

3.72 (m, 16H), 3.41 – 3.03 (m, 6H), 2.65 – 1.02 (m, 382H), 0.99 – 0.62 (m, 34H). M_n^{cal}=5748, M_n^{GPC}=3291, M_w^{GPC}=4252, $Đ_M$ =1.29.

poly(**1b**-*alt*-**6d**)$_{10}$.

The reaction was monitored by ^{1}H NMR. The NMR tube was evacuated under high vacuum for 15 min, and then was purged with N_2 gas for another 15 min. Under an N_2 atmosphere, a solution of monomer **1a (**29.6 mg**,** 0.060 mmol**)** in CD_2Cl_2 (300 μL) was added to the NMR tube. Then a solution of **G4** (5.3 mg, 6.0 μmol) in CD_2Cl_2 (300 μL) was added to the NMR tube. After complete mixing of the solution, the NMR tube was spun for 60 min at 25 °C until the precatalyst had reacted as can be observed by disappearance of ruthenium alkylidene proton at 19.1 ppm. Monomer **6c** (26.8 mg, 0.120 mmol) in CD_2Cl_2 (100 μL) was added to the NMR tube. The reaction was quenched in 6 h with ethyl vinyl ether (50 μL) and the resulting solution was stirred for another 1 h. The mixture was condensed to give a dark brown oil which was further purified by column chromatography (100:1/CH_2Cl_2:MeOH) to yield an orange solid in 75% yield. ^{1}H NMR (600 MHz, $CDCl_3$) δ 7.84 (m, 20H), 7.32 (m, 20H), 6.98 – 6.56 (m, 30H), 5.33 (m, 13H), 4.11 (s, 3H), 292 – 1.25 (m, 366H), 0.95 (m, 30H). The resulting polymer poly(**1b**-*alt*-**6c**)$_{10}$ (27.2 mg, 3.7 μmol) was dissolved in dry THF and cooled in an ice bath. EDC•HCl (7.1 mg, 37 μmol), DIEA (9.7 mg, 74 μmol), and 2-(6-aminohexyl)-6-decylpyrrolo[3,4-*f*]isoindole-1,3,5,7(2*H*,6*H*)-tetraone (**10**) (**34** mg, 74 μmol) were added. The mixture was stirred for 2 days and then filtered, followed by column chromatography (5:95/acetone/CH_2Cl_2) to yield an orange solid in 20% yield. ^{1}H NMR of poly(**1b**-*alt*-**6d**)$_{10}$ (600 MHz, $CDCl_3$) δ 8.26 – 7.92 (m, 9H), 7.80 (dd, J = 14.4, 6.1 Hz, 20H), 7.42 – 7.18 (m, 20H), 6.93 – 6.62 (m, 30H), 5.66 – 5.17 (m, 12H), 4.30 – 3.91 (m, 59H), 3.72 (dd, J = 14.7, 7.1 Hz, 15H), 3.41 – 3.03 (m, 6H), 2.65 – 0.99 (m, 545H), 0.99 – 0.62 (m, 86H). M_n^{Cal}=10948, M_n^{GPC}=7966, M_w^{GPC}=10221, $Đ_M$ =1.28.

Synthesis of orthogonally functionalized alternating copolymers and post polymerization modification to make FRET polymers.

poly(**4e**-*alt*-**6e**)$_{27}$.

Under an N_2 atmosphere, **4e** (61.8 mg, 0.24 mmol) and **G4** (5.3 mg, 0.006 mmol) were mixed in CD_2Cl_2 (600 μL) in an NMR tube. NMR spectra were acquired at 25 °C until the **G4** had completely reacted as determined by the disappearance of its alkylidene α proton signal. Cyclohex-3-enecarbaldehyde **6e** (52.7 mg, 0.48 mmol) was added to the NMR tube. When no further propagation occurred, the reaction was quenched with ethyl vinyl ether and stirred for 30 min. The solvent was evaporated, and the alternating copolymer was purified by chromatography on silica gel (97:3/CH_2Cl_2:acetone). ^{1}H NMR (500 MHz, CD_2Cl_2): δ 9.59 (m, 27H), 7.25 (m, 5H), 6.59 (m, 27H), 5.83 (m, 27H), 5.36 (m, 27H), 4.39 (m, 54H), 3.59 (m, 54H), 3.0-1.25 (m, 560H). M_n^{calc} = 9700, M_n^{GPC} = 14823, M_w^{GPC} = 31649, $Đ_M$ = 2.13.

poly(**4e'**-*alt*-**6e**)$_{27}$.

To a solution of poly(**4e**-*alt*-**6e**)$_{27}$ (44.0 mg, 4.51 μmol) in anhydrous DMF (1 mL) was added NaN_3 (23.0 mg, 353 μmol). The mixture was stirred at 60 °C for 3 h, and water (5 mL) was added and the mixture was extracted with CH_2Cl_2 (3 × 5 mL). The combined organic layers were washed with water and dried over $MgSO_4$. After filtration, the solvent was evaporated by vacuum to give a yellow oil (31.0 mg, 80 %). ^{1}H NMR (500 MHz, CD_3OD): δ 9.50 (m, 27H), 7.24 (m, 5H), 6.48 (m, 27H), 5.78 (m, 27H), 5.30 (m, 27H), 4.20 (m, 59H), 3.50 (m, 59H), 3.00 - 1.35 (m, 863H). IR (KBr): 3418, 2924, 2854, 2718, 2104, 1716, 1633 cm^{-1}.

poly(**4e'**-*alt*-**6e-DH**)$_{27}$.

poly(**4e'**-*alt*-**6e**)$_{27}$ (4.7 mg, 0.54 μmol) and dansyl hydrazide (5.5 mg, 21 μmol) were dissolved in THF (2 mL). The mixture was stirred at 65 °C for 2 h and the solution was concentrated under vacuum. The residue was purified sephadex LH-20 with eluting solvent as THF. ^{1}H NMR (400 MHz, CD_2Cl_2): δ 8.56 (bs, 47H), 8.42 (bs, 39H), 8.28 (bs, 39H), 8.00 (bs, 47H), 7.54 (bs, 87H), 7.20 (bs, 96H), 6.43 (bs, 27H), 5.68 (bs, 29H), 5.13 (bs, 31H), 4.30 (bs, 137H), 3.46 (bs, 131H), 2.94 (bs, 155H), 2.88 (bs, 243H), 2.86 (s, 172H), 2.80 – 1.01 (m, 1618H). M_n^{calc} = 16369, M_n^{GPC} = 19325, M_w^{GPC} = 34382, $Đ_M$ = 1.78.

poly(**4e'-Trp**-*alt*-**6e**)$_{27}$.

Under an N_2 atmosphere, poly(**4e'**-*alt*-**6e**)$_{27}$ (5.9 mg, 0.67 μmol), Boc-Trp-alkyne (10.6 mg, 25.6 μmol), CuBr (1.7 mg, 0.20 μmol) and PEDTA (6.7 μL) were mixed in THF (1 mL). After stirring for 12 h, the solution was concentrated and the residue was purified by sephadex LH-20 with eluting solvent as THF. M_n^{calc} = 16715, M_n^{GPC} = 12472, M_w^{GPC} = 20226, $Đ_M$ = 1.62.

poly(**4e'-Trp**-*alt*-**6e-DH**)$_{27}$.

Under an N_2 atmosphere, poly(**4e'**-*alt*-**6e**)$_{27}$ (7.0 mg, 0.80 mmol), dansyl hydrazide (8.2 mg, 31 μmol), Boc-Trp-alkyne (12.5 mg, 30.0 mmol), CuBr (2.0 mg, 0.24 mmol) and PEDTA (7.9 μL) were mixed in THF (1 mL). The mixture was stirred at 65 °C for 12 h, the solution was concentrated and the residue was purified by sephadex LH-20 with eluting solvent as THF. M_n^{calc} = 22491, M_n^{GPC} = 21645, M_w^{GPC} = 38312, $Đ_M$ = 1.77. IR (KBr): 3413, 2929, 2854, 1707, 1690 cm^{-1}.

Bibliography

[1] Song, A., Parker, K. A., and Sampson, N. S. (2009) Synthesis of copolymers by alternating ROMP (AROMP), *J. Am. Chem. Soc. 131*, 3444-3445.

[2] McCrum, N. G., Buckley, C. P., and Bucknall, C. B. (1997) Principles of polymer engineering, In *New York: Oxford University Press*, p 1.

[3] Feizi, T., and Chai, W. G. (2004) Oligosaccharide microarrays to decipher the glyco code, *Nat Rev Mol Cell Bio 5*, 582-588.

[4] Lienkamp, K., Madkour, A., and Tew, G. (2013) Antibacterial peptidomimetics: polymeric synthetic mimics of antimicrobial peptides, In *Polym. Composite.* (Abe, A., Kausch, H.-H., Möller, M., and Pasch, H., Eds.), pp 141-172, Springer Berlin Heidelberg.

[5] Gabriel, G. J., Maegerlein, J. A., Nelson, C. F., Dabkowski, J. M., Eren, T., Nüsslein, K., and Tew, G. N. (2009) Comparison of facially amphiphilic versus segregated monomers in the design of antibacterial copolymers, *Chem. Eur. J. 15*, 433-439.

[6] Kuroda, K., and DeGrado, W. F. (2005) Amphiphilic polymethacrylate derivatives as antimicrobial agents, *J. Am. Chem. Soc. 127*, 4128-4129.

[7] Arnt, L., Nüsslein, K., and Tew, G. N. (2004) Nonhemolytic abiogenic polymers as antimicrobial peptide mimics, *J. Polym. Sci., Part A: Polym. Chem. 42*, 3860-3864.

[8] Choi, S., Isaacs, A., Clements, D., Liu, D., Kim, H., Scott, R. W., Winkler, J. D., and DeGrado, W. F. (2009) De novo design and in vivo activity of conformationally restrained antimicrobial arylamide foldamers, *P. Natl. Acad. Sci. USA 106*, 6968-6973.

[9] Sambhy, V., Peterson, B. R., and Sen, A. (2008) Antibacterial and hemolytic activities of pyridinium polymers as a function of the spatial relationship between the positive charge and the pendant alkyl tail, *Angew. Chem. Int. Ed. 47*, 1250-1254.

[10] KWON, I., BAE, Y., and KIM, S. (1991) Electrically erodible polymer gel for controlled release of drugs. , *Nature 354*, 291-293.

[11] Gupta, P., Vermani, K., and Garg, S. (2002) Hydrogels: from controlled release to pH-responsive drug delivery, *Drug Discov. Today 7*, 569-579.

[12] Uhrich, K. E., Cannizzaro, S. M., Langer, R. S., and Shakesheff, K. M. (1999) Polymeric systems for controlled drug release, *Chem. Rev. 99*, 3181-3198.

[13] Jeong, B., Bae, Y. H., Lee, D. S., and Kim, S. W. (1997) Biodegradable block copolymers as injectable drug-delivery systems, *Nature 388*, 860-862.

[14] Langer, R., and Chasin, M. (1990) *Biodegradable polymers as drug delivery systems*, Vol. 45, Marcel Dekker, Inc., New York.

[15] Loeffler, J. P., Tartaglia, J. M., and Turnlund, T. H. (1997) Polymer film for wrapping a stent structure, US Patent 08/701,405.

[16] Stone, G. W., Ellis, S. G., Cox, D. A., Hermiller, J., O'Shaughnessy, C., Mann, J. T., Turco, M., Caputo, R., Bergin, P., Greenberg, J., Popma, J. J., and Russell, M. E. (2004) A polymer-based, paclitaxel-eluting stent in patients with coronary artery disease, *New Engl. J. Med. 350*, 221-231.

[17] Stone, G. W., Ellis, S. G., Cannon, L., and et al. (2005) Comparison of a polymer-based paclitaxel-eluting stent with a bare metal stent in patients with complex coronary artery disease: A randomized controlled trial, *J. A. M. A. 294*, 1215-1223.

[18] Frazza, E. J., and Schmitt, E. E. (1971) A new absorbable suture, *J. Biomed. Mater. Res. 5*, 43-58.

[19] Dardik, H., Dardik, I., and Laufman, H. (1971) Clinical use of polyglycolic acid polymer as a new absorbable synthetic suture, *Am. J. Surg. 121*, 656-660.

[20] Lipatova, T. E. (1986) Medical polymer adhesives, In *Biopolymers/Non-Exclusion HPLC*, pp 65-93, Springer Berlin Heidelberg.

[21] English, J. P., McNeely, G. W., and Dunn, R. L. (1989) Method for making a biodegradable adhesive for soft living tissue, US Patent 4804691 A.

[22] Dunn, R. L., Southard, J. L., Urheim, J. E., and Yewey, G. L. (1998) Adjunctive polymer system for use with medical device, US Patent 08/749,029.

[23] Helmus, M. N., Raleigh, C. L., and Tolkoff, J. (1996) Medical device polymer, US Patent 08/479,513.

[24] Jenkins, A. D., Kratochvil, P., Stepto, R. F. T., and Suter, U. W. (1996) Glosssary of basic terms in polymer science, pp 2287-2311, Pure Appl. Chem.

[25] Kelly A. Davis, K. a. (2002) Statistical Copolymers, In *Statistical, dradient, block and graft copolymers by controlled/living Radical polymerizations*, pp 14-29, Springer Berlin Heidelberg.

[26] Cowie, J. M. G. (2008) *Polymers: chemistry and physics of modern materials*, 3rd ed., Scotland: CRC Press.

[27] Kato, M., Kamigaito, M., Sawamoto, M., and Higashimura, T. (1995) Polymerization of methyl methacrylate with the carbon tetrachloride/dichlorotris-(triphenylphosphine)ruthenium(II)/methylaluminum bis(2,6-di-tert-butylphenoxide) initiating system: possibility of living radical polymerization, *Macromolecules 28*, 1721-1723.

[28] Wang, J.-S., and Matyjaszewski, K. (1995) Controlled/"living" radical polymerization. Atom transfer radical polymerization in the presence of transition-metal complexes, *J. Am. Chem. Soc. 117*, 5614-5615.

[29] Chiefari, J., Chong, Y. K., Ercole, F., Krstina, J., Jeffery, J., Le, T. P. T., Mayadunne, R. T. A., Meijs, G. F., Moad, C. L., Moad, G., Rizzardo, E., and Thang, S. H. (1998) Living free-radical polymerization by reversible addition−fragmentation chain transfer: The RAFT Process, *Macromolecules 31*, 5559-5562.

[30] William, A. A., and George, M. N. (1955) Polymeric bicyclo-(2, 2, 1)-2-heptene, US Patent 2721189 A.

[31] Bielawski, C. W., and Grubbs, R. H. (2007) Living ring-opening metathesis polymerization, *Prog. Polym. Sci. 32*, 1-29.

[32] Walker, R., Conrad, R. M., and Grubbs, R. H. (2009) The living ROMP of trans-cyclooctene, *Macromolecules 42*, 599-605.

[33] Hejl, A., Scherman, O. A., and Grubbs, R. H. (2005) Ring-opening metathesis polymerization of functionalized low-atrain monomers with ruthenium-based catalysts, *Macromolecules 38*, 7214-7218.

[34] Ilker, M. F., and Coughlin, E. B. (2001) Alternating copolymerizations of polar and nonpolar cyclic olefins by ring-opening metathesis polymerization, *Macromolecules 35*, 54-58.

[35] Al Samak, B., Carbill, A. G., Hamilton, J. G., Rooney, J. J., and Thompson, J. M. (1997) Alternating ring-opening metathesis copolymerization of bicyclo[2.2.1]hept-2-ene and cyclopentene, *Chem. Comm.*, 2057-2058.

[36] Bornand, M., Torker, S., and Chen, P. (2007) Mechanistically designed dual-site datalysts for the alternating ROMP of norbornene and cyclooctene, *Organometallics 26*, 3585-3596.

[37] Wu, Z., Benedicto, A. D., and Grubbs, R. H. (1993) Living ring-opening metathesis polymerization of bicyclo[3.2.0]heptene catalyzed by a ruthenium alkylidene complex, *Macromolecules 26*, 4975-4977.

[38] Schleyer, P. R., Williams, J. E., and Blanchard, K. R. (1970) The evaluation of strain in hydrocarbons. The strain in adamantane and its origin *J. Am. Chem. Soc. 92*, 2377-2386.

[39] Banks, R. L., and Bailey, G. C. (1964) Olefin disproportionation. A new catalytic process, *Ind. Eng. Chem. Prod. Rd. 3*, 170-173.

[40] Natta, G., Dall'Asta, G., and Mazzanti, G. (1964) Stereospecific homopolymerization of cyclopentene, *Angew. Chem. Int. Ed. 3*, 723-729.

[41] Fischer, E. O., and Maasböl, A. (1964) Zur frage eines wolfram-carbonyl-carben-komplexes, *Angew. Chem. 76*, 645-645.

[42] Chauvin, Y., Commereuc, D., and Cruypelinck, D. (1976) Catalysis of olefin transformation by tungsten complexes, 5. Tungsten carbonyl carbenes activated by titanium tetrahalides as catalysts for the ring-opening polymerization of cyclopentene, *Macromol. Chem. Phys. 177*, 2637-2646.

[43] Chauvin, Y. (2006) Olefin metathesis: the early days (Nobel Lecture), *Angew. Chem. Int. Ed. 45*, 3740-3747.

[44] Chauvin, Y., and Commereuc, D. (1995) Metathesis process for olefins using an enhanced rhenium catalyst, CA Patent 2130492 A1.

[45] Hillmyer, M. A., Lepetit, C., McGrath, D. V., Novak, B. M., and Grubbs, R. H. (1992) Aqueous ring-opening metathesis polymerization of carboximide-functionalized 7-oxanorbornenes, *Macromolecules 25*, 3345-3350.

[46] McGrath, D. V., and Grubbs, R. H. (1994) The mechanism of aqueous ruthenium(II)-catalyzed olefin isomerization, *Organometallics 13*, 224-235.

[47] Dias, E. L., Nguyen, S. T., and Grubbs, R. H. (1997) Well-defined ruthenium olefin metathesis catalysts: mechanism and activity, *J. Am. Chem. Soc. 119*, 3887-3897.

[48] Trnka, T. M., and Grubbs, R. H. (2000) The development of L_2X_2RuCHR olefin metathesis catalysts: an organometallic success story, *Accounts Chem. Res. 34*, 18-29.

[49] Grubbs, R. H. (2003) *Handbook of Metathesis*, Vol. 3, Wiley-VCH, Weinheim, Germany.

[50] Schwab, P., France, M. B., Ziller, J. W., and Grubbs, R. H. (1995) A series of well-defined metathesis catalysts-synthesis of $[RuCl_2(=CHR')(PR_3)_2]$ and its reactions, *Angew. Chem. Int. Ed. 34*, 2039-2041.

[51] Schwab, P., Grubbs, R. H., and Ziller, J. W. (1996) Synthesis and applications of $RuCl_2(=CHR')(PR_3)_2$: The influence of the alkylidene moiety on metathesis activity, *J. Am. Chem. Soc. 118*, 100-110.

[52] Hoveyda, A. H., and Schrock, R. R. (2001) Catalytic asymmetric olefin metathesis, *Chem. Eur. J. 7*, 945-950.

[53] Feldman, J., and Schrock, R. R. (1991) Recent advances in the chemistry of "d^0" alkylidene and metallacyclobutane complexes, *Prog. Inorg. Chem. 39*, 1.

[54] Schrock, R. R., DePue, R. T., Feldman, J., Yap, K. B., Yang, D. C., Davis, W. M., Park, L., DiMare, M., and Schofield, M. (1990) Further studies of imido alkylidene complexes of tungsten, well-characterized olefin metathesis catalysts with controllable activity, *Organometallics 9*, 2262-2275.

[55] Schrock, R. R., Murdzek, J. S., Bazan, G. C., Robbins, J., DiMare, M., and O'Regan, M. (1990) Synthesis of molybdenum imido alkylidene complexes and some reactions involving acyclic olefins, *J. Am. Chem. Soc. 112*, 3875-3886.

[56] Osborn, J. A., and Schrock, R. R. (1971) Coordinatively unsaturated cationic complexes of rhodium(I), iridium(I), palladium(II), and platinum(II). Generation, synthetic utility, and some catalytic studies, *J. Am. Chem. Soc. 93*, 3089-3091.

[57] Schrock, R. R. (1990) Living ring-opening metathesis polymerization catalyzed by well-characterized transition-metal alkylidene complexes, *Acc. Chem. Res. 23*, 158-165.

[58] Kingsbury, J. S., Harrity, J. P. A., Bonitatebus, P. J., and Hoveyda, A. H. (1999) A recyclable Ru-based metathesis catalyst, *J. Am. Chem. Soc. 121*, 791-799.

[59] Garber, S. B., Kingsbury, J. S., Gray, B. L., and Hoveyda, A. H. (2000) Efficient and recyclable monomeric and dendritic Ru-based metathesis catalysts, *J. Am. Chem. Soc. 122*, 8168-8179.

[60] Grela, K., Harutyunyan, S., and Michrowska, A. (2002) A highly efficient ruthenium catalyst for metathesis reactions, *Angew. Chem. 114*, 4210-4212.

[61] Michrowska, A., Bujok, R., Harutyunyan, S., Sashuk, V., Dolgonos, G., and Grela, K. (2004) Nitro-substituted Hoveyda−Grubbs ruthenium carbenes: enhancement of catalyst activity through electronic activation, *J. Am. Chem. Soc. 126*, 9318-9325.

[62] Samojlowicz, C., Bieniek, M., and Grela, K. (2009) Ruthenium-based olefin metathesis catalysts bearing N-heterocyclic carbene ligands, *Chem. Rev. 109*, 3708-3742.

[63] Bourgeois, D., Pancrazi, A., Nolan, S. P., and Prunet, J. (2002) The $Cl_2(PCy_3)(IMes)Ru(=CHPh)$ catalyst: olefin metathesis versus olefin isomerization, *J. Organomet. Chem. 643–644*, 247-252.

[64] Huang, J., Stevens, E. D., Nolan, S. P., and Petersen, J. L. (1999) Olefin metathesis-active ruthenium complexes bearing a nucleophilic carbene ligand, *J. Am. Chem. Soc. 121*, 2674-2678.

[65] Casey, C. P. (2006) 2005 Nobel Prize in Chemistry. Development of the olefin metathesis method in organic synthesis, *J. Chem. Educ. 83*, 192.

[66] Pu, L., Wagaman, M. W., and Grubbs, R. H. (1996) Synthesis of poly(1,4-naphthylenevinylenes): metathesis polymerization of benzobarrelenes, *Macromolecules 29*, 1138-1143.

[67] Ivin, K. J., Kenwright, A. M., Khosravi, E., and Hamilton, J. G. (2000) Ring-opening metathesis polymerization of 7-methylbicyclo[2.2.1]hepta-2,5-diene initiated by well-defined molybdenum and ruthenium carbene complexes., *J. Organomet. Chem.*

[68] Ivin, K. J., Kenwright, A. M., Khosravi, E., and Hamilton, J. G. (2001) Ring-opening metathesis polymerization of 7-tert-butoxybicyclo[2.2.1]hepta-2,5-diene initiated by well-defined molybdenum and ruthenium carbene complexes., *Macromol. Chem. Phys. 202*, 3624-3633.

[69] Nomura, K., Takahashi, S., and Imanishi, Y. (2001) Synthesis of poly(macromonomer)s by repeating ring-opening metathesis polymerization (ROMP) with $Mo(CHCMe_2Ph)(NAr)(OR_2)$ initiators, *Macromolecules 34*, 4712-4723.

[70] Singh, R., Czekelius, C., and Schrock, R. R. (2006) Living ring-opening metathesis polymerization of cyclopropenes, *Macromolecules 39*, 1316-1317.

[71] Wagaman, M. W., and Grubbs, R. H. (1997) Synthesis of organic and water soluble poly(1,4-phenylenevinylenes) containing carboxyl groups: living ring-opening metathesis polymerizatin (ROMP) of 2,3-dicarboxybarrelenes, *Macromolecules 30*, 3978-3985.

[72] Singh, R., and Schrock, R. R. (2008) Stereospecific ring-opening metathesis polymerization of 3-methyl-3-phenylcyclopropene bymolybdenum alkylidene initiators, *Macromolecules 41*, 2990-2993.

[73] Porri, L., Diversi, P., Lucherini, A., and Rossi, R. (1975) Catalysts derived from ruthenium and iridium for the ring-opening polymerization of cycloolefins, *Macromol. Chem. Phys. 176*, 3121-3125.

[74] Porri, L., Rossi, R., Diversi, P., and Lucherini, A. (1974) Ring-Opening polymerization of cycloolefins with catalysts derived from ruthenium and iridium, *Macromol. Chem. Phys. 175*, 3097-3115.

[75] Lu, S.-Y., Amass, J. M., Majid, N., Glennon, D., Byerley, A., Heatley, F., Quayle, P., Booth, C., Yeates, S. G., and Padget, J. C. (1994) Aqueous ring-opening metathesis polymerisation of 7-oxanorbornene derivatives with oxygen-containing functionalities, *Macromol. Chem. Phys. 195*, 1273-1288.

[76] Nguyen, S. T., Johnson, L. K., Grubbs, R. H., and Ziller, J. W. (1992) Ring-opening metathesis polymerization (ROMP) of norbornene by a Group VIII carbene complex in protic media, *J. Am. Chem. Soc. 114*, 3974-3975.

[77] Lynn, D. M., Kanaoka, S., and Grubbs, R. H. (1996) Living ring-opening metathesis polymerization in aqueous media catalyzed by well-defined ruthenium carbene complexes, *J. Am. Chem. Soc. 118*, 784-790.

[78] Miller, S. J., and Grubbs, R. H. (1995) Synthesis of conformationally restricted amino acids and peptides employing olefin metathesis, *J. Am. Chem. Soc. 117*, 5855-5856.

[79] Ulman, M., and Grubbs, R. H. (1999) Ruthenium carbene-based olefin metathesis initiators: catalyst decomposition and longevity, *J. Org. Chem. 64*, 7202-7207.

[80] Maughon, B. R., and Grubbs, R. H. (1997) Ruthenium alkylidene initiated living ring-opening metathesis polymerization (ROMP) of 3-substituted cyclobutenes, *Macromolecules 30*, 3459-3469.

[81] Adlhart, C., Hinderling, C., Baumann, H., and Chen, P. (2000) Mechanistic studies of olefin metathesis by ruthenium carbene complexes using electrospray ionization tandem mass spectrometry, *J. Am. Chem. Soc. 122*, 8204-8214.

[82] Tallarico, J. A., Bonitatebus, P. J., and Snapper, M. L. (1997) Ring-opening metathesis. A ruthenium catalyst caught in the act, *J. Am. Chem. Soc. 119*, 7157-7158.

[83] Hinderling, C., Adlhart, C., and Chen, P. (1998) Olefin metathesis of a ruthenium carbene complex by electrospray ionization in the gas phase, *Angew. Chem. Int. Ed. 37*, 2685-2689.

[84] Aagaard, O. M., Meier, R. J., and Buda, F. (1998) Ruthenium-catalyzed olefin metathesis: a quantum molecular dynamics study, *J. Am. Chem. Soc. 120*, 7174-7182.

[85] Weskamp, T., Schattenmann, W. C., Spiegler, M., and Herrmann, W. A. (1998) A novel class of ruthenium catalysts for olefin metathesis, *Angew. Chem. Int. Ed. 37*, 2490-2493.

[86] Arduengo, A. J. (1999) Looking for stable carbenes: the difficulty in starting anew, *Accounts Chem. Res. 32*, 913-921.

[87] Bourissou, D., Guerret, O., Gabba ̈ı F. P., and Bertrand, G. (1999) Stable Carbenes, *Chem. Rev. 100*, 39-92.

[88] Scholl, M., Ding, S., Lee, C. W., and Grubbs, R. H. (1999) Synthesis and activity of a new generation of ruthenium-based olefin metathesis catalysts coordinated with 1,3-dimesityl-4,5-dihydroimidazol-2-ylidene ligands, *Org. Lett. 1*, 953-956.

[89] Gessler, S., Randl, S., and Blechert, S. (2000) Synthesis and metathesis reactions of a phosphine-free dihydroimidazole carbene ruthenium complex, *Tetrahedron Lett. 41*, 9973-9976.

[90] Vougioukalakis, G. C., and Grubbs, R. H. (2010) Ruthenium-based heterocyclic carbene-coordinated olefin metathesis catalysts, *Chem. Rev. 110*, 1746-1787.

[91] Love, J. A., Morgan, J. P., Trnka, T. M., and Grubbs, R. H. (2002) A practical and highly active ruthenium-based catalyst that effects the cross metathesis of acrylonitrile, *Angew. Chem. Int. Ed. 41*, 4035-4037.

[92] Bielawski, C. W., and Grubbs, R. H. (2001) Increasing the initiation efficiency of ruthenium-based ring-opening metathesis initiators: effect of excess phosphine, *Macromolecules 34*, 8838-8840.

[93] Sanford, M. S., Love, J. A., and Grubbs, R. H. (2001) Mechanism and activity of ruthenium olefin metathesis catalysts, *J. Am. Chem. Soc. 123*, 6543-6554.

[94] Matson, J. B., and Grubbs, R. H. (2008) ROMP−ATRP block copolymers prepared from monotelechelic poly(oxa)norbornenes using a difunctional terminating agent, *Macromolecules 41*, 5626-5631.

[95] Klavetter, F. L., and Grubbs, R. H. (1988) Polycyclooctatetraene (polyacetylene): synthesis and properties, *J. Am. Chem. Soc. 110*, 7807-7813.

[96] Chen, Z.-R., Claverie, J. P., Grubbs, R. H., and Kornfield, J. A. (1995) Modeling ring-chain equilibria in ring-opening polymerization of cycloolefins, *Macromolecules 28*, 2147-2154.

[97] Reif, L., and Hoecker, H. (1984) Kinetics and thermodynamics of the metathesis reaction of cycloolefins. 2. Molecular weight distribution, *Macromolecules 17*, 952-956.

[98] Maynard, H. D., and Grubbs, R. H. (1999) Purification technique for the removal of ruthenium from olefin metathesis reaction products, *Tetrahedron Lett. 40*, 4137-4140.

[99] Pederson, R. L., Fellows, I. M., Ung, T. A., Ishihara, H., and Hajela, S. P. (2002) Applications of olefin cross metathesis to commercial products, *Adv. Synth. Catal. 344*, 728-735.

[100] French, J. M., Caras, C. A., and Diver, S. T. (2013) Removal of ruthenium using a silica gel supported reagent, *Org. Lett. 15*, 5416-5419.

[101] Amir-Ebrahimi, V., Corry, D. A., Hamilton, J. G., Thompson, J. M., and Rooney, J. J. (2000) Characteristics of $RuCl_2(CHPh)(PCy_3)_2$ as a catalyst for ring-opening metathesis polymerization, *Macromolecules 33*, 717-724.

[102] Maynard, H. D., Okada, S. Y., and Grubbs, R. H. (2000) Synthesis of norbornenyl polymers with bioactive oligopeptides by ring-opening metathesis polymerization, *Macromolecules 33*, 6239-6248.

[103] Lee, J. C., Parker, K. A., and Sampson, N. S. (2006) Amino acid-bearing ROMP polymers with a stereoregular backbone, *J. Am. Chem. Soc. 128*, 4578-4579.

[104] Song, A., Lee, J. C., Parker, K. A., and Sampson, N. S. (2010) Scope of the ring-opening metathesis polymerization (ROMP) reaction of 1-substituted cyclobutenes, *J. Am. Chem. Soc. 132*, 10513-10520.

[105] Lutz, J.-F., Ouchi, M., Liu, D. R., and Sawamoto, M. (2013) Sequence-controlled polymers, *Science 341*.

[106] Badi, N., and Lutz, J.-F. (2009) Sequence control in polymer synthesis, *Chemi. Soc. Rev. 38*, 3383-3390.

[107] Lutz, J.-F. (2010) Sequence-controlled polymerizations: the next holy grail in polymer science, *J. Polym. Sci., Part A: Polym. Chem. 1*, 55-62.

[108] Ouchi, M., Meyer, T., and Lutz, J.-F. (2014) *Sequence-controlled polymers by ruthenium-mediated ring-opening metathesis polymerization*, ACS Books.

[109] Castner, K. F., and Calderon, N. (1982) Ring-opening polymerization of cyclic olefins substituted with polar groups. 5-Norbornene-2,3-dicarboxy anhydride (CPD-MA), *J. Mol. Catal. 15*, 47-59.

[110] Al Samak, B., Amir-Ebrahimi, V., Corry, D. G., Hamilton, J. G., Rigby, S., Rooney, J. J., and Thompson, J. M. (2000) Dramatic solvent effects on ring-opening metathesis polymerization of cycloalkenes, *J. Mol. Catal. A: Chem. 160*, 13-21.

[111] Bornand, M., and Chen, P. (2005) Mechanism-based design of a ROMP catalyst for sequence-selective copolymerization, *Angew. Chem. Int. Ed. 44*, 7909-7911.

[112] Torker, S., Müller, A., Sigrist, R., and Chen, P. (2010) Tuning the steric properties of a metathesis catalyst for copolymerization of norbornene and cyclooctene toward complete alternation, *Organometallics 29*, 2735-2751.

[113] Torker, S., Müller, A., and Chen, P. (2010) Building stereoselectivity into a chemoselective ring-opening metathesis polymerization catalyst for alternating copolymerization, *Angew. Chem. 122*, 3850-3854.

[114] Vehlow, K., Wang, D., Buchmeiser, M. R., and Blechert, S. (2008) Alternating copolymerizations using a Grubbs-type initiator with an unsymmetrical, chiral N-heterocyclic carbene ligand, *Angew. Chem., Int. Ed. 47*, 2615-2618.

[115] Lichtenheldt, M., Wang, D., Vehlow, K., Reinhardt, I., Kuhnel, C., Decker, U., Blechert, S., and Buchmeiser, M. R. (2009) Alternating ring-opening metathesis copolymerization by Grubbs-type initiators with unsymmetrical N-heterocyclic carbenes, *Chemistry 15*, 9451-9457.

[116] Ilker, M. F., and Coughlin, E. B. (2002) Alternating copolymerizations of polar and nonpolar cyclic olefins by ring-opening metathesis polymerization, *Macromolecules 35*, 54-58.

[117] Sutthasupa, S., Shiotsuki, M., Masuda, T., and Sanda, F. (2009) Alternating ring-opening metathesis copolymerization of amino acid derived norbornene monomers carrying nonprotected carboxy and amino groups based on acid-base interaction, *J. Am. Chem. Soc. 131*, 10546-10551.

[118] Choi, T.-L., Rutenberg, I. M., and Grubbs, R. H. (2002) Synthesis of A,B-alternating copolymers by ring-opening-insertion-metathesis polymerization, *Angew. Chem. Int. Ed. 41*, 3839-3841.

[119] Zhang, J., Matta, M. E., and Hillmyer, M. A. (2012) Synthesis of sequence-specific vinyl copolymers by regioselective ROMP of multiply substituted cyclooctenes, *ACS Macro. Lett. 1*, 1383-1387.

[120] Song, A. (2010) ROMP of cyclobutenes and its application in antimicrobial studies: from homopolymers to alternating copolymers, *Ph. D. Thesis, Stony Brook University*

[121] Siegwart, D. J., Oh, J. K., and Matyjaszewski, K. (2012) ATRP in the design of functional materials for biomedical applications, *Prog. Polym. Sci. 37*, 18-37.

[122] Cölfen, H. (2001) Double-hydrophilic block copolymers: synthesis and application as novel surfactants and crystal growth modifiers, *Macromol. Rapid Commun. 22*, 219-252.

[123] Schacher, F. H., Rupar, P. A., and Manners, I. (2012) Functional block bopolymers: nanostructured materials with emerging applications, *Angew. Chem. Int. Ed. 51*, 7898-7921.

[124] Furuta, P. T., Deng, L., Garon, S., Thompson, M. E., and Frechet, J. M. (2004) Platinum-functionalized random copolymers for use in solution-processible, efficient, near-white organic light-emitting diodes, *J. Am. Chem. Soc. 126*, 15388-15389.

[125] Furuta, P., Brooks, J., Thompson, M. E., and Fréchet, J. M. J. (2003) Simultaneous light emission from a mixture of dendrimer encapsulated chromophores: a model for single-layer multichromophoric organic light-emitting diodes, *J. Am. Chem. Soc. 125*, 13165-13172.

[126] Romulus, J., Tan, L., Weck, M., and Sampson, N. S. (2013) Alternating ring-opening metathesis polymerization copolymers containing charge-transfer units, *Macromol. Lett. 2*, 749-752.

[127] Kim, H. K., Baek, N. S., Paik, K. L., Lee, Y., and Lee, J. H. (2004) Synthesis, photophysical property, and electroluminescent applications of silicon-based alternating copolymers, In *Chromogenic Phenomena in Polymers*, pp 247-263, American Chemical Society.

[128] ten Brummelhuis, N., and Weck, M. (2012) Orthogonal multifunctionalization of random and alternating copolymers, *Macromol. Lett. 1*, 1216-1218.

[129] Chen, G.-Q., Wu, Z.-Q., Wu, J.-R., Li, Z.-C., and Li, F.-M. (1999) Synthesis of alternating copolymers of N-substituted maleimides with styrene via atom transfer radical polymerization, *Macromolecules 33*, 232-234.

[130] Shirota, Y., Yoshimura, M., Matsumoto, A., and Mikawa, H. (1974) Mechanism of charge-transfer polymerization. VI. alternating radical copolymerization of N-vinylcarbazole with electron-accepting monomers, *Macromolecules 7*, 4-11.

[131] Lutz, J.-F., Kirci, B., and Matyjaszewski, K. (2003) Synthesis of well-defined alternating copolymers by controlled/lRadical polymerization in the presence of lewis acids, *Macromolecules 36*, 3136-3145.

[132] Kamigaito, M., Ando, T., and Sawamoto, M. (2001) Metal-catalyzed living radical polymerization, *Chem. Rev. 101*, 3689-3746.

[133] Ouchi, M., Terashima, T., and Sawamoto, M. (2009) Transition metal-catalyzed living radical polymerization: toward perfection in catalysis and precision polymer synthesis, *Chem. Rev. 109*, 4963-5050.

[134] Moad, G., Rizzardo, E., and Thang, S. H. (2012) Living radical polymerization by the RAFT process - a third update, *Aust. J. Chem. 65*, 985-1076.

[135] Amir-Ebrahimi, V., and Rooney, J. J. (2004) Remarkable alternating effect in metathesis copolymerization of norbornene and cyclopentene using modified Grubbs ruthenium initiators, *J. Mol. Catal. A: Chem. 208*, 115-121.

[136] Vehlow, K., Lichtenheldt, M., Wang, D., Blechert, S., and Buchmeiser, M. R. (2010) Alternating ring-opening metathesis copolymerization of norborn-2-ene with *cis*-cyclooctene and cyclopentene, *Macromol. Symp. 296*, 44-48.

[137] Buchmeiser, M. R., Ahmad, I., Gurram, V., and Kumar, P. S. (2011) Pseudo-halide and nitrate derivatives of Grubbs and Grubbs–Hoveyda initiators: some structural features related to the alternating ring-opening metathesis copolymerization of norborn-2-ene with cyclic olefins, *Macromolecules 44*, 4098-4106.

[138] Choi, T.-L., Lee, C. W., Chatterjee, A. K., and Grubbs, R. H. (2001) Olefin metathesis involving ruthenium enoic carbene complexes, *J. Am. Chem. Soc. 123*, 10417-10418.

[139] Song, A., Parker, K. A., and Sampson, N. S. (2010) Cyclic alternating ring-opening metathesis polymerization (CAROMP). Rapid access to functionalized cyclic polymers, *Org. Lett. 12*, 3729-3731.

[140] Choi, T.-L., and Grubbs, R. H. (2003) Controlled living ring-opening-metathesis polymerization by a fast-initiating ruthenium catalyst, *Angew. Chem. Int. Ed. 42*, 1743-1746.

[141] Elsheimer, S., Slattery, D. K., Michael, M., Weeks, J., and Topoleski, K. (1989) Alkaline hydrolysis of 1,3-dibromo-1,1-difluoroalkanes: a two-step vinyl carboxylation, *J. Org. Chem. 54*, 3992-3993.

[142] Yong, L., and Butenschon, H. (2002) The first cobalt catalyzed [2 + 2 + 2] alkyne cyclotrimerization in aqueous medium at room temperature, *Chem Commun (Camb)*, 2852-2853.

[143] Yamamoto, Y., Arakawa, T., Ogawa, R., and Itoh, K. (2003) Ruthenium(II)-catalyzed selective intramolecular [2+2+2] alkyne cyclotrimerizations, *J. Am. Chem. Soc. 125*, 12143-12160.

[144] Breslow, R. (2005) *Organic reaction mechanisms*, Vol. 41, John Wiley & Sons Ltd.

[145] Snider, B. B., Rodini, D. J., Cionn, R. S. E., and Sealfon, S. (1979) Lewis acid catalyzed reactions of methyl propiolate with unactivated alkenes, *J. Am. Chem. Soc. 101*, 5283-5493.

[146] Baird, N. C. (1970) The calculation of strain energy by molecular orbital theories, *Tetrahedron 26*, 2185-2190.

[147] Elsheimer, S., Swanson, J. L., and Gonzalez, J. (2000) Mechanisms for the alkaline hydrolysis of dibromodifluoromethane-alkene adducts to α,β-unsaturated carboxylates., *J. Fluorine Chem. 102*, 3-9.

[148] Wiberg, K. B. (2003) The concept of strain in organic chemistry, *Angew. Chem. Int. Ed. 25*, 312-322.

[149] Rankin, D. A., Schanz, H.-J., and Lowe, A. B. (2007) Effect of the halide counterion in the ROMP of exo-benzyl-[2-(3,5-dioxo-10-oxa-4-aza-tricyclo[5.2.1.$0^{2,6}$]dec-8-en-4-yl)ethyl]dimethyl ammonium bromide/chloride, *Macromol. Chem. Phys. 208*, 2389-2395.

[150] Jordan, R., Marquand, P. L., and Tam, W. (2008) Ruthenium(II)-Catalyzed [2+2] Cycloadditions of *anti-7-Substituted* Norbornenes, *Eur. J. Org. Chem.*, 80-86.

[151] Myers, S. B., and Register, R. A. (2008) Crystalline-crystalline diblock copolymers of linear polyethylene and hydrogenated polynorbornene, *Macromolecules 41*, 6773-6779.

[152] Beak, P., Kempf, D. J., and Wilson, K. D. (1985) The beta'-lithiation of alpha,beta-unsaturated amides, *J. Am. Chem. Soc. 107*, 4745-4756.

[153] Allinger, N. L., Tribble, M. T., Miller, M. A., and Wertz, D. H. (1971) Conformational analysis. LXIX. Improved force field for the calculation of the structures and energies of hydrocarbons, *J. Am. Chem. Soc. 93*, 1637-1648.

[154] Hoyland, J. R. (1969) Ab initio calculation of the relative energy of some conformations of cyclopentane and cyclohexane, *J. Chem. Phys. 50*, 2775-2775.

[155] Allinger, N. L., Hirsch, J. A., Miller, M. A., Tyminski, I. J., and Van Catledge, F. A. (1968) Conformational analysis. LX. Improved calculations of the structures and energies of hydrocarbons by the Westheimer method, *J. Am. Chem. Soc. 90*, 1199-1210.

[156] Fuchs, B. (1978) Conformations of five-membered rings, In *Topics in Stereochemistry* (Eliel, E. L., Wilen, S. H., and Allinger, N. L., Eds.), pp 1-94 (96), Interscience.

[157] Wilson, N. K., Stochters, J. B., Bucourt, R., Kellie, G. M., Friddell, F. G., and Moriarty, R. M. (1974) Topics in stereochemsitry, In *Topics in Stereochemsitry* (Eliel, E. L., Wilen, S. H., and Allinger, N. L., Eds.), pp 1-158, Interscience.

[158] Testa, B., Vistoli, G., and Pedretti, A. (2013) Organic stereochemistry. Part 41) Isomerisms about single bonds and in cyclic systems, *Helv. Chim. Acta 96*, 564-623.

[159] Abraham, R. J., Koniotou, R., and Sancassan, F. (2002) Conformational analysis. Part 39. A theoretical and lanthanide induced shift (LIS) investigation of the conformations of cyclopentanol and cis- and trans-cyclopentane-1,2-diol, *J. Chem. Soc., Perkin Trans. 2*, 2025-2030.

[160] Abraham, R. J., and Koniotou, R. (2003) Conformational analysis. Part 40: A theoretical and NMR investigation of the conformations of cis- and trans-cyclopentane-1,3-diol, *Magn. Reson. Chem. 41*, 1000-1008.

[161] Romulus, J., Patel, S., and Weck, M. (2011) Facile synthesis of flexible, donor–acceptor side-chain functionalized copolymers via ring-opening metathesis polymerization, *Macromolecules 45*, 70-77.

[162] Flook, M. M., Ng, V. W. L., and Schrock, R. R. (2011) Synthesis of cis,syndiotactic ROMP polymers containing alternating enantiomers, *J. Am. Chem. Soc. 133*, 1784-1786.

[163] Lokey, R. S., and Iverson, B. L. (1995) Synthetic molecules that fold into a pleated secondary structure in solution, *Nature 375*, 303-305.

[164] Hill, D. J., Mio, M. J., Prince, R. B., Hughes, T. S., and Moore, J. S. (2001) A field guide to foldamers, *Chem. Rev. 101*, 3893-4011.

[165] Gellman, S. H. (1998) Foldamers: A manifesto, *Acc. Chem. Res. 31*, 173-180.

[166] Chang, A. B., Miyake, G. M., and Grubbs, R. (2014) Sequence-controlled polymers by ruthenium-mediated ring-opening metathesis polymerization, In *Sequence-Controlled Polymers: Synthesis, Self-Assembly, and Properties* (Ouchi, M. O., Meyer, T., and Lutz, J.-F., Eds.), ACS, Washington, D.C.

[167] Leitgeb, A., Wappel, J., and Slugovc, C. (2010) The ROMP toolbox upgraded, *Polymer 51*, 2927-2946.

[168] Sutthasupa, S., Shiotsuki, M., and Sanda, F. (2010) Recent advances in ring-opening metathesis polymerization, and application to synthesis of functional materials, *Polymer journal 42*, 905-915.

[169] Tan, L., Parker, K. A., and Sampson, N. S. (2014) A bicyclo[4.2.0]octene-derived monomer provides completely linear alternating copolymers via alternating ring-opening metathesis polymerization (AROMP). *Macromolecules* 10.1021/ma5012039.

[170] Song, A., Walker, S. G., Parker, K. A., and Sampson, N. S. (2011) Antibacterial studies of cationic polymers with alternating, random, and uniform backbones, *ACS Chem. Bio. 6*, 590-599.

[171] Stewart, I. C., Ung, T., Pletnev, A. A., Berlin, J. M., Grubbs, R. H., and Schrodi, Y. (2007) Highly efficient ruthenium catalysts for the formation of tetrasubstituted olefins via ring-closing metathesis, *Org. Lett. 9*, 1589-1592.

[172] Berlin, J. M., Campbell, K., Ritter, T., Funk, T. W., Chlenov, A., and Grubbs, R. H. (2007) Ruthenium-catalyzed ring-closing metathesis to form tetrasubstituted olefins, *Org. Lett. 9*, 1339-1342.

[173] Rost, D., Porta, M., Gessler, S., and Blechert, S. (2008) A hexafluorobenzene promoted ring-closing metathesis to form tetrasubstituted olefins, *Tetrahedron Lett. 49*, 5968-5971.

[174] Ackermann, L., Fürstner, A., Weskamp, T., Kohl, F. J., and Herrmann, W. A. (1999) Ruthenium carbene complexes with imidazolin-2-ylidene ligands allow the formation of tetrasubstituted cycloalkenes by RCM, *Tetrahedron Lett. 40*, 4787-4790.

[175] Curran, K., Risse, W., Hamill, M., Saunders, P., Muldoon, J., Asensio del la Rosa, R., and Tritto, I. (2012) Palladium(II)-catalyzed rearrangement and oligomerization reactions of *cis*-bicyclo[4.2.0]oct-7-ene, *Organometallics 31*, 882-889.

[176] Cadot, C., Dalko, P. I., and Cossy, J. (2002) Olefin isomerization by a ruthenium carbenoid complex. Cleavage of allyl and homoallyl groups, *Tetrahedron Lett. 43*, 1839-1841.

[177] Dinger, M. B., and Mol, J. C. (2003) Degradation of the first-generation Grubbs metathesis catalyst with primary alcohols, water, and oxygen. formation and catalytic activity of ruthenium(II) monocarbonyl species, *Organometallics 22*, 1089-1095.

[178] Dinger, Maarten B., and Mol, Johannes C. (2003) Degradation of the second-generation Grubbs metathesis catalyst with primary alcohols and oxygen − isomerization and hydrogenation activities of monocarbonyl complexes, *Eur. J. Inorg. Chem. 2003*, 2827-2833.

[179] Schmidt, B. (2004) Catalysis at the interface of ruthenium carbene and ruthenium hydride chemistry: organometallic aspects and applications to organic synthesis, *Eur. J. Org. Chem. 2004*, 1865-1880.

[180] Janse van Rensburg, W., Steynberg, P. J., Meyer, W. H., Kirk, M. M., and Forman, G. S. (2004) DFT prediction and experimental observation of substrate-induced catalyst decomposition in ruthenium-catalyzed olefin metathesis, *J. Am. Chem. Soc. 126*, 14332-14333.

[181] van Rensburg, W. J., Steynberg, P. J., Kirk, M. M., Meyer, W. H., and Forman, G. S. (2006) Mechanistic comparison of ruthenium olefin metathesis catalysts: DFT insight into relative reactivity and decomposition behavior, *J. Organometallic Chem. 691*, 5312-5325.

[182] Ashworth, I. W., Hillier, I. H., Nelson, D. J., Percy, J. M., and Vincent, M. A. (2012) Searching for the hidden hydrides: the competition between alkene isomerization and metathesis with grubbs catalysts, *Eur. J. Org. Chem. 2012*, 5673-5677.

[183] Higman, C. S., Plais, L., and Fogg, D. E. (2013) Isomerization during olefin metathesis: an assessment of potential catalyst culprits, *Chem. Cat. Chem 5*, 3548-3551.

[184] Schmidt, B. (2006) Olefin metathesis and isomerization: From undesired side reactions to useful synthetic methodology, *J. Mol. Catal. A: Chem. 254*, 53-57.

[185] Trost, B. M., and Kulawiec, R. J. (1993) Chemoselectivity in the ruthenium-catalyzed redox isomerization of allyl alcohols, *J. Am. Chem. Soc. 115*, 2027-2036.

[186] McGrath, D. V., and Grubbs, R. H. (1994) The mechanism of aqueous ruthenium (II)-catalyzed olefin isomerization, *Organometallics 13*, 224-235.

[187] Hong, S. H., Sanders, D. P., Lee, C. W., and Grubbs, R. H. (2005) Prevention of undesirable isomerization during olefin metathesis, *J. Am. Chem. Soc. 127*, 17160-17161.

[188] Bielawski, C., Scherman, O., and Grubbs, R. (2001) Highly efficient syntheses of acetoxy- and hydroxy-terminated telechelic poly (butadiene) s using ruthenium catalysts containing *N*-heterocyclic ligands, *Polymer 42*, 4939-4945.

[189] Hillmyer, M. A., Nguyen, S. T., and Grubbs, R. H. (1997) Utility of a ruthenium metathesis catalyst for the preparation of end-functionalized polybutadiene, *Macromolecules 30*, 718-721.

[190] Stone, M. T., Heemstra, J. M., and Moore, J. S. (2005) The chain-length dependence test, *Acc. Chem. Res. 39*, 11-20.

[191] Hosono, N., Gillissen, M. A. J., Li, Y., Sheiko, S. S., Palmans, A. R. A., and Meijer, E. W. (2012) Orthogonal self-assembly in folding block copolymers, *J. Am. Chem. Soc. 135*, 501-510.

[192] Wu, Z., and Grubbs, R. H. (1995) Preparation of alternating copolymers from the ring-opening metathesis polymerization of 3-methylcyclobutene and 3,3-dimethylcyclobutene, *Macromolecules 28*, 3502-3508.

[193] Yoshida, Y., Mohri, J.-i., Ishii, S.-i., Mitani, M., Saito, J., Matsui, S., Makio, H., Nakano, T., Tanaka, H., Onda, M., Yamamoto, Y., Mizuno, A., and Fujita, T. (2004) Living copolymerization of ethylene with norbornene catalyzed by bis(pyrrolide−imine) titanium complexes with MAO, *J. Am. Chem. Soc. 126*, 12023-12032.

[194] Braunecker, W. A., and Matyjaszewski, K. (2007) Controlled/living radical polymerization: features, developments, and perspectives, *Prog. Polym. Sci. 32*, 93-146.

[195] Maruo, N., Uchiyama, M., Kato, T., Arai, T., Nishino, N., and Akisada, H. (1999) Hemispherical synthesis of dendritic poly(L-lysine) combining sixteen free-base porphyrins and sixteen zinc porphyrins, *Chem. Commun. 0*, 2057-2058.

[196] Burattini, S., Colquhoun, H. M., Greenland, B. W., Hayes, W., and Wade, M. (2009) Pyrene-functionalised, alternating copolyimide for sensing nitroaromatic compounds, *Macromol. Rapid Commun. 30*, 459-463.

[197] Nakade, H., Ilker, M. F., Jordan, B. J., Uzun, O., LaPointe, N. L., Coughlin, E. B., and Rotello, V. M. (2005) Duplex strand formation using alternating copolymers, *Chem. Commun. 0*, 3271-3273.

[198] Anslyn, E. V., and Dougherty, D. A., (Eds.) (2006) *Modern Physical Organic Chemistry*, Vol. 83.

[199] Zych, A. J., and Iverson, B. L. (2000) Synthesis and conformational characterization of tethered, self-complexing 1,5-dialkoxynaphthalene/1,4,5,8-naphthalenetetracarboxylic diimide systems, *J. Am. Chem. Soc. 122*, 8898-8909.

[200] Ghosh, S., and Ramakrishnan, S. (2004) Aromatic donor–acceptor charge-transfer and metal-ion-complexation-assisted folding of a synthetic polymer, *Angew. Chem., Int. Ed. 43*, 3264-3268.

[201] Arnett, E. M., Joris, L., Mitchell, E., Murty, T. S. S. R., Gorrie, T. M., and Schleyer, P. v. R. (1970) Hydrogen-bonded complex formation. III. Thermodynamics of complexing by infrared spectroscopy and calorimetry, *J. Am. Chem. Soc. 92*, 2365-2377.

[202] Baird, N. C. (1970) *Tetrahedron 26*, 2185-2190.

[203] Tan, L., Parker, K. A., and Sampson, N. S. (2014) Alkene isomerization as an entry to efficient alternating ring-opening metathesis polymerization (*i*-AROMP).

[204] De Angelis, D. A. (1999) *Why FRET over genomics*, Vol. 1.

[205] Buchowicz, W., Holerca, M. N., and Percec, V. (2001) Self-inhibition of propagating carbenes in ROMP of 7-oxa-bicyclo[2.2.1]hept-2-ene-5,6-dicarboxylic acid dendritic diesters initiated with $Ru(CHPh)Cl_2(PCy_3)$(1,3-dimesityl-4,5-dihydroimidazol-2-ylidene), *Macromolecules 34*, 3842-3848.

[206] Haigh, D. M., Kenwright, A. M., and Khosravi, E. (2005) Nature of the propagating species in ring-opening metathesis polymerizations of oxygen-containing monomers using well-defined ruthenium initiators, *Macromolecules 38*, 7571-7579.

[207] Johnson, J. A., Lu, Y. Y., Burts, A. O., Lim, Y.-H., Finn, M. G., Koberstein, J. T., Turro, N. J., Tirrell, D. A., and Grubbs, R. H. (2010) Core-clickable PEG-branch-azide bivalent-bottle-brush polymers by ROMP: grafting-through and clicking-to, *J. Am. Chem. Soc. 133*, 559-566.

[208] Boren, B. C., Narayan, S., Rasmussen, L. K., Zhang, L., Zhao, H., Lin, Z., Jia, G., and Fokin, V. V. (2008) Ruthenium-catalyzed azide−alkyne cycloaddition: scope and mechanism, *J. Am. Chem. Soc. 130*, 8923-8930.

[209] Yang, S. K., and Weck, M. (2007) Modular covalent multifunctionalization of copolymers, *Macromolecules 41*, 346-351.

[210] Fenderson, B. A. (2006) Molecular imaging: FRET microscopy and spectroscopy, *Shock 25*, 317 310.1097/1001.shk.0000214139.0000249166.0000214131b.

[211] Gryczynski, I., Wiczk, W., Johnson, M. L., Cheung, H. C., Wang, C. K., and Lakowicz, J. R. (1988) Resolution of end-to-end distance distributions of flexible molecules using quenching-induced variations of the Forster distance for fluorescence energy transfer, *Biophys. J. 54*, 577-586.

[212] Campbell, A., and Rydon, H. N. (1953) 596. The synthesis of caryophyllenic acid, *J. Chem. Soc. 0*, 3002-3008.

[213] Mathias, L. J. (1979) Esterification and alkylation reactions employing isoureas, *Synthesis-Stuttgart*, 561-576.

[214] Fleming, I., and Harley-Mason, J. (1964) 403. The reaction of enamines with electrophilic olefins. A synthesis of cyclobutanes, *J. Chem. Soc.* , 2165-2174.

Appendix

Checklist for compounds

Compound	Reference	1H NMR	13C NMR	Other
1b	119	✓	✓	
2	156	✓	✓	
3	156	✓	✓	
4a	156	✓	✓	
4e		✓	✓	
5	156	✓	✓	
6b	119	✓	✓	
6c	119	✓	✓	
8a		✓	✓	
8b		✓	✓	
8c		✓	✓	
8d		✓	✓	
8e		✓	✓	
8f		✓	✓	
8f*		✓	✓	
8a'		✓		
8b'		✓		
8c'		✓	✓	HSQC
8d'		✓		
8e'		✓	✓	
8f'		✓		
8f*'		✓		
9		✓		
poly(**3**-*alt*-**6a**)$_{13}$		✓		
poly(**4a**-*alt*-**6a**)$_{20}$		✓	✓	HSQC
poly(**4a**-*alt*-**6a-D$_{10}$**)$_{20}$		✓		
poly(**4a**-*alt*-**6a**)$_{35}$		✓		
poly(**5**-*alt*-**6a**)$_{10}$		✓		
E-stilbene		✓	✓	HSQC
Ph-(**3**-*alt*-**6a**)-Ph		✓	✓	HSQC
cyc-(**3**-*alt*-**6a**)		✓		

poly(**8c'**-*alt*-**6a**)$_{10}$		✓		
poly(**8c'**-*alt*-**6a**)$_{50}$		✓		HSQC
poly(**8c'**-*alt*-**6a**)$_{97}$		✓		
poly(**8c'**-*alt*-**6a**)$_{424}$		✓	✓	
poly(**8d'**-*alt*-**6a**)$_{50}$		✓		
poly(**8d'**-*alt*-**6a-D$_{10}$**)$_{10}$		✓		
poly(**8d'**-*alt*-**6a**)$_{20}$		✓		
poly(**1a**-*alt*-**6b**)$_5$	119	✓		
poly(**1a**-*alt*-**6c**)$_{10}$	119	✓		
Poly(**1a**-*alt*-**6d**)$_{10}$	119	✓		
Boc-Trp-alkyne		✓	✓	
poly(**4e**-*alt*-**6e**)$_{27}$		✓	✓	
poly(**4e'**-*alt*-**6e**)$_{27}$		✓		IR
poly(**4e'**-*alt*-**6e-DH**)$_{27}$		✓		
poly(**4e'-Trp**-*alt*-**6e**)$_{27}$		✓		
poly(**4e'-Trp**-*alt*-**6e-DH**)$_{27}$		✓		IR